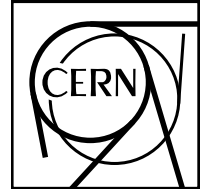
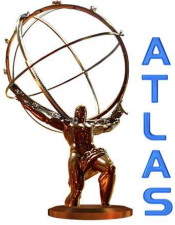


EUROPEAN ORGANISATION FOR NUCLEAR RESEARCH (CERN)



CERN-PH-EP-2012-140

Submitted to: JHEP

**Search for the Standard Model Higgs boson in the $H \rightarrow \tau^+\tau^-$
decay mode in $\sqrt{s} = 7$ TeV pp collisions with ATLAS**

The ATLAS Collaboration

Abstract

A search for the Standard Model Higgs boson decaying into a pair of τ leptons is reported. The analysis is based on a data sample of proton-proton collisions collected by the ATLAS experiment at the LHC and corresponding to an integrated luminosity of 4.7fb^{-1} . No significant excess over the expected background is observed in the Higgs boson mass range of 100–150 GeV. The observed (expected) upper limits on the cross section times the branching ratio for $H \rightarrow \tau^+\tau^-$ are found to be between 2.9 (3.4) and 11.7 (8.2) times the Standard Model prediction for this mass range.

Search for the Standard Model Higgs boson in the $H \rightarrow \tau^+\tau^-$ decay mode in $\sqrt{s} = 7$ TeV pp collisions with ATLAS

The ATLAS Collaboration

ABSTRACT: A search for the Standard Model Higgs boson decaying into a pair of τ leptons is reported. The analysis is based on a data sample of proton-proton collisions collected by the ATLAS experiment at the LHC and corresponding to an integrated luminosity of 4.7 fb^{-1} . No significant excess over the expected background is observed in the Higgs boson mass range of 100–150 GeV. The observed (expected) upper limits on the cross section times the branching ratio for $H \rightarrow \tau^+\tau^-$ are found to be between 2.9 (3.4) and 11.7 (8.2) times the Standard Model prediction for this mass range.

Contents

1	Introduction	1
2	Data and Monte Carlo simulated samples	2
3	Selection and reconstruction of physics objects	3
4	Preselection	5
4.1	$H \rightarrow \tau_{\text{lep}}\tau_{\text{lep}}$	5
4.2	$H \rightarrow \tau_{\text{lep}}\tau_{\text{had}}$	6
4.3	$H \rightarrow \tau_{\text{had}}\tau_{\text{had}}$	6
5	Analysis categories	6
5.1	$H \rightarrow \tau_{\text{lep}}\tau_{\text{lep}}$	6
5.2	$H \rightarrow \tau_{\text{lep}}\tau_{\text{had}}$	7
5.3	$H \rightarrow \tau_{\text{had}}\tau_{\text{had}}$	8
6	Background estimation and modelling	8
6.1	$H \rightarrow \tau_{\text{lep}}\tau_{\text{lep}}$	10
6.2	$H \rightarrow \tau_{\text{lep}}\tau_{\text{had}}$	14
6.3	$H \rightarrow \tau_{\text{had}}\tau_{\text{had}}$	18
7	Systematic uncertainties	22
8	Statistical analysis	23
9	Results	24
10	Conclusions	24

1 Introduction

The Higgs boson is the only fundamental particle in the Standard Model (SM) of particle physics that has not yet been observed. It is predicted by the Higgs mechanism [1–6], which in the SM gives mass to particles. The search for the Higgs boson is a centrepiece of the Large Hadron Collider (LHC) physics programme.

An indirect constraint on the Higgs boson mass of $m_H < 185$ GeV at the 95% confidence level (CL) has been set using global fits to electroweak precision data [7]. Direct searches at LEP and the Tevatron have placed exclusion limits at 95% CL for $m_H < 114.4$ GeV and in

the region $147 \text{ GeV} < m_H < 179 \text{ GeV}$ [8, 9], respectively. The results of searches in various channels using data corresponding to an integrated luminosity of up to 5 fb^{-1} have recently been reported by both the ATLAS and CMS Collaborations [10, 11] excluding the mass range between 112.9 GeV and 115.5 GeV and the region between 127 GeV and 600 GeV, again at the 95% CL.

In the Higgs boson mass range 100-150 GeV, the $H \rightarrow \tau^+\tau^-$ decay mode is a promising channel for the search at the LHC with branching ratios between 8% and 1.8%. The $H \rightarrow \tau^+\tau^-$ search is complementary to searches with other decays in the same mass range and enhances the overall sensitivity. Also, if the Higgs boson is discovered, the measurement of the $H \rightarrow \tau^+\tau^-$ decay rate provides a test of the SM prediction for the τ Yukawa coupling.

The process with the largest cross section to produce a SM Higgs boson at the LHC is gluon fusion $gg \rightarrow H$. However, Higgs boson production via vector boson (WW, ZZ) fusion $qq \rightarrow qqH$ (VBF) and via Higgs-strahlung $qq \rightarrow VH$, in association with a hadronically decaying vector boson ($V = W$ or Z), are highly relevant as well because they lead to additional jets in the final state, which provide distinct experimental signatures. In particular the VBF topology of two high-energy jets with a large rapidity separation offers a good discrimination against background processes. For all production processes above, the Higgs boson is typically more boosted in the transverse plane if there are additional high- p_T jets in the event, which increases the transverse momentum of the τ decay products and thus facilitates the measurement of the $\tau^+\tau^-$ invariant mass and the discrimination of the signal from background processes.

This paper presents SM Higgs boson searches in the the $H \rightarrow \tau_{\text{lep}}^+\tau_{\text{lep}}^-$, $H \rightarrow \tau_{\text{lep}}^+\tau_{\text{had}}^-$, and $H \rightarrow \tau_{\text{had}}^+\tau_{\text{had}}^-$ channels,¹ where τ_{lep} and τ_{had} denote leptonically and hadronically decaying τ leptons, respectively. The data analyses use proton-proton (pp) collisions at $\sqrt{s} = 7 \text{ TeV}$ collected by the ATLAS experiment in 2011, which correspond to an integrated luminosity of 4.7 fb^{-1} . In order to enhance the sensitivity of the search, the selected events are analysed in several separate categories according to the number and topology of reconstructed jets.

2 Data and Monte Carlo simulated samples

The ATLAS detector is a multipurpose apparatus with a forward-backward symmetric cylindrical geometry and nearly 4π coverage in solid angle [12]. It consists of an inner tracking detector surrounded by a thin superconducting solenoid, electromagnetic and hadronic calorimeters, and an external muon spectrometer incorporating three large superconducting air-core toroid magnets. Electrons, muons, τ leptons and jets can be reconstructed and identified in the ATLAS detector.² Only data taken with all sub-systems relevant to this analysis

¹ Charge-conjugated decay modes are implied. Throughout the remainder of the paper, a simplified notation without the particle charges is used.

² ATLAS uses a right-handed coordinate system with its origin at the nominal interaction point (IP) in the centre of the detector and the z -axis along the beam pipe. The x -axis points from the IP to the centre of the LHC ring, and the y -axis points upwards. Cylindrical coordinates (r, ϕ) are used in the transverse plane,

operational are used. This results in an integrated luminosity of 4.7 fb^{-1} for the full 2011 data sample.

The signal contributions considered here include the gluon fusion production process, the VBF production process, and the Higgs-strahlung VH production in association with a hadronically-decaying vector boson $V = W, Z$. For the decay of the Higgs boson, the $H \rightarrow \tau\tau$ mode is considered. Next-to-next-to-leading-order (NNLO) Quantum Chromodynamics (QCD) corrections, soft-gluon resummations calculated in the next-to-next-to-leading-log-approximation and next-to-leading-order (NLO) electroweak (EW) corrections are applied to the signal cross sections for the $gg \rightarrow H$ production process [13–24]. The cross sections of the VBF process are calculated with full NLO QCD and electroweak corrections [25–27], and approximate NNLO QCD corrections [28]. The WH/ZH processes are calculated with NNLO QCD corrections [29, 30] and NLO EW radiative corrections are applied [31]. The Higgs boson decay branching ratios are calculated using HDECAY [32]. The $gg \rightarrow H$ and VBF processes are modelled using the POWHEG [33, 34] Monte Carlo (MC) generator, interfaced to PYTHIA [35] for showering and hadronisation. In the $gg \rightarrow H$ process, the Higgs boson p_T spectrum is reweighted to agree with the prediction of the HqT program [36]. The associated VH production process is modelled using PYTHIA.

ALPGEN [37], interfaced to HERWIG [38], with the MLM matching scheme [39] is used to model the production of single W and Z/γ^* bosons decaying to charged leptons in association with jets. MC@NLO [40] is used to model $t\bar{t}$, WW , WZ and ZZ production processes, using HERWIG for the parton shower and hadronisation and JIMMY [41] for the underlying event modelling. AcerMC [42] is used to model single top-quark production for all three production channels (s -channel, t -channel, and Wt production).

The TAUOLA [43] and PHOTOS [44] programs are used to model the decay of τ leptons and the Quantum Electrodynamics (QED) radiation of photons, respectively.

The set of parton distribution functions (PDF) CT10 [45] is used for the MC@NLO samples, as well as CTEQ6L1 [46] for the ALPGEN samples, and MRST2007 [47] for the PYTHIA and HERWIG samples. Acceptances and efficiencies are based on a simulation of the ATLAS detector using GEANT4 [48, 49]. Since the data are affected by the detector response to multiple interactions (pileup) occurring in the same or nearby bunch crossings, the simulation includes a treatment of the event pileup conditions present in the 2011 data.

The $Z/\gamma^* \rightarrow \tau\tau$ background processes are modelled with a τ -embedded $Z/\gamma^* \rightarrow \mu\mu$ data sample as described in Section 6.

3 Selection and reconstruction of physics objects

Electron candidates are formed from an energy deposit in the electromagnetic calorimeter and associated to a track measured in the inner detector. They are selected if they have a transverse energy $E_T > 15 \text{ GeV}$, lie within $|\eta| < 2.47$ but outside the transition region between

ϕ being the azimuthal angle around the beam pipe. The pseudorapidity is defined in terms of the polar angle θ as $\eta = -\ln \tan(\theta/2)$.

the barrel and end-cap calorimeters ($1.37 < |\eta| < 1.52$), and meet quality requirements based on the expected shower shape [50].

Muon candidates are formed from a track measured in the inner detector and linked to a track in the muon spectrometer [51]. They are required to have a transverse momentum $p_T > 10$ GeV and to lie within $|\eta| < 2.5$. Additionally, the difference between the z -position of the point of closest approach of the muon inner detector track to the beam-line and the z -coordinate of the primary vertex is required to be less than 1 cm.³ This requirement reduces the contamination due to cosmic ray muons and beam-induced backgrounds. Muon quality criteria based on, e.g., inner detector hit requirements are applied in order to achieve a precise measurement of the muon momentum and reduce the misidentification rate.

Identified electrons and muons are required to be isolated: the additional transverse energy in the electromagnetic and hadronic calorimeters must be less than 8% (4%) of the electron transverse energy (muon transverse momentum) in a cone of radius $\Delta R = \sqrt{(\Delta\eta)^2 + (\Delta\phi)^2} = 0.2$ around the electron (muon) direction. The sum of the transverse momenta of all tracks with p_T above 1 GeV located within a cone of radius $\Delta R = 0.4$ around the electron (muon) direction and originating from the same primary vertex must be less than 6% of the electron transverse energy (muon transverse momentum).

Jets are reconstructed using the anti- k_t algorithm [52] with a distance parameter value of $R = 0.4$, taking as input three-dimensional noise-suppressed clusters in the calorimeters. Reconstructed jets with $p_T > 20$ GeV and within $|\eta| < 4.5$ are selected. Events are discarded if a jet is associated with out-of-time activity or calorimeter noise. After having associated tracks to jets by requiring $\Delta R < 0.4$ between tracks and the jet direction, a jet-vertex fraction (JVF) is computed for each jet as the scalar p_T sum of all associated tracks from the primary vertex divided by the scalar p_T sum of all tracks associated with the jet. Conventionally, $\text{JVF} = -1$ is assigned to jets with no associated tracks. Jets with $|\eta| < 2.4$ are required to have $|\text{JVF}| > 0.75$ in order to suppress pileup contributions. In the pseudorapidity range $|\eta| < 2.5$, b -jets are identified using a tagging algorithm based on the discrimination power of the impact parameter information and of the reconstruction of the displaced vertices of the hadron decays inside the jets [53]. The b -tagging algorithm has an average efficiency of 58% for b -jets in $t\bar{t}$ events [54]. The corresponding light-quark jet misidentification probability is 0.1–0.5%, depending on the jet p_T and η [55].

Hadronic decays of τ leptons are characterised by the presence of one or three charged hadrons accompanied by a neutrino and possibly neutral hadrons, which results in a collimated shower profile in the calorimeters and only a few nearby tracks. The visible decay products are combined into τ_{had} candidates. These candidates are reconstructed as jets, which are recalibrated to account for the different calorimeter response to hadronic decays as compared to hadronic jets. The four-momentum of the τ_{had} candidates are reconstructed from the energy deposits in the calorimeters and the rejection of jets misidentified as hadronic τ decays is performed by a multivariate discriminator based on a boosted decision tree [56] that uses

³The primary vertex is defined as the vertex with the largest $\sum p_T^2$ of the associated tracks.

both tracking and calorimeter information. The identification is optimised to be 50% efficient while the jet misidentification probability is kept below 1%. A τ_{had} candidate must lie within $|\eta| < 2.5$, have a transverse momentum greater than 20 GeV, one or three associated tracks (with $p_{\text{T}} > 1$ GeV) and a total charge of ± 1 computed from the associated tracks. Dedicated electron and muon veto algorithms are used.

When different objects selected according to the above criteria overlap with each other geometrically (within $\Delta R < 0.2$), only one of them is considered for further analysis. The overlap is resolved by selecting muon, electron, τ_{had} and jet candidates in this order of priority.

The magnitude of the missing transverse momentum [57] ($E_{\text{T}}^{\text{miss}}$) is reconstructed including contributions from muon tracks and energy deposits in the calorimeters. Calorimeter cells belonging to three-dimensional noise-suppressed clusters are used and they are calibrated taking into account the reconstructed physics object to which they belong.

4 Preselection

An initial selection of events is performed by requiring a vertex from the primary pp collisions that is consistent with the beam spot position, with at least three associated tracks, each with $p_{\text{T}} > 500$ MeV. Overall quality criteria are applied to suppress events with fake $E_{\text{T}}^{\text{miss}}$, produced by non-collision activity such as cosmic ray muons, beam-related backgrounds, or noise in the calorimeters.

The $\ell\ell$, $\ell\tau_{\text{had}}$ and $\tau_{\text{had}}\tau_{\text{had}}$ final states.⁴ considered in this search are defined in a mutually exclusive way: a requirement of exactly two, one, or zero electrons or muons is imposed, respectively.

4.1 $H \rightarrow \tau_{\text{lep}}\tau_{\text{lep}}$

Signal events in this channel are selected by requiring exactly two isolated and oppositely-charged light leptons (electrons and/or muons). Single lepton and di-lepton triggers are used to preselect the data. The trigger object quality requirements were tightened during the data-taking period to cope with increasing instantaneous luminosity. The single muon trigger requires $p_{\text{T}} > 18$ GeV; for the single electron trigger the E_{T} threshold changes from 20 GeV to 22 GeV depending on the LHC instantaneous luminosity; the di-muon trigger requires $p_{\text{T}} > 15$ GeV for the leading muon and $p_{\text{T}} > 10$ GeV for the sub-leading muon; the di-electron trigger requires $E_{\text{T}} > 12$ GeV for each of the two electrons; the $e\mu$ trigger requires $E_{\text{T}} > 10$ GeV for the electron and $p_{\text{T}} > 6$ GeV for the muon. In addition to the trigger requirements, the preselection requires $E_{\text{T}} > 22$ GeV if the electron satisfies only the single electron trigger. The E_{T} requirement is increased to 24 GeV when the trigger threshold is 22 GeV. If a muon is associated only with the single muon trigger object, it is required to have $p_{\text{T}} > 20$ GeV. For the $e\mu$ channel the di-lepton invariant mass is required to be in the range of $30 \text{ GeV} < m_{\ell\ell} < 100 \text{ GeV}$, whereas for the ee and $\mu\mu$ channels $30 \text{ GeV} < m_{\ell\ell} < 75 \text{ GeV}$ is required, reducing the contamination from $Z/\gamma^* \rightarrow \ell\ell$.

⁴Here ℓ denotes an electron or a muon (also referred to below as light leptons).

4.2 $H \rightarrow \tau_{\text{lep}}\tau_{\text{had}}$

Signal events in this channel are characterised by exactly one isolated light lepton ℓ , a τ_{had} candidate, and large $E_{\text{T}}^{\text{miss}}$ due to the undetected neutrinos. For the $e\tau_{\text{had}}$ ($\mu\tau_{\text{had}}$) final states, events are preselected using the single electron (muon) trigger described in Section 4.1. Exactly one electron with $E_{\text{T}} > 25$ GeV or one muon with $p_{\text{T}} > 20$ GeV, and one oppositely-charged τ_{had} candidate with $p_{\text{T}} > 20$ GeV are required in the event. Events with more than one electron or muon candidate are rejected to suppress events from $Z/\gamma^* \rightarrow \ell^+\ell^-$ decays and from $t\bar{t}$ or single top-quark production.⁵ The transverse mass of the lepton and $E_{\text{T}}^{\text{miss}}$ is calculated as

$$m_{\text{T}} = \sqrt{2p_{\text{T}}^{\ell}E_{\text{T}}^{\text{miss}}(1 - \cos \Delta\phi)}, \quad (4.1)$$

where p_{T}^{ℓ} denotes the magnitude of the transverse momentum of the lepton and $\Delta\phi$ is the angle between the lepton and $E_{\text{T}}^{\text{miss}}$ directions in the plane perpendicular to the beam direction. In order to reduce contributions from the W +jets and $t\bar{t}$ background processes, only events with $m_{\text{T}} < 30$ GeV are considered for further analysis. In addition, $E_{\text{T}}^{\text{miss}}$ is used for further event selection and categorisation, as described in Section 5.

4.3 $H \rightarrow \tau_{\text{had}}\tau_{\text{had}}$

Signal events in this channel are characterised by two identified hadronic τ decays and large $E_{\text{T}}^{\text{miss}}$ from the undetected neutrinos. The corresponding event selection starts with a double hadronic τ trigger, where the p_{T} thresholds are 29 GeV and 20 GeV for the leading and sub-leading hadronic τ objects, respectively. A requirement of exactly zero charged light leptons, as defined in Section 3, is imposed. Two identified opposite charge τ_{had} candidates with $p_{\text{T}} > 35$ GeV and $p_{\text{T}} > 25$ GeV are required, each matching a τ trigger object [58].

5 Analysis categories

For further analysis, the selected event samples are split into several categories according to the number and topology of reconstructed jets. The sensitivity of the search is usually higher for categories where the presence of one or more jets is required, as discussed in Section 1, but events without any reconstructed high- p_{T} jets are also considered in order to maximise the sensitivity.

5.1 $H \rightarrow \tau_{\text{lep}}\tau_{\text{lep}}$

Four categories defined by their jet multiplicity and kinematics are used for this channel: H +2-jet VBF, H +2-jet VH , H +1-jet and H +0-jet. The first two categories require the presence of at least two jets and the cuts are optimised in one case for the VBF process [59–61], and in the other for the VH and $gg \rightarrow H$ processes [62].

⁵For the purpose of vetoing additional light leptons, the isolation requirements are removed from the muon selection and a looser identification requirement is used for electrons. The transverse momentum (energy) threshold for muons (electrons) is lowered to 10 GeV (15 GeV).

The $H + 0$ -jet category uses an inclusive selection to collect part of the signal not selected by the categories with jets. In the $H + 0$ -jet category, only the $e\mu$ final state is considered because of the overwhelming $Z/\gamma^* \rightarrow \ell\ell$ background in the ee and $\mu\mu$ final states. In order to suppress the $t\bar{t}$ background, it is required that the di-lepton azimuthal opening angle be $\Delta\phi_{\ell\ell} > 2.5$ rad and that the leptonic transverse energy be $H_T^{\text{lep}} = p_T^{\ell 1} + p_T^{\ell 2} + E_T^{\text{miss}} < 120$ GeV, where $p_T^{\ell 1}$ and $p_T^{\ell 2}$ are the magnitudes of the transverse momenta of the leading and sub-leading leptons, respectively.

In categories with jets ($H + 2$ -jet VBF, $H + 2$ -jet VH and $H + 1$ -jet), the presence of a hadronic jet with a transverse momentum $p_T > 40$ GeV is required and, to suppress the $t\bar{t}$ background, the event is rejected if any jet with $p_T > 25$ GeV is identified as a b -jet. In addition, $E_T^{\text{miss}} > 40$ GeV ($E_T^{\text{miss}} > 20$ GeV) for the $ee, \mu\mu$ ($e\mu$) channels is also required.

The collinear approximation technique [63] is used to reconstruct the kinematics of the $\tau\tau$ system. The approximation is based on two assumptions: that the neutrinos from each τ decay are nearly collinear with the corresponding visible τ decay products and that the E_T^{miss} in the event is due only to neutrinos. In this case, the total invisible momentum carried away by neutrinos in each τ decay can be estimated from the polar and azimuthal angles of the visible products of each τ decay. Then, the invariant mass of the $\tau\tau$ system can be calculated as $m_{\tau\tau} = m_{\ell\ell}/\sqrt{x_1 \cdot x_2}$, where x_1 and x_2 are the momentum fractions of the two τ candidates carried away by their visible decay products. Events that do not satisfy $0.1 < x_1, x_2 < 1.0$ are rejected. In categories with jets, there is an additional requirement that $0.5 \text{ rad} < \Delta\phi_{\ell\ell} < 2.5 \text{ rad}$ to suppress the $Z/\gamma^* \rightarrow \ell\ell$ background.

For the $H + 2$ -jet categories, a subleading jet with $p_T > 25$ GeV is required in addition. For the $H + 2$ -jet VBF category, a pseudorapidity difference between the two selected jets of $\Delta\eta_{jj} > 3$ and a di-jet invariant mass of $m_{jj} > 350$ GeV are required. Finally, the event is rejected in the $H + 2$ -jet VBF category if any additional jet with $p_T > 25$ GeV and $|\eta| < 2.4$ is found in the pseudorapidity range between the two leading jets.

For the $H + 2$ -jet VH category, the requirement on the pseudorapidity separation of the jets and on the di-jet invariant mass are instead: $\Delta\eta_{jj} < 2$ and $50 \text{ GeV} < m_{jj} < 120 \text{ GeV}$.

Only events failing the cuts for the $H + 2$ -jet categories are considered in the $H + 1$ -jet category. For the $H + 1$ -jet category, the invariant mass of the two τ leptons and the leading jet is required to fulfil $m_{\tau\tau j} > 225$ GeV, where the τ momenta are taken from the collinear approximation. The main Higgs production mechanism in this category is the $gg \rightarrow H$ process plus a high- p_T parton.

The $m_{\tau\tau}$ calculated with the collinear approximation (“collinear mass”) is used in categories with jets. Because this variable displays poor resolution in the $H + 0$ -jet category due to the back-to-back configuration of the two leptons, the effective mass ($m_{\tau\tau}^{\text{eff}}$), defined as the invariant mass of the two leptons and the E_T^{miss} , is used instead.

5.2 $H \rightarrow \tau_{\text{lep}}\tau_{\text{had}}$

The selected data are split into seven categories based on jet properties and E_T^{miss} .

The $H+2$ -jet VBF category includes all selected events with $E_T^{\text{miss}} > 20$ GeV and at least two jets with $p_T > 25$ GeV, where the two leading jets are found in opposite hemispheres of the detector ($\eta_{jet1} \cdot \eta_{jet2} < 0$), with $\Delta\eta_{jj} > 3$ and $m_{jj} > 300$ GeV. Both the lepton and the τ_{had} candidate are required to be found in the pseudorapidity range between the two leading jets. Due to the limited size of the selected event samples, the VBF category combines the $e\tau_{\text{had}}$ and $\mu\tau_{\text{had}}$ final states.

Two $H+1$ -jet categories include all selected events with $E_T^{\text{miss}} > 20$ GeV and at least one jet with $p_T > 25$ GeV, that fail the VBF selection. The $e\tau_{\text{had}}$ and $\mu\tau_{\text{had}}$ final states are considered separately.

Four $H+0$ -jet categories include all selected events without any jet with $p_T > 25$ GeV. The $e\tau_{\text{had}}$ and $\mu\tau_{\text{had}}$ final states are considered separately. In addition, the analysis is separated into events with $E_T^{\text{miss}} > 20$ GeV and $E_T^{\text{miss}} < 20$ GeV. The low- E_T^{miss} region is included here because, in the absence of high- p_T jets, the Higgs decay products, including the neutrinos, are typically less boosted than for events with additional jet activity.

For each category, the mass of the $\tau\tau$ system is reconstructed using the Missing Mass Calculator (MMC) [64]. This technique provides a full reconstruction of event kinematics in the $\tau\tau$ final state with 99% efficiency and 13–20% resolution in $m_{\tau\tau}$, depending on the event topology (better resolution is obtained for events with high- p_T jets). Conceptually, the MMC is a more sophisticated version of the collinear approximation. The main improvement comes from requiring that relative orientations of the neutrinos and other decay products are consistent with the mass and kinematics of a τ lepton decay. This is achieved by maximising a probability defined in the kinematically allowed phase space region.

5.3 $H \rightarrow \tau_{\text{had}}\tau_{\text{had}}$

In the $H \rightarrow \tau_{\text{had}}\tau_{\text{had}}$ channel, only a single $H+1$ -jet category is defined. After selecting two hadronic τ candidates, the collinear mass approximation cuts $0 < x_1, x_2 < 1$ are applied. Events at this stage are used as a control sample to derive the normalisation of the $Z/\gamma^* \rightarrow \tau\tau$ background. Then, events are selected if $E_T^{\text{miss}} > 20$ GeV and if the leading jet has a transverse momentum $p_T > 40$ GeV. The two τ candidates are required to be separated by $\Delta R(\tau, \tau) < 2.2$. Also, only events with an invariant mass of the $\tau\tau$ pair and the leading jet $m_{\tau\tau j} > 225$ GeV are considered for further analysis. The event selection criteria described here are effective against the multi-jet and $Z/\gamma^* \rightarrow \tau\tau$ backgrounds. The collinear mass approximation is used for the Higgs mass reconstruction.

6 Background estimation and modelling

The background composition and normalisation are determined using data-driven methods and the simulated event samples described in Section 2.

The main background to the Higgs boson signal in all selected final states is the largely irreducible $Z/\gamma^* \rightarrow \tau\tau$ process. While it is not possible to select a Higgs signal-free $Z/\gamma^* \rightarrow \tau\tau$ sample directly from the data, this background is still modelled in a data-driven way, by

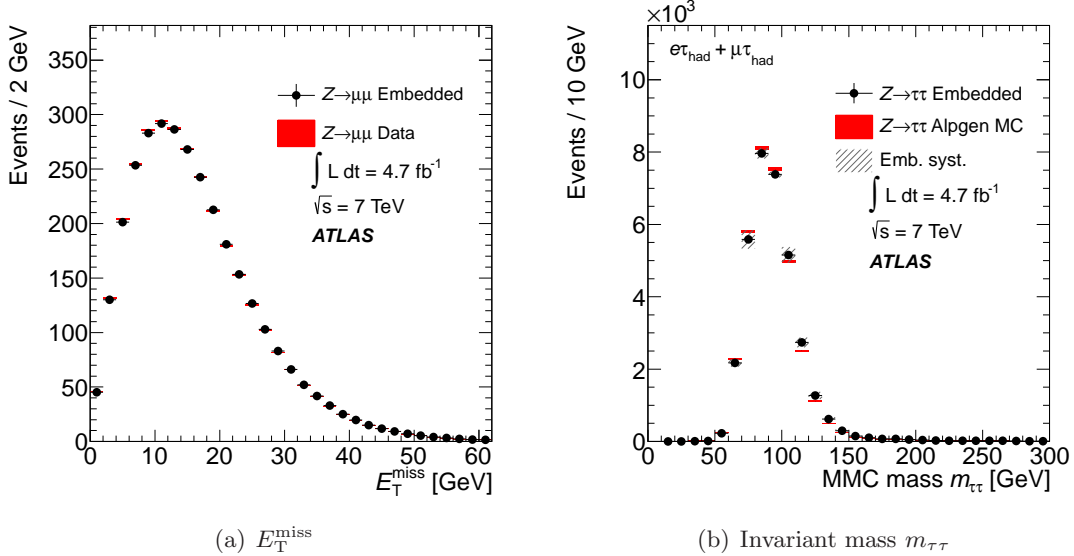


Figure 1. (a) E_T^{miss} distributions for the $Z/\gamma^* \rightarrow \mu\mu$ data before and after muon embedding and (b) MMC mass distributions (defined in Section 5) for the τ -embedded $Z/\gamma^* \rightarrow \mu\mu$ data and simulated $Z/\gamma^* \rightarrow \tau\tau$ events. For (a) only statistical uncertainties are shown; (b) also includes systematic uncertainties associated with the embedding procedure as discussed in Section 7.

choosing a control sample where the expected signal contamination is negligible. In a sample of selected $Z/\gamma^* \rightarrow \mu\mu$ data events, the muon tracks and associated calorimeter cells are replaced by τ leptons from a simulated $Z/\gamma^* \rightarrow \tau\tau$ decay with the same kinematics, where the τ polarisation and spin correlations are modelled with the TAUOLA program and the τ - μ mass difference is taken into account as well. Thus, only the τ decays and the corresponding detector response are taken from the simulation, whereas the underlying event kinematics and all other properties—including pileup effects—are obtained from the data. These embedded data are used to model the shape of the relevant $Z/\gamma^* \rightarrow \tau\tau$ background distributions as well as the efficiency for selecting $Z/\gamma^* \rightarrow \tau\tau$ events from the preselected sample. The overall normalisation at the preselection level is obtained from simulation.

The procedure is extensively validated: example results for the $H \rightarrow \tau_{\text{lep}}\tau_{\text{had}}$ channel are shown in Figure 1. Systematic effects intrinsic to the method are studied by replacing the muons selected in data by simulated muons instead of τ decays. Figure 1(a) shows a comparison of the E_T^{miss} distributions from the selected $Z/\gamma^* \rightarrow \mu\mu$ events in data before and after this muon embedding, demonstrating that the embedding procedure does not introduce any significant bias to the reconstruction of the event properties. Figure 1(b) compares the MMC mass distributions reconstructed from the τ -embedded $Z/\gamma^* \rightarrow \mu\mu$ data and simulated $Z/\gamma^* \rightarrow \tau\tau$ events after the preselection described in Section 4; good agreement is found and similar studies for the other channels yield the same conclusions.

6.1 $H \rightarrow \tau_{\text{lep}} \tau_{\text{lep}}$

The $Z/\gamma^* \rightarrow \tau\tau$ background is modelled using the embedding procedure described above. The contribution from $Z/\gamma^* \rightarrow \ell^+\ell^-$ is determined by scaling the yields in the Monte Carlo simulation using correction factors obtained by comparing data to simulation in low- and high- $E_{\text{T}}^{\text{miss}}$ control regions enriched in these backgrounds. The correction factors are obtained separately for $Z/\gamma^* \rightarrow ee$ and $Z/\gamma^* \rightarrow \mu\mu$ and for the different analysis categories and are on the order of 10%.

The fake lepton background consists of events that have a reconstructed lepton that did not originate from the decay of a τ lepton or the leptonic decay of a W or Z boson. The normalisation and shape of relevant distributions are obtained from data with a template method using a control region in which the lepton isolation requirement is reversed. The chosen template shape is the p_{T} distribution of the sub-leading lepton. For this method to be applied, it is first verified that the template shapes of the fake lepton distribution in the control and signal regions agree within uncertainties. This is performed at intermediate steps of the event selection where the data sample is dominated by background events and where the number of expected signal events is negligible.

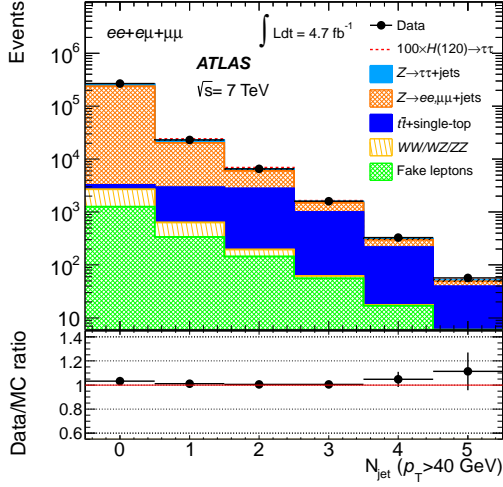
After subtracting the simulated backgrounds, the template shape in a given distribution is obtained from the control region, while the normalisation is obtained from a fit of the distribution of the events in the signal region with the template shape. The uncertainty related to the estimation of backgrounds with fake leptons is calculated from the uncertainty on the subtraction of other processes from Monte Carlo simulation and from the difference in the p_{T} shape of the events in the control region and signal regions. Such systematic uncertainties lie in the range of 30–40%.

The contributions of the $t\bar{t}$, single top-quark and electroweak di-boson backgrounds are estimated from simulation. The Monte Carlo description of the top-quark backgrounds has been validated using data by selecting control regions enriched in top-quark background processes. The control regions are defined by inverting the b -jet selection for the $H + 2$ -jet VBF, $H + 2$ -jet VH , $H + 1$ -jet categories and by inverting the $H_{\text{T}}^{\text{lep}}$ selection for the $H + 0$ -jet category.

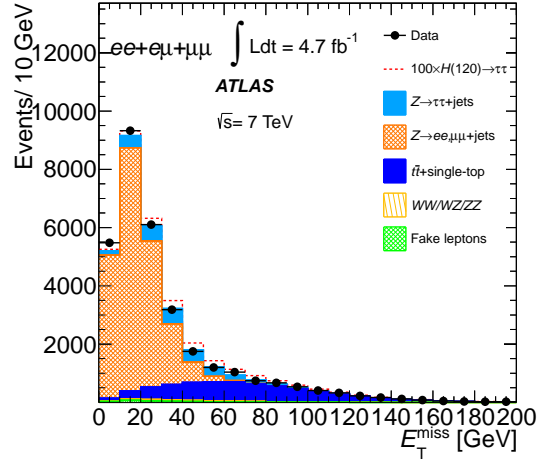
Table 1 displays the number of events expected and observed in the four categories after all selection criteria including all systematic uncertainties described in Section 7. The estimated combined background contributions are found to give a good description of all quantities relevant to the analysis. As examples, the distributions of the jet multiplicity, $E_{\text{T}}^{\text{miss}}$, the invariant mass of the two leading jets and their pseudorapidity difference are shown in Figure 2. Figure 3 displays the invariant mass spectra of the selected events for the four categories.

Table 1. Number of events after the $H \rightarrow \tau_{\text{lep}}\tau_{\text{lep}}$ selection for the four categories in data and predicted number of background events, for an integrated luminosity of 4.7 fb^{-1} . Expectations for the Higgs boson signal ($m_H = 120 \text{ GeV}$) are also given. Statistical and systematic uncertainties are quoted, in that order.

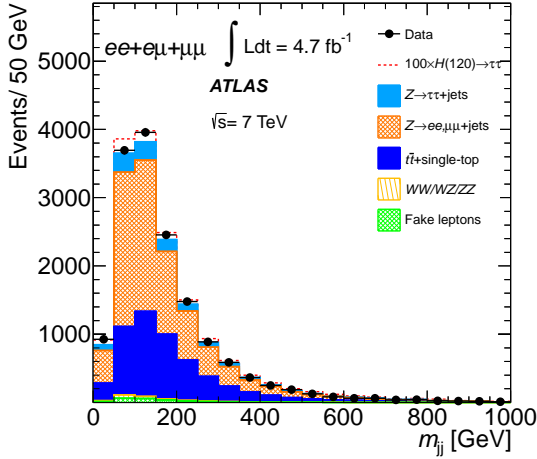
	$ee + \mu\mu + e\mu$ $H + 2\text{-jet VBF}$	$ee + \mu\mu + e\mu$ $H + 2\text{-jet VH}$	$ee + \mu\mu + e\mu$ $H + 1\text{-jet}$	$e\mu$ $H + 0\text{-jet}$
$gg \rightarrow H$ signal	$0.26 \pm 0.06 \pm 0.10$	$0.8 \pm 0.1 \pm 0.2$	$3.9 \pm 0.2 \pm 1.0$	$23 \pm 1 \pm 3$
VBF H signal	$1.08 \pm 0.03 \pm 0.11$	$0.10 \pm 0.01 \pm 0.01$	$1.15 \pm 0.03 \pm 0.01$	$0.75 \pm 0.03 \pm 0.06$
VH signal	$0.01 \pm 0.01 \pm 0.01$	$0.53 \pm 0.02 \pm 0.07$	$0.40 \pm 0.02 \pm 0.03$	$0.52 \pm 0.02 \pm 0.04$
$Z/\gamma^* \rightarrow \tau^+\tau^-$	$24 \pm 3 \pm 2$	$107 \pm 12 \pm 9$	$(0.52 \pm 0.01 \pm 0.04) \cdot 10^3$	$(9.68 \pm 0.05 \pm 0.07) \cdot 10^3$
$Z/\gamma^* \rightarrow \ell^+\ell^-$ ($\ell=e,\mu$)	$2 \pm 1 \pm 1$	$25 \pm 4 \pm 9$	$83 \pm 10 \pm 30$	$185 \pm 11 \pm 14$
$t\bar{t}$ +single top	$7 \pm 1 \pm 2$	$42 \pm 2 \pm 6$	$98 \pm 3 \pm 12$	$169 \pm 4 \pm 14$
$WW/WZ/ZZ$	$0.9 \pm 0.3 \pm 0.3$	$6 \pm 1 \pm 1$	$21 \pm 1 \pm 3$	$221 \pm 3 \pm 18$
Fake leptons	$1.3 \pm 0.8 \pm 0.6$	$13 \pm 2 \pm 5$	$30 \pm 4 \pm 12$	$(1.2 \pm 0.5) \cdot 10^3$
Total background	$35 \pm 3 \pm 4$	$193 \pm 7 \pm 20$	$(0.75 \pm 0.01 \pm 0.05) \cdot 10^3$	$(11.4 \pm 0.5) \cdot 10^3$
Observed data	27	185	702	11420



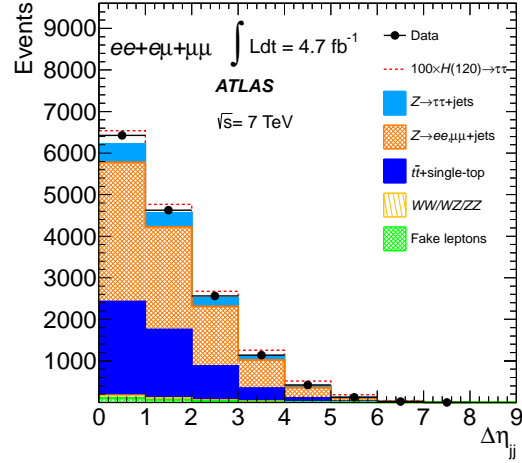
(a) Jet multiplicity ($p_T > 40$ GeV)



(b) E_T^{miss}



(c) Invariant mass of the two leading jets



(d) η difference of the two leading jets

Figure 2. Distributions of (a) the jet multiplicity, (b) the E_T^{miss} , (c) the invariant mass of the two leading jets and (d) the η difference of the two leading jets in the $H \rightarrow \tau_{\text{lep}}\tau_{\text{lep}}$ channel for the selection criteria described in the text. Simulated samples are normalised to an integrated luminosity of 4.7 fb^{-1} . For illustration only, the signal contributions have been scaled by factors given in the legends. $30 \text{ GeV} < m_{\ell\ell} < 100 \text{ GeV}$ is required for the ee and $\mu\mu$ channels and $30 \text{ GeV} < m_{\ell\ell} < 75 \text{ GeV}$ for the $e\mu$ channel. For the E_T^{miss} distribution the presence of a leading jet with $p_T > 40 \text{ GeV}$ is required; for the invariant mass and for the η difference of the two leading jets, the presence of a sub-leading jet with $p_T > 25 \text{ GeV}$ is required in addition.

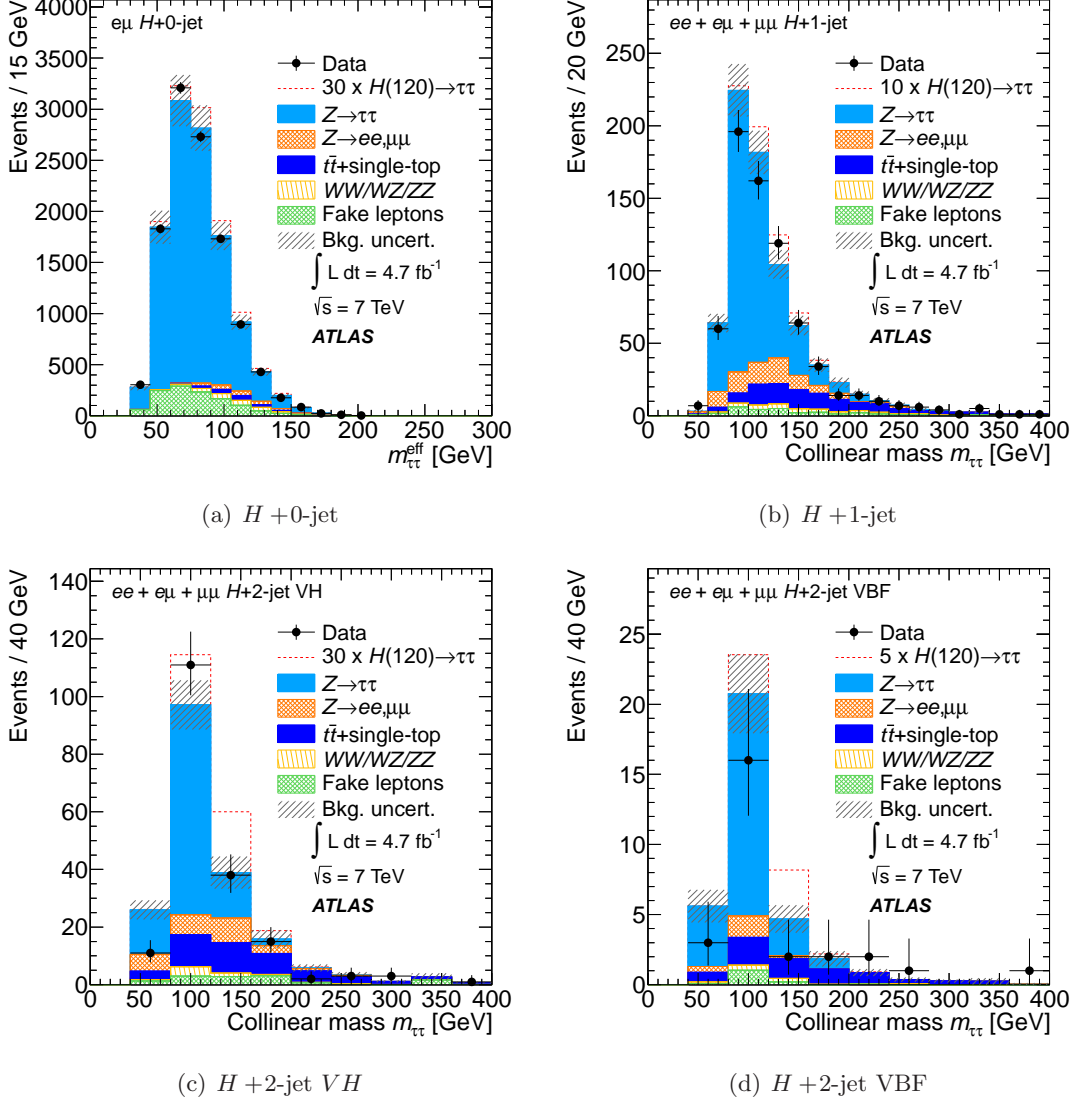


Figure 3. Reconstructed $m_{\tau\tau}$ of the selected events in the $H \rightarrow \pi_{ep}\pi_{ep}$ channel for the four categories described in the text. Simulated samples are normalised to an integrated luminosity of 4.7fb^{-1} . Predictions from the Higgs boson signal ($m_H = 120\text{ GeV}$) and from backgrounds are given. In the case of the $H + 0\text{-jet}$ category $m_{\tau\tau}^{\text{eff}}$ is used. For illustration only, the signal contributions have been scaled by factors given in the legends.

6.2 $H \rightarrow \tau_{\text{lep}}\tau_{\text{had}}$

In order to estimate the background contributions to the selected $H \rightarrow \tau_{\text{lep}}\tau_{\text{had}}$ candidate events, a control sample in data is obtained by applying the signal selection described in Section 5.2 but now requiring that the light lepton and the τ_{had} candidate have the same charge. This control sample is referred to as the same-sign (SS) sample here, in contrast to the opposite-sign (OS) signal sample. The number of OS background events in the signal region ($n_{\text{OS}}^{\text{bkg}}$) can be expressed as

$$n_{\text{OS}}^{\text{bkg}} = n_{\text{SS}}^{\text{all}} + n_{\text{OS-SS}}^{W+\text{jets}} + n_{\text{OS-SS}}^{Z/\gamma^* \rightarrow \tau\tau} + n_{\text{OS-SS}}^{\text{other}}, \quad (6.1)$$

where $n_{\text{SS}}^{\text{all}}$ is the sum of all SS backgrounds in the signal region and the remaining terms are the differences between the number of OS and SS events for $W + \text{jets}$, $Z/\gamma^* \rightarrow \tau\tau$ and other backgrounds, respectively. Due to their large production cross sections, multi-jet processes provide a significant background if quark/gluon jets are misidentified as hadronic τ decays. The ratio of OS to SS events for the multi-jet background ($r_{\text{OS/SS}}^{\text{QCD}}$) is expected to be close to unity and therefore $n_{\text{OS-SS}}^{\text{QCD}} = 0$ is assumed. This assumption is validated with a control sample that is dominated by low- p_{T} jets from multi-jet processes. This sample is selected by replacing the requirement $E_{\text{T}}^{\text{miss}} > 20$ GeV with $E_{\text{T}}^{\text{miss}} < 15$ GeV and removing the isolation criteria of the electron or muon candidate. After subtraction of the other backgrounds using simulation, a value of $r_{\text{OS/SS}}^{\text{QCD}} = 1.10 \pm 0.01(\text{stat.}) \pm 0.09(\text{syst.})$ is obtained. The observed deviation of $r_{\text{OS/SS}}^{\text{QCD}}$ from unity is taken into account as a systematic uncertainty for the final result.

The $Z/\gamma^* \rightarrow \tau\tau$ contribution is estimated from the τ -embedded $Z/\gamma^* \rightarrow \mu\mu$ sample in the data, as described previously. For the $W + \text{jets}$ background, a significant deviation of the ratio of OS and SS events ($r_{\text{OS/SS}}^W$) from unity is expected since $W + \text{jets}$ production is dominated by gu/gd -processes that often give rise to a jet originating from a quark, the charge of which is anti-correlated with the W boson charge. The predicted number of $W + \text{jets}$ background events is obtained from the simulation after applying a normalisation correction factor determined from W -dominated data control samples.⁶ The remaining contributions $n_{\text{OS-SS}}^{\text{other}}$ are taken from the simulation.

Table 2 displays the number of events expected and observed in the seven categories after the full signal selection, including all systematic uncertainties as described in Section 7. The estimated combined background contributions are found to give a good description of all quantities relevant to the analysis. As examples, the distributions of $E_{\text{T}}^{\text{miss}}$, the transverse mass of the lepton- $E_{\text{T}}^{\text{miss}}$ system as well as the invariant mass of the two leading jets and their pseudorapidity difference are shown in Figure 4. Figure 5 shows the corresponding $\tau\tau$ invariant mass spectra, where the electron and muon categories have been combined for illustration purposes. The data are found to be consistent with the estimated combined background contributions in both normalisation and shape within the uncertainties.

⁶ These control samples are defined by replacing the $m_{\text{T}} < 30$ GeV requirement in the nominal selection with $m_{\text{T}} > 50$ GeV.

Table 2. Predicted number of signal events (for $m_H = 120$ GeV) and predicted backgrounds obtained as described in the text, together with the observed number of events in data for the $H \rightarrow \tau_{\text{lep}}\tau_{\text{had}}$ categories. The total background yield predicted by the alternative estimation method is given as well for comparison. The listed uncertainties are statistical and systematic, in that order.

	$H + 0\text{-jet (low } E_T^{\text{miss}})$		$H + 0\text{-jet (high } E_T^{\text{miss}})$	
	Electron	Muon	Electron	Muon
ggH signal	11 \pm 1 \pm 2	17 \pm 1 \pm 4	7.1 \pm 0.8 \pm 1.5	9.8 \pm 0.9 \pm 2.1
VBF H signal	0.08 \pm 0.02 \pm 0.12	0.11 \pm 0.03 \pm 0.03	0.09 \pm 0.02 \pm 0.02	0.14 \pm 0.03 \pm 0.03
VH signal	0.07 \pm 0.02 \pm 0.05	0.10 \pm 0.03 \pm 0.01	0.08 \pm 0.02 \pm 0.01	0.08 \pm 0.02 \pm 0.01
$n_{\text{SS}}^{\text{all}}$	(3.3 \pm 0.2 \pm 0.7) $\cdot 10^3$	(2.0 \pm 0.1 \pm 0.4) $\cdot 10^3$	(0.69 \pm 0.06 \pm 0.14) $\cdot 10^3$	(0.47 \pm 0.04 \pm 0.09) $\cdot 10^3$
$n_{\text{OS-SS}}^{W+\text{jets}}$	(0.33 \pm 0.02 \pm 0.04) $\cdot 10^3$	(0.50 \pm 0.02 \pm 0.07) $\cdot 10^3$	(0.15 \pm 0.01 \pm 0.02) $\cdot 10^3$	(0.18 \pm 0.01 \pm 0.03) $\cdot 10^3$
$n_{\text{OS-SS}}^{Z \rightarrow \tau\tau}$	(3.70 \pm 0.06 \pm 0.61) $\cdot 10^3$	(7.29 \pm 0.06 \pm 1.21) $\cdot 10^3$	(1.49 \pm 0.04 \pm 0.23) $\cdot 10^3$	(2.80 \pm 0.04 \pm 0.42) $\cdot 10^3$
$n_{\text{OS-SS}}^{\text{other}}$	(0.97 \pm 0.04 \pm 0.22) $\cdot 10^3$	(0.59 \pm 0.04 \pm 0.14) $\cdot 10^3$	(0.27 \pm 0.02 \pm 0.08) $\cdot 10^3$	(0.14 \pm 0.02 \pm 0.04) $\cdot 10^3$
Total background	(8.2 \pm 0.2 \pm 0.8) $\cdot 10^3$	(10.4 \pm 0.2 \pm 1.2) $\cdot 10^3$	(2.59 \pm 0.07 \pm 0.26) $\cdot 10^3$	(3.59 \pm 0.06 \pm 0.43) $\cdot 10^3$
Observed data	8363	10911	2545	3570
Altern. estimate	(8.7 \pm 0.1 \pm 0.8) $\cdot 10^3$	(10.7 \pm 0.1 \pm 1.0) $\cdot 10^3$	(2.76 \pm 0.05 \pm 0.33) $\cdot 10^3$	(3.75 \pm 0.05 \pm 0.47) $\cdot 10^3$

	$H + 1\text{-jet}$		$H + 2\text{-jet VBF}$
	Electron	Muon	Electron + Muon
ggH signal	8.1 \pm 0.7 \pm 1.6	10.8 \pm 0.8 \pm 2.2	0.9 \pm 0.2 \pm 0.3
VBF H signal	1.6 \pm 0.1 \pm 0.1	1.9 \pm 0.1 \pm 0.1	2.2 \pm 0.1 \pm 0.2
VH signal	1.1 \pm 0.1 \pm 0.1	1.4 \pm 0.1 \pm 0.1	0.02 \pm 0.01 \pm 0.01
$n_{\text{SS}}^{\text{all}}$	(0.93 \pm 0.07 \pm 0.19) $\cdot 10^3$	(0.49 \pm 0.04 \pm 0.10) $\cdot 10^3$	45 \pm 7 \pm 9
$n_{\text{OS-SS}}^{W+\text{jets}}$	(0.25 \pm 0.01 \pm 0.03) $\cdot 10^3$	(0.26 \pm 0.01 \pm 0.03) $\cdot 10^3$	5 \pm 1 \pm 2
$n_{\text{OS-SS}}^{Z \rightarrow \tau\tau}$	(1.23 \pm 0.03 \pm 0.17) $\cdot 10^3$	(1.76 \pm 0.03 \pm 0.25) $\cdot 10^3$	54 \pm 6 \pm 8
$n_{\text{OS-SS}}^{\text{other}}$	(0.28 \pm 0.02 \pm 0.04) $\cdot 10^3$	(0.24 \pm 0.01 \pm 0.03) $\cdot 10^3$	20 \pm 3 \pm 5
Total background	(2.69 \pm 0.08 \pm 0.26) $\cdot 10^3$	(2.75 \pm 0.05 \pm 0.27) $\cdot 10^3$	124 \pm 10 \pm 13
Observed data	2610	2711	122
Altern. estimate	(2.63 \pm 0.05 \pm 0.25) $\cdot 10^3$	(2.72 \pm 0.04 \pm 0.28) $\cdot 10^3$	131 \pm 11 \pm 23

In order to validate these results, an alternative background estimation is performed. This second method provides an estimate of the multi-jet background using control samples that are defined by separately inverting the light-lepton isolation and the $\tau_{\text{had}}\text{-}\ell$ charge cor-

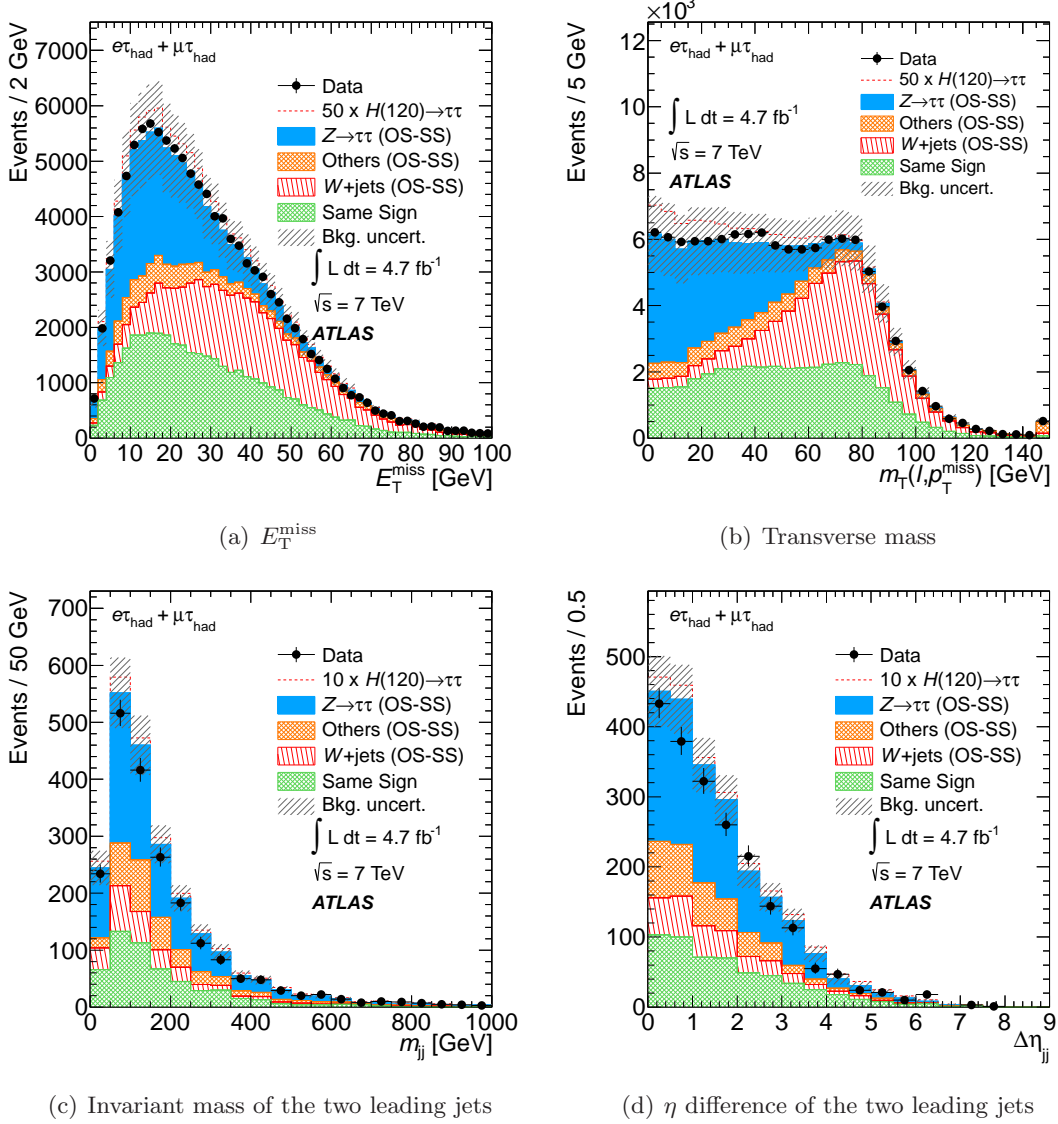


Figure 4. (a) Missing transverse momentum, (b) transverse mass of the lepton- E_T^{miss} system as well as (c) invariant mass and (d) pseudorapidity difference of the two leading jets in the $H \rightarrow \tau_{\text{lep}}\tau_{\text{had}}$ channel. The preselection criteria and an $E_T^{\text{miss}} > 20$ GeV requirement are applied except those for the displayed quantity; for (c) and (d) the presence of at least two jets with $p_T > 25$ GeV is required in addition. Simulated samples are normalised to an integrated luminosity of 4.7 fb^{-1} . The selected events in data are shown together with the predicted Higgs boson signal ($m_H = 120$ GeV) stacked above the background contributions (see text). For illustration only, the signal contributions have been scaled by factors given in the legends.

relation requirements, respectively. In addition to the signal region (A) this results in three background-dominated regions B (SS $l\tau_{\text{had}}$, l isolated), C (OS $l\tau_{\text{had}}$, l anti-isolated) and D (SS $l\tau_{\text{had}}$, l anti-isolated). The shape of the MMC mass distribution for multi-jet contributions in the signal region A is taken from the control region B and the normalisation is derived from the relation $n_A = n_C/n_D \times n_B$. Here, n_B , n_C and n_D denote the event yields in regions

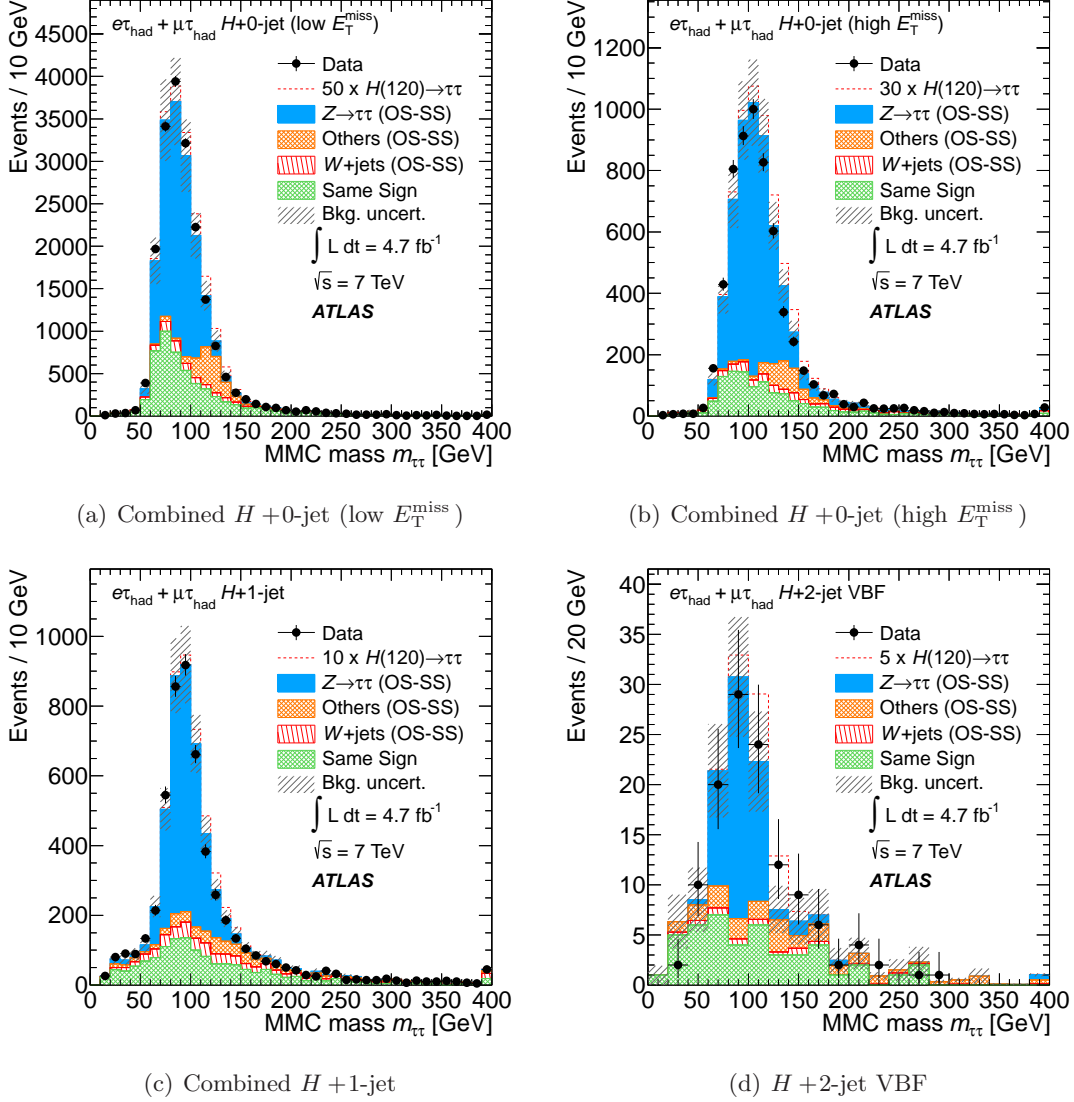


Figure 5. MMC mass (defined in Section 5) distributions of the selected events in the $H \rightarrow \pi_{\text{ep}}\tau_{\text{had}}$ channel. The corresponding electron and muon categories for the $H + 0$ -jet and $H + 1$ -jet categories are shown combined here, while in the data analysis they are considered separately. The selected events in data are shown together with the predicted Higgs boson signal ($m_H = 120$ GeV) stacked above the background contributions (see text). For illustration only, the signal contributions have been scaled by factors given in the legends.

B, C and D, after subtracting the contribution from non-multi-jet backgrounds in all control regions. The $Z/\gamma^* \rightarrow \tau\tau$ contribution is estimated from the τ -embedded $Z/\gamma^* \rightarrow \mu\mu$ data and the estimate of the $W + \text{jets}$ background is obtained from the simulation after applying normalisation correction factors determined from W -dominated (high- m_T) OS and SS data control samples. The remaining contributions are obtained from the simulation. The resulting total background estimates are also included in Table 2 and are found to be consistent with both the observed number of data events and the predictions of the default background estimate within the uncertainties.

Further studies of specific background contributions are performed by estimating the probability to misidentify jets as τ_{had} candidates in the signal region and using data control regions for the background from $t\bar{t}$ production processes. Results are consistent with the background estimates in Table 2 in both cases.

6.3 $H \rightarrow \tau_{\text{had}}\tau_{\text{had}}$

The dominant backgrounds in the $H \rightarrow \tau_{\text{had}}\tau_{\text{had}}$ channel are $Z/\gamma^* \rightarrow \tau\tau$ and multi-jet production. For both, the normalisation and shape of the mass distribution are estimated using data-driven methods.

The normalisation of the $Z/\gamma^* \rightarrow \tau\tau$ background is obtained by using collision data events at an early stage of the event selection. This data-driven control sample is defined by requiring that events contain two τ_{had} candidates that pass the hadronic selections including the collinear approximation cuts ($0 < x_{1,2} < 1$ and $\Delta R(\tau\tau) < 2.8$). To avoid signal contamination in this control sample, a requirement that $m_{\tau\tau} < 100$ GeV is applied; this results in a SM Higgs signal contamination of less than 0.2%. The $Z/\gamma^* \rightarrow \tau\tau$ contribution is obtained by fitting the track multiplicity of the two τ candidates simultaneously. The tracks associated to the τ_{had} candidates are counted in the cone defined by $\Delta R < 0.6$, as motivated by the momentum correlation between tracks in τ_{had} candidates [56]. A two-dimensional distribution of the track multiplicities for these two τ candidates is formed, and a track multiplicity fit is performed. The multi-jet template is modelled from the same-sign (SS) candidates in the data while the $Z/\gamma^* \rightarrow \tau\tau$ contribution is modelled by the simulation. The less significant backgrounds are estimated from the simulation and subtracted before the fit is performed. The result of the fit is used to normalise the τ -embedded $Z/\gamma^* \rightarrow \mu\mu$ sample described above, and then this sample is used to model the acceptance of the later cuts and the mass shape in the signal region.

The multi-jet contribution is estimated by the same two-dimensional track multiplicity fitting technique, where the fit is now performed in the signal region. The contribution from di- τ events is allowed to float in the fit, where the shape comes from the simulation. It is assumed that the shape of the two-dimensional track multiplicity in the $Z/\gamma^* \rightarrow \tau\tau$ and Higgs boson signal processes are the same.

The systematic uncertainties considered for the background prediction arise from the jet template statistics, alternative multi-jet track multiplicity templates, the presence of non-di- τ

background, signal contamination, charge misidentification probability and variations in the pileup conditions.

Instead of using the SS events for the multi-jet track template, the alternative multi-jet track multiplicity template is built from events with one additional electron or muon which enhances the contribution of W +jets events, where two jets are misidentified as the hadronic

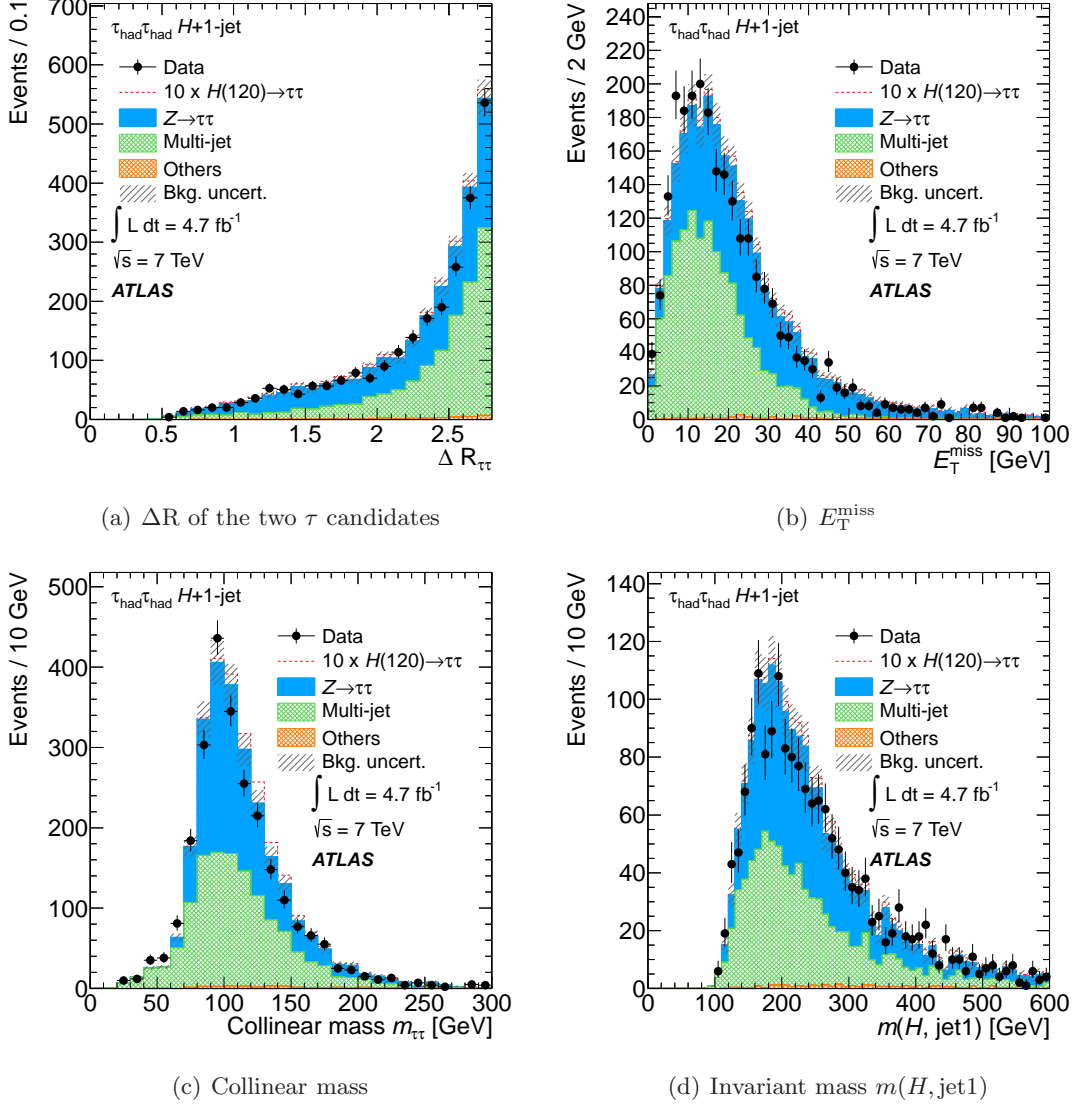


Figure 6. (a) ΔR of the two τ candidates, (b) missing transverse momentum, (c) collinear mass and (d) invariant mass of the reconstructed Higgs boson and the leading jet in the $H \rightarrow \tau_{\text{had}}\tau_{\text{had}}$ control region. Expectations from the Higgs boson signal ($m_H = 120$ GeV) and from backgrounds are given. The error band indicates the total background uncertainty. For illustration only, the signal contributions, which are expected to be small in this control region, have been scaled by factors given in the legends.

taus. This provides a different mix of quark- and gluon-initiated jets from the inclusive multi-jet sample, addressing a possible flavour dependence of the track multiplicity distribution.

The overall systematic uncertainties are 11.6% and 22% for $Z/\gamma^* \rightarrow \tau\tau$ and multi-jet backgrounds, respectively.

The mass shape from the multi-jet events is modelled by dropping the opposite-sign and τ_{had} track multiplicity requirements. In order to obtain a data sample that is enriched with the multi-jet background, events are accepted if they are same-sign events or if the sum of the charges of the products of a single τ decay is 0 or ± 2 . This mass shape model is tested against several other hypothesis obtained, e.g., from pure SS samples or events selected with looser τ identification criteria.

Figure 6 shows the kinematic distributions of (a) the ΔR of the two τ candidates, (b) the missing transverse momentum, (c) the collinear mass and (d) the invariant mass of the reconstructed Higgs boson and the leading jet in the $H \rightarrow \tau_{\text{had}}\tau_{\text{had}}$ control region.

Table 3 presents the event yields after the full event selection, where the yields are normalised to 4.7 fb^{-1} . The collinear mass distribution after full selection is presented in Figure 7.

Table 3. Number of events after the $H \rightarrow \tau_{\text{had}}\tau_{\text{had}}$ selection in data and predicted number of background events, for an integrated luminosity of 4.7 fb^{-1} . Predictions for the Higgs boson signal ($m_H = 120 \text{ GeV}$) are also given. Statistical errors and systematic uncertainties are quoted, in that order.

	$H \rightarrow \tau_{\text{had}}\tau_{\text{had}}$		
	$H + 1\text{-jet}$		
$gg \rightarrow H$ signal	3.1	± 0.2	± 0.6
VBF H signal	1.51	± 0.05	± 0.18
VH signal	0.61	± 0.04	± 0.06
$Z/\gamma^* \rightarrow \tau^+\tau^-$	287	± 23	± 34
$W + \text{jets} / Z + \text{jets}$	6.1 ± 1.3	± 1.4	
$t\bar{t} + \text{single top}$	1.9 ± 0.3	± 0.4	
$WW/WZ/ZZ$	2.1 ± 0.4	± 0.4	
Multi-jet	54	± 21	± 12
Total background	348	± 31	± 36
Observed data	317		

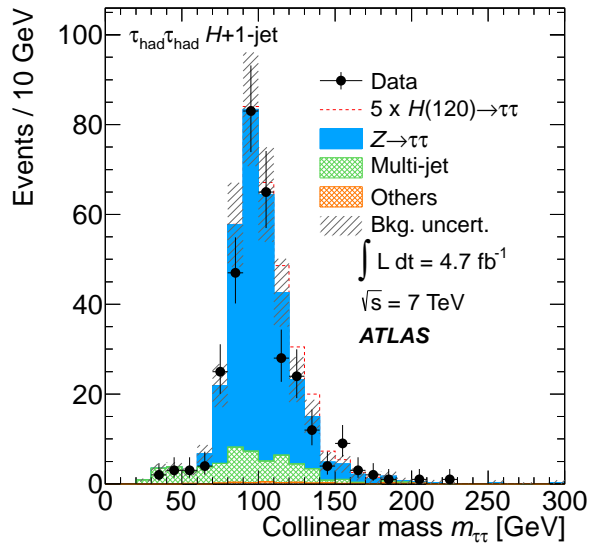


Figure 7. Reconstructed $m_{\tau\tau}$ of the selected events in the $H \rightarrow \tau_{\text{had}}\tau_{\text{had}}$ channel. Expectations from the Higgs boson signal ($m_H = 120$ GeV) and from backgrounds are given. Results are shown after all selection criteria (see text). For illustration only, the signal contribution has been scaled by a factor given in the legend.

7 Systematic uncertainties

Systematic uncertainties on the normalisation and shape of the signal and background mass distributions are taken into account. These are treated either as fully correlated or uncorrelated across categories. In the case of partial correlations, the source is separated into correlated and uncorrelated components. The dominant correlated systematic uncertainties are those on the measurement of the integrated luminosity and on the theoretical predictions of the signal production cross sections and decay branching ratios, as well as those related to detector response that impact the analyses through the reconstruction of electrons, muons, hadronic τ decays, jets, E_T^{miss} and b -tagging.

Theoretical uncertainties: The Higgs boson cross section, branching ratios and their uncertainties are compiled in Refs. [65, 66]. The QCD scale uncertainties on the signal cross sections depend on m_H and are of the order of 1% for the VBF and VH production modes and in the range of 8–25% for $gg \rightarrow H$ depending on jet multiplicity [67, 68]. An uncertainty of 4–5% is assumed for the inclusive cross section of the single vector boson and di-boson production mechanisms and a relative uncertainty of 24% is added in quadrature per additional jet. For both $t\bar{t}$ production and single top-quark production, the QCD scale uncertainties are in the range of 3–6% [69–71]. The uncertainties related to the PDF amount to 8% for the predominantly gluon-initiated processes, $gg \rightarrow H$ and $t\bar{t}$, and 4% for the predominantly quark-initiated processes, VBF, VH , single vector boson and di-boson production [72–75]. The systematic uncertainty arising from the choice of different sets of PDF is included. In addition to the theoretical errors considered in Ref. [66], other effects are taken into account. Uncertainties related to hadronisation effects are estimated by replacing PYTHIA with HERWIG. Effects due to initial and final state radiation are assessed with PYTHIA samples where the gluon emission is changed according to Ref. [76]. The effect of a different choice of parton shower and underlying event parametrisation yields a total uncertainty of about 10% on the acceptance of the Higgs boson produced via the VBF mechanism in the H+2jet VBF channel.

Detector-related uncertainties: The uncertainty on the integrated luminosity is considered as fully correlated across all analysis categories and amounts to 3.9% [77, 78]. The effect of pileup on the signal and background expectations is modelled in the Monte Carlo simulations and the corresponding uncertainty is taken into account.

Appropriate scale factors for the trigger efficiencies of electron, muon and hadronic τ triggers are obtained from data and applied to the Monte Carlo simulations. The associated systematic uncertainties are typically 1–2%. Differences between data and Monte Carlo simulations in the reconstruction and identification efficiencies of τ leptons, electrons and muons are taken into account, as well as the differences in the momentum scales and resolutions.

The systematic uncertainties on the hadronic τ decay identification efficiency are estimated from data samples enriched in $W \rightarrow \tau\nu$ and $Z/\gamma^* \rightarrow \tau\tau$ events and they are less than 4%. The energy scale uncertainties on the hadronic τ and jets are evaluated based on the single hadron response in the calorimeters [79]. In addition, the τ_{had} energy scale is validated

in data samples enriched in $Z/\gamma^* \rightarrow \tau\tau$ events. The systematic uncertainties related to the τ and jet energy scale, resolution and b -veto are modelled as functions of η and p_T . The jet and τ energy scale and resolution uncertainties are treated as correlated and propagated to the E_T^{miss} calculation. Uncertainties associated with the remaining pileup noise and cluster activity in the calorimeters are also considered as independent E_T^{miss} uncertainties.

The detector-related uncertainties depend on the event topology and are typically small compared to the theoretical uncertainties. The main exceptions are the jet energy scale uncertainty, which reaches up to 12%, and the τ energy scale uncertainty, which is in the range 2–5%.

Background modelling uncertainties: The modelling of the $Z/\gamma^* \rightarrow \tau\tau$ background is performed with the data, as described in Section 2. Corresponding uncertainties are obtained by propagating variations of the $Z/\gamma^* \rightarrow \mu\mu$ event selection and the muon energy subtraction procedure through the τ -embedding procedure. Backgrounds with misreconstructed leptons and τ_{had} candidates are estimated with data and the uncertainty in the estimation lies in the range of 6–40%. The uncertainty takes into account the dependence on the number of jets. The treatment of the other background processes varies across channels and the uncertainties related to the modelling are taken into account as described in Section 6.

8 Statistical analysis

The statistical analysis of the data employs a binned likelihood function constructed as the product of the likelihood terms for each category. A total of twelve categories are considered from the $H \rightarrow \tau_{\text{lep}}\tau_{\text{lep}}$, $H \rightarrow \tau_{\text{lep}}\tau_{\text{had}}$ and $H \rightarrow \tau_{\text{had}}\tau_{\text{had}}$ channels. The likelihood in each category is a product over bins in the distributions of the MMC mass, collinear mass or effective mass shown in Figs. 3, 5 and 7.

The expected signal and background, as well as the observed number of events, in each bin of the mass distributions enter in the definition of the likelihood function $\mathcal{L}(\mu, \theta)$. A “signal strength” parameter (μ) multiplies the expected signal in each bin. The signal strength is a free parameter in the fit procedure. The value $\mu = 0$ ($\mu = 1$) corresponds to the absence (presence) of a Higgs boson signal with the SM production cross-section. Signal and background predictions (s and b) depend on systematic uncertainties that are parametrised by nuisance parameters θ , which in turn are constrained using Gaussian functions. The correlation of the systematic uncertainties across categories are taken into account:

$$\mathcal{L}(\mu, \theta) = \prod_{\text{bin } j} \text{Poisson}(N_j | \mu(s_j) + b_j) \prod_{\theta} \text{Gaussian}(\theta | 0, 1). \quad (8.1)$$

The expected signal and background event counts in each bin are functions of θ . The parametrisation is chosen such that the rates in each channel are log-normally distributed for a normally distributed θ .

The test statistic q_μ is defined as:

$$q_\mu = -2 \ln \left(\mathcal{L}(\mu, \hat{\theta}_\mu) / \mathcal{L}(\hat{\mu}, \hat{\theta}) \right), \quad (8.2)$$

where $\hat{\mu}$ and $\hat{\theta}$ refer to the global maximum of the likelihood (with the constraint $0 \leq \hat{\mu} \leq \mu$) and $\hat{\theta}_\mu$ corresponds to the conditional maximum likelihood of θ for a given μ . This test statistic is used to compute exclusion limits following the modified frequentist method known as CL_s [80]. The asymptotic approximation [81] is used to evaluate the Gaussian probability density functions rather than performing pseudo-experiments and the procedure has been validated using ensemble tests.

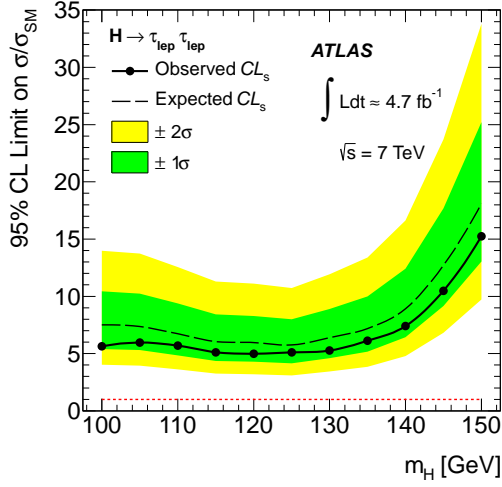
The profile likelihood formalism used in this statistical analysis incorporates the information on the observed and expected number of events, nuisance parameters, probability density functions and parameters of interest. The statistical significance of an excess is evaluated in terms of the same profile likelihood test statistic. The expected sensitivity and the $\pm 1, 2\sigma$ bands are obtained for the background expectation in the absence of a Standard Model Higgs boson signal. The consistency with the background-only hypothesis is quantified using the p -value, the probability that the test statistic of a background-only experiment fluctuates to at least the observed one.

9 Results

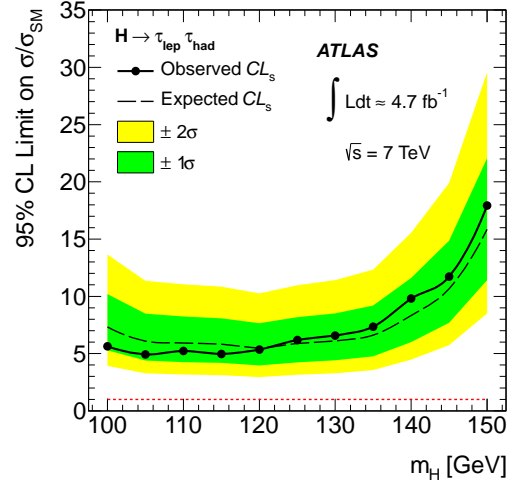
No significant excess is observed in the data compared to the SM expectation in any of the channels studied here. Exclusion limits at the 95% confidence level, normalised to the Standard Model cross section times the branching ratio of $H \rightarrow \tau^+\tau^-$ (σ_{SM}), are set as a function of the Higgs boson mass. Figure 8 shows expected and observed limits for the individual channels and for the combined result. The combined expected limits vary between 3.4 and 8.2 times the predicted Standard Model cross section times branching ratio for the mass range 100–150 GeV. The most sensitive categories are the $H + 1$ -jet category in the $\tau_{\text{had}}\tau_{\text{had}}$ channel, the $H + 2$ -jet VBF category in the $\tau_{\text{lep}}\tau_{\text{had}}$ channel and the $H + 2$ -jet VBF category in the $\tau_{\text{lep}}\tau_{\text{lep}}$ channel. The observed limits are in the range between 2.9 and 11.7 times the predicted Standard Model cross section times branching ratio for the same mass range. The most significant deviation from the background-only hypothesis is observed in the combined limit for $m_H = 150$ GeV with a local p -value of 10%, corresponding to a significance of 1.3σ .

10 Conclusions

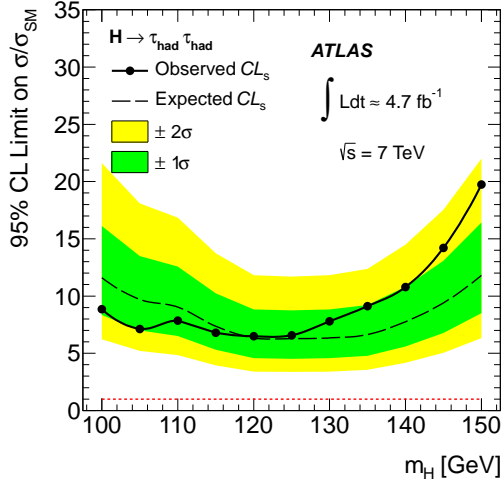
A search for a Higgs boson decaying in the $H \rightarrow \tau\tau$ channel has been performed with the ATLAS detector at the Large Hadron Collider. It uses the full 2011 data sample of 4.7fb^{-1} collected at a centre-of-mass energy of 7 TeV. The $H \rightarrow \tau_{\text{lep}}\tau_{\text{lep}}$, $H \rightarrow \tau_{\text{lep}}\tau_{\text{had}}$ and $H \rightarrow \tau_{\text{had}}\tau_{\text{had}}$ decays are considered in this search. No significant excess is observed in the mass range of 100–150 GeV. The observed (expected) upper limits on the cross section times the branching ratio of $H \rightarrow \tau\tau$ are between 2.9 (3.4) and 11.7 (8.2) times the SM prediction. These limits are similar to results recently reported by the CMS experiment [82].



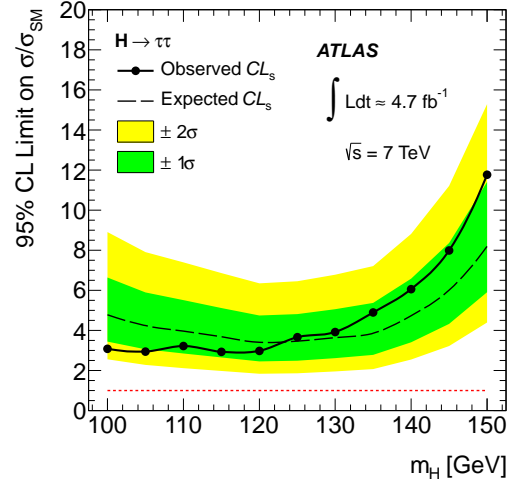
(a) $H \rightarrow \tau_{\text{lep}}\tau_{\text{lep}}$



(b) $H \rightarrow \tau_{\text{lep}}\tau_{\text{had}}$



(c) $H \rightarrow \tau_{\text{had}}\tau_{\text{had}}$



(d) Combined

Figure 8. Observed (solid) and expected (dashed) 95% confidence level upper limits on the Higgs boson cross section times branching ratio, normalised to the Standard Model expectation, as a function of the Higgs boson mass. Expected limits are given for the scenario with no signal. The bands around the dashed line indicate the expected statistical fluctuations of the limit. Results are given for the $H \rightarrow \tau_{\text{lep}}\tau_{\text{lep}}$, $H \rightarrow \tau_{\text{lep}}\tau_{\text{had}}$, and $H \rightarrow \tau_{\text{had}}\tau_{\text{had}}$ channels independently and for all channels combined.

Acknowledgments

We thank CERN for the very successful operation of the LHC, as well as the support staff from our institutions without whom ATLAS could not be operated efficiently.

We acknowledge the support of ANPCyT, Argentina; YerPhI, Armenia; ARC, Australia; BMWF, Austria; ANAS, Azerbaijan; SSTC, Belarus; CNPq and FAPESP, Brazil; NSERC, NRC and CFI, Canada; CERN; CONICYT, Chile; CAS, MOST and NSFC, China; COLCIENCIAS, Colombia; MSMT CR, MPO CR and VSC CR, Czech Republic; DNRF, DNSRC and Lundbeck Foundation, Denmark; EPLANET and ERC, European Union; IN2P3-CNRS, CEA-DSM/IRFU, France; GNAS, Georgia; BMBF, DFG, HGF, MPG and AvH Foundation, Germany; GSRT, Greece; ISF, MINERVA, GIF, DIP and Benoziyo Center, Israel; INFN, Italy; MEXT and JSPS, Japan; CNRST, Morocco; FOM and NWO, Netherlands; RCN, Norway; MNiSW, Poland; GRICES and FCT, Portugal; MERYS (MECTS), Romania; MES of Russia and ROSATOM, Russian Federation; JINR; MSTD, Serbia; MSSR, Slovakia; ARRS and MVZT, Slovenia; DST/NRF, South Africa; MICINN, Spain; SRC and Wallenberg Foundation, Sweden; SER, SNSF and Cantons of Bern and Geneva, Switzerland; NSC, Taiwan; TAEK, Turkey; STFC, the Royal Society and Leverhulme Trust, United Kingdom; DOE and NSF, United States of America.

The crucial computing support from all WLCG partners is acknowledged gratefully, in particular from CERN and the ATLAS Tier-1 facilities at TRIUMF (Canada), NDGF (Denmark, Norway, Sweden), CC-IN2P3 (France), KIT/GridKA (Germany), INFN-CNAF (Italy), NL-T1 (Netherlands), PIC (Spain), ASGC (Taiwan), RAL (UK) and BNL (USA) and in the Tier-2 facilities worldwide.

References

- [1] F. Englert and R. Brout, *Phys. Rev. Lett.* **13** (1964) 321.
- [2] P. W. Higgs, *Phys. Lett.* **12** (1964) 132.
- [3] P. W. Higgs, *Phys. Rev. Lett.* **13** (1964) 508.
- [4] G. S. Guralnik, C. R. Hagen, and T. W. B. Kibble, *Phys. Rev. Lett.* **13** (1964) 585–587.
- [5] P. W. Higgs, *Phys. Rev. D* **145** (1966) 1156.
- [6] T. W. B. Kibble, *Phys. Rev.* **155** (1967) 1554–1561.
- [7] **ALEPH, DELPHI, L3, OPAL, SLD, CDF, and DØ** Collaborations, The LEP Tevatron SLD Electroweak Working Group, [arXiv:1012.2367](https://arxiv.org/abs/1012.2367).
- [8] **ALEPH, DELPHI, L3, and OPAL** Collaborations, The LEP Working Group for Higgs Boson Searches, *Phys. Lett. B* **565** (2003) 61, [[hep-ex/0306033](https://arxiv.org/abs/hep-ex/0306033)].
- [9] **TEVNPH (Tevatron New Phenomena and Higgs Working Group), CDF and D0** Collaboration, [arXiv:1203.3774](https://arxiv.org/abs/1203.3774). Preliminary results prepared for the Winter 2012 Conferences.
- [10] **ATLAS** Collaboration, *Phys. Lett. B* **710** (2012) 49, [[arXiv:1202.1408](https://arxiv.org/abs/1202.1408)].

- [11] CMS Collaboration, *Phys. Lett. B* **710** (2012) 26, [[arXiv:1202.1488](#)].
- [12] ATLAS Collaboration, *JINST* **3** (2008) S08003.
- [13] A. Djouadi, M. Spira, and P. M. Zerwas, *Phys. Lett. B* **264** (1991) 440–446.
- [14] S. Dawson, *Nucl. Phys. B* **359** (1991) 283–300.
- [15] M. Spira, A. Djouadi, D. Graudenz, and P. M. Zerwas, *Nucl. Phys. B* **453** (1995) 17–82, [[hep-ph/9504378](#)].
- [16] R. Harlander and W. B. Kilgore, *Phys. Rev. Lett.* **88** (2002) 201801, [[hep-ph/0201206](#)].
- [17] C. Anastasiou and K. Melnikov, *Nucl. Phys. B* **646** (2002) 220, [[hep-ph/0207004](#)].
- [18] V. Ravindran, J. Smith, W. L. van Neerven, *Nucl. Phys. B* **665** (2003) 325, [[hep-ph/0302135](#)].
- [19] S. Catani, D. de Florian, M. Grazzini, and P. Nason, *JHEP* **0307** (2003) 028, [[hep-ph/0306211](#)].
- [20] U. Aglietti, R. Bonciani, G. Degrossi, and A. Vicini, *Phys. Lett. B* **595** (2004) 432, [[hep-ph/0404071](#)].
- [21] S. Actis, G. Passarino, C. Sturm, and S. Uccirati, *Phys. Lett. B* **670** (2008) 12–17, [[arXiv:0809.1301](#)].
- [22] C. Anastasiou, R. Boughezal, and F. Petriello, *JHEP* **0904** (2009) 003, [[arXiv:0811.3458](#)].
- [23] D. de Florian and M. Grazzini, *Phys. Lett. B* **674** (2009) 291, [[arXiv:0901.2427](#)].
- [24] J. Baglio and A. Djouadi, *JHEP* **1103** (2011) 055, [[arXiv:1012.0530](#)].
- [25] M. Ciccolini, A. Denner, and S. Dittmaier, *Phys. Rev. Lett.* **99** (2007) 161803, [[arXiv:0707.0381](#)].
- [26] M. Ciccolini, A. Denner, and S. Dittmaier, *Phys. Rev. D* **77** (2008) 013002, [[arXiv:0710.4749](#)].
- [27] K. Arnold, M. Bahr, G. Bozzi, F. Campanario, C. Englert, *et. al.*, *Comput.Phys.Commun.* **180** (2009) 1661–1670, [[arXiv:0811.4559](#)].
- [28] P. Bolzoni, F. Maltoni, S.-O. Moch, and M. Zaro, *Phys. Rev. Lett.* **105** (2010) 011801, [[arXiv:1003.4451](#)].
- [29] T. Han and S. Willenbrock, *Phys. Lett. B* **273** (1991) 167–172.
- [30] O. Brein, A. Djouadi, and R. Harlander, *Phys. Lett. B* **579** (2004) 149, [[hep-ph/0307206](#)].
- [31] M. L. Ciccolini, S. Dittmaier, and M. Kramer, *Phys. Rev. D* **68** (2003) 073003, [[hep-ph/0306234](#)].
- [32] A. Djouadi, J. Kalinowski, and M. Spira, *Comput. Phys. Commun.* **108** (1998) 56, [[hep-ph/9704448](#)].
- [33] S. Alioli, P. Nason, and C. Oleari, and E. Re, *JHEP* **0904** (2009) 002, [[arXiv:0812.0578](#)].
- [34] P. Nason and C. Oleari, *JHEP* **1002** (2010) 037, [[arXiv:0911.5299](#)].
- [35] T. Sjostrand, S. Mrenna, and P. Z. Skands, *JHEP* **0605** (2006) 026.
- [36] D. de Florian *et al.*, *JHEP* **11** (2011) 064, [[arXiv:1109.2109](#)]. For Higgs boson $p_T > m_H$, the calculation is switched from NLO+NLL to NLO.
- [37] M. L. Mangano *et. al.*, *JHEP* **0307** (2003) 001.

- [38] G. Corcella *et. al.*, *JHEP* **0101** (2001) 010.
- [39] J. Alwall *et al.*, *Eur. Phys. J. C* **53** (2008) 473.
- [40] S. Frixione and B. R. Webber, *JHEP* **06** (2002) 029, [[hep-ph/0204244](#)].
- [41] J. M. Butterworth, J. R. Forshaw, and M. H. Seymour, *Z. Phys. C* **72** (1996) 637–646, [[hep-ph/9601371](#)].
- [42] B. P. Kersevan and E. Richter-Was, [hep-ph/0405247](#).
- [43] S. Jadach, Z. Was, R. Decker, and J. H. Kuhn, *Comput. Phys. Commun.* **76** (1993) 361–380.
- [44] P. Golonka and Z. Was, *Eur. Phys. J. C* **45** (2006) 97–107, [[hep-ph/0506026](#)].
- [45] H.-L. Lai *et. al.*, *Phys. Rev. D* **82** (2010) 074024, [[arXiv:1007.2241](#)].
- [46] J. Pumplin *et. al.*, *JHEP* **07** (2002) 012, [[hep-ph/0201195](#)].
- [47] A. Sherstnev and R. S. Thorne, *Eur. Phys. J C* **55** (2009) 553.
- [48] S. Agostinelli *et al.*, *Nucl. Instrum. Meth. A* **506** (2003) 250.
- [49] **ATLAS** Collaboration, *Eur. Phys. J. C* **70** (2010) 823–874, [[arXiv:1005.4568](#)].
- [50] **ATLAS** Collaboration, *Eur.Phys.J. C* **72** (2012) 1909, [[arXiv:1110.3174](#)].
- [51] **ATLAS** Collaboration, *JHEP* **1012** (2010) 060, [[arXiv:1010.2130](#)].
- [52] M. Cacciari, G. P. Salam, and G. Soyez, *JHEP* **0804** (2008) 063, [[arXiv:0802.1189](#)].
- [53] **ATLAS** Collaboration, ATLAS-CONF-2011-102, [<http://cdsweb.cern.ch/record/1369219>].
- [54] **ATLAS** Collaboration, ATLAS-CONF-2012-043, [<http://cdsweb.cern.ch/record/1435197>].
- [55] **ATLAS** Collaboration, ATLAS-CONF-2012-040, [<http://cdsweb.cern.ch/record/1435194>].
- [56] **ATLAS** Collaboration, ATLAS-CONF-2011-152, [<http://cdsweb.cern.ch/record/1398195>].
- [57] **ATLAS** Collaboration, *Eur. Phys. J. C* **72** (2012) 1844, [[arXiv:1108.5602](#)].
- [58] **ATLAS** Collaboration, *Eur.Phys.J. C* **72** (2012) 1849, [[arXiv:1110.1530](#)].
- [59] D. L. Rainwater, D. Zeppenfeld, and K. Hagiwara, *Phys. Rev. D* **59** (1998) 014037, [[hep-ph/9808468](#)].
- [60] T. Plehn, D. L. Rainwater and D. Zeppenfeld, *Phys. Rev. D* **61** (2000) 093005, [[hep-ph/9911385](#)].
- [61] S. Asai *et. al.*, *Eur. Phys. J. C* **32S2** (2004) 19–54, [[hep-ph/0402254](#)].
- [62] B. Mellado, W. Quayle, and S. L. Wu, *Phys. Lett. B* **611** (2005) 60–65, [[hep-ph/0406095](#)].
- [63] R.K. Ellis, I. Hinchliffe, M. Soldate and J.J. Van der Bij, *Nucl. Phys. B* **297** (1988) 221.
- [64] A. Elagin, P. Murat, A. Pranko, and A. Safonov, *Nucl. Instrum. Meth. A* **654** (2011) 481–489, [[arXiv:1012.4686](#)].
- [65] S. Dittmaier *et al.* (LHC Higgs Cross Section Working Group), [arXiv:1101.0593](#).
- [66] S. Dittmaier *et al.* (LHC Higgs Cross Section Working Group), [arXiv:1201.3084](#).
- [67] I. W. Stewart and F. J. Tackmann, *Phys. Rev. D* **85** (2012) 034011, [[arXiv:1107.2117](#)].
- [68] **ATLAS** and **CMS** Collaborations, ATL-PHYS-PUB-2011-011, CMS-NOTE-2011-005.

- [69] S. Moch and P. Uwer, *Phys. Rev. D* **78** (2008) 034003.
- [70] M. Beneke et al., *Phys. Lett. B* **690** (2010) 483.
- [71] N. Kidonakis, *Phys. Rev. D* **83** (2011) 091503, [[arXiv:1103.2792](#)].
- [72] M. Botje et al., [arXiv:1101.0538](#).
- [73] H.-L. Lai et al., *Phys. Rev. D* **82** (2010) [[arXiv:1007.2241](#)].
- [74] A. D. Martin, W. J. Stirling, R. S. Thorne, and G. Watt, *Eur. Phys. J. C* **63** (2009) 189–285, [[arXiv:0901.0002](#)].
- [75] R. D. Ball et al., *Nucl. Phys. B* **849** (2011) [[arXiv:1101.1300](#)].
- [76] P. Z. Skands, *Phys. Rev. D* **82** (2010) 074018, [[arXiv:1005.3457](#)].
- [77] **ATLAS** Collaboration, *Eur. Phys. J. C* **71** (2011) 1630, [[arXiv:1101.2185](#)].
- [78] **ATLAS** Collaboration, ATLAS-CONF-2011-116 [<http://cdsweb.cern.ch/record/1376384>].
- [79] **ATLAS** Collaboration, [arXiv:1112.6426](#). Submitted to EPJC.
- [80] A.L. Read, *J. Phys. G* **28** (2002) 2693.
- [81] G. Cowan, K. Cranmer, E. Gross, and O. Vitells, *Eur. Phys. J. C* **71** (2011) 1554.
- [82] **CMS** Collaboration, *Phys. Lett. B* **713** (2012) 68, [[arXiv:1202.4083](#)].

The ATLAS Collaboration

G. Aad⁴⁸, B. Abbott¹¹¹, J. Abdallah¹¹, S. Abdel Khalek¹¹⁵, A.A. Abdelalim⁴⁹,
O. Abidinov¹⁰, B. Abi¹¹², M. Abolins⁸⁸, O.S. AbouZeid¹⁵⁸, H. Abramowicz¹⁵³, H. Abreu¹³⁶,
E. Acerbi^{89a,89b}, B.S. Acharya^{164a,164b}, L. Adamczyk³⁷, D.L. Adams²⁴, T.N. Addy⁵⁶,
J. Adelman¹⁷⁶, S. Adomeit⁹⁸, P. Adragna⁷⁵, T. Adye¹²⁹, S. Aefsky²²,
J.A. Aguilar-Saavedra^{124b,a}, M. Agustoni¹⁶, M. Aharrouche⁸¹, S.P. Ahlen²¹, F. Ahles⁴⁸,
A. Ahmad¹⁴⁸, M. Ahsan⁴⁰, G. Aielli^{133a,133b}, T. Akdogan^{18a}, T.P.A. Åkesson⁷⁹,
G. Akimoto¹⁵⁵, A.V. Akimov⁹⁴, M.S. Alam¹, M.A. Alam⁷⁶, J. Albert¹⁶⁹, S. Albrand⁵⁵,
M. Aleksa²⁹, I.N. Aleksandrov⁶⁴, F. Alessandria^{89a}, C. Alexa^{25a}, G. Alexander¹⁵³,
G. Alexandre⁴⁹, T. Alexopoulos⁹, M. Alhroob^{164a,164c}, M. Aliev¹⁵, G. Alimonti^{89a},
J. Alison¹²⁰, B.M.M. Allbrooke¹⁷, P.P. Allport⁷³, S.E. Allwood-Spiers⁵³, J. Almond⁸²,
A. Aloisio^{102a,102b}, R. Alon¹⁷², A. Alonso⁷⁹, B. Alvarez Gonzalez⁸⁸, M.G. Alviggi^{102a,102b},
K. Amako⁶⁵, C. Amelung²², V.V. Ammosov¹²⁸, A. Amorim^{124a,b}, N. Amram¹⁵³,
C. Anastopoulos²⁹, L.S. Ancu¹⁶, N. Andari¹¹⁵, T. Andeen³⁴, C.F. Anders^{58b}, G. Anders^{58a},
K.J. Anderson³⁰, A. Andreazza^{89a,89b}, V. Andrei^{58a}, X.S. Anduaga⁷⁰, P. Anger⁴³,
A. Angerami³⁴, F. Anghinolfi²⁹, A. Anisenkov¹⁰⁷, N. Anjos^{124a}, A. Annovi⁴⁷, A. Antonaki⁸,
M. Antonelli⁴⁷, A. Antonov⁹⁶, J. Antos^{144b}, F. Anulli^{132a}, S. Aoun⁸³, L. Aperio Bella⁴,
R. Apolle^{118,c}, G. Arabidze⁸⁸, I. Aracena¹⁴³, Y. Arai⁶⁵, A.T.H. Arce⁴⁴, S. Arfaoui¹⁴⁸,
J-F. Arguin¹⁴, E. Arik^{18a,*}, M. Arik^{18a}, A.J. Armbruster⁸⁷, O. Arnaez⁸¹, V. Arnal⁸⁰,
C. Arnault¹¹⁵, A. Artamonov⁹⁵, G. Artoni^{132a,132b}, D. Arutinov²⁰, S. Asai¹⁵⁵,
R. Asfandiyarov¹⁷³, S. Ask²⁷, B. Åsman^{146a,146b}, L. Asquith⁵, K. Assamagan²⁴,
A. Astbury¹⁶⁹, B. Aubert⁴, E. Auge¹¹⁵, K. Augsten¹²⁷, M. Aourousseau^{145a}, G. Avolio¹⁶³,
R. Avramidou⁹, D. Axen¹⁶⁸, G. Azuelos^{93,d}, Y. Azuma¹⁵⁵, M.A. Baak²⁹, G. Baccaglioni^{89a},
C. Bacci^{134a,134b}, A.M. Bach¹⁴, H. Bachacou¹³⁶, K. Bachas²⁹, M. Backes⁴⁹, M. Backhaus²⁰,
E. Badescu^{25a}, P. Bagnaia^{132a,132b}, S. Bahinipati², Y. Bai^{32a}, D.C. Bailey¹⁵⁸, T. Bain¹⁵⁸,
J.T. Baines¹²⁹, O.K. Baker¹⁷⁶, M.D. Baker²⁴, S. Baker⁷⁷, E. Banas³⁸, P. Banerjee⁹³,
Sw. Banerjee¹⁷³, D. Banfi²⁹, A. Bangert¹⁵⁰, V. Bansal¹⁶⁹, H.S. Bansil¹⁷, L. Barak¹⁷²,
S.P. Baranov⁹⁴, A. Barbaro Galtieri¹⁴, T. Barber⁴⁸, E.L. Barberio⁸⁶, D. Barberis^{50a,50b},
M. Barbero²⁰, D.Y. Bardin⁶⁴, T. Barillari⁹⁹, M. Barisonzi¹⁷⁵, T. Barklow¹⁴³, N. Barlow²⁷,
B.M. Barnett¹²⁹, R.M. Barnett¹⁴, A. Baroncelli^{134a}, G. Barone⁴⁹, A.J. Barr¹¹⁸,
F. Barreiro⁸⁰, J. Barreiro Guimarães da Costa⁵⁷, P. Barrillon¹¹⁵, R. Bartoldus¹⁴³,
A.E. Barton⁷¹, V. Bartsch¹⁴⁹, R.L. Bates⁵³, L. Batkova^{144a}, J.R. Batley²⁷, A. Battaglia¹⁶,
M. Battistin²⁹, F. Bauer¹³⁶, H.S. Bawa^{143,e}, S. Beale⁹⁸, T. Beau⁷⁸, P.H. Beauchemin¹⁶¹,
R. Beccherle^{50a}, P. Bechtel²⁰, H.P. Beck¹⁶, A.K. Becker¹⁷⁵, S. Becker⁹⁸, M. Beckingham¹³⁸,
K.H. Becks¹⁷⁵, A.J. Beddall^{18c}, A. Beddall^{18c}, S. Bedikian¹⁷⁶, V.A. Bednyakov⁶⁴,
C.P. Bee⁸³, M. Begel²⁴, S. Behar Harpaz¹⁵², M. Beimforde⁹⁹, C. Belanger-Champagne⁸⁵,
P.J. Bell⁴⁹, W.H. Bell⁴⁹, G. Bella¹⁵³, L. Bellagamba^{19a}, F. Bellina²⁹, M. Bellomo²⁹,
A. Belloni⁵⁷, O. Beloborodova^{107,f}, K. Belotskiy⁹⁶, O. Beltramello²⁹, O. Benary¹⁵³,
D. Benchekroun^{135a}, K. Bendtz^{146a,146b}, N. Benekos¹⁶⁵, Y. Benhammou¹⁵³,
E. Benhar Noccioli⁴⁹, J.A. Benitez Garcia^{159b}, D.P. Benjamin⁴⁴, M. Benoit¹¹⁵,

J.R. Bensing²², K. Benslama¹³⁰, S. Bentvelsen¹⁰⁵, D. Berge²⁹, E. Bergeaas Kuutmann⁴¹,
 N. Berger⁴, F. Berghaus¹⁶⁹, E. Berglund¹⁰⁵, J. Beringer¹⁴, P. Bernat⁷⁷, R. Bernhard⁴⁸,
 C. Bernius²⁴, T. Berry⁷⁶, C. Bertella⁸³, A. Bertin^{19a,19b}, F. Bertolucci^{122a,122b},
 M.I. Besana^{89a,89b}, G.J. Besjes¹⁰⁴, N. Besson¹³⁶, S. Bethke⁹⁹, W. Bhimji⁴⁵, R.M. Bianchi²⁹,
 M. Bianco^{72a,72b}, O. Biebel⁹⁸, S.P. Bieniek⁷⁷, K. Bierwagen⁵⁴, J. Biesiada¹⁴, M. Biglietti^{134a},
 H. Bilokon⁴⁷, M. Bindi^{19a,19b}, S. Binet¹¹⁵, A. Bingul^{18c}, C. Bini^{132a,132b}, C. Biscarat¹⁷⁸,
 U. Bitenc⁴⁸, K.M. Black²¹, R.E. Blair⁵, J.-B. Blanchard¹³⁶, G. Blanchot²⁹, T. Blazek^{144a},
 C. Blocker²², J. Blocki³⁸, A. Blondel⁴⁹, W. Blum⁸¹, U. Blumenschein⁵⁴, G.J. Bobbink¹⁰⁵,
 V.B. Bobrovnikov¹⁰⁷, S.S. Bocchetta⁷⁹, A. Bocci⁴⁴, C.R. Boddy¹¹⁸, M. Boehler⁴¹,
 J. Boek¹⁷⁵, N. Boelaert³⁵, J.A. Bogaerts²⁹, A. Bogdanchikov¹⁰⁷, A. Bogouch^{90,*},
 C. Boehm^{146a}, J. Boehm¹²⁵, V. Boisvert⁷⁶, T. Bold³⁷, V. Boldea^{25a}, N.M. Bolnet¹³⁶,
 M. Bomben⁷⁸, M. Bona⁷⁵, M. Boonekamp¹³⁶, C.N. Booth¹³⁹, S. Bordoni⁷⁸, C. Borer¹⁶,
 A. Borisov¹²⁸, G. Borissov⁷¹, I. Borjanovic^{12a}, M. Borri⁸², S. Borroni⁸⁷,
 V. Bortolotto^{134a,134b}, K. Bos¹⁰⁵, D. Boscherini^{19a}, M. Bosman¹¹, H. Boterenbrood¹⁰⁵,
 D. Botterill¹²⁹, J. Bouchami⁹³, J. Boudreau¹²³, E.V. Bouhova-Thacker⁷¹, D. Boumediene³³,
 C. Bourdarios¹¹⁵, N. Bousson⁸³, A. Boveia³⁰, J. Boyd²⁹, I.R. Boyko⁶⁴,
 I. Bozovic-Jelisavcic^{12b}, J. Bracinik¹⁷, P. Branchini^{134a}, A. Brandt⁷, G. Brandt¹¹⁸,
 O. Brandt⁵⁴, U. Bratzler¹⁵⁶, B. Brau⁸⁴, J.E. Brau¹¹⁴, H.M. Braun¹⁷⁵, S.F. Brazzale^{164a,164c},
 B. Brelief¹⁵⁸, J. Bremer²⁹, K. Brendlinger¹²⁰, R. Brenner¹⁶⁶, S. Bressler¹⁷², D. Britton⁵³,
 F.M. Brochu²⁷, I. Brock²⁰, R. Brock⁸⁸, E. Brodet¹⁵³, F. Broggi^{89a}, C. Bromberg⁸⁸,
 J. Bronner⁹⁹, G. Brooijmans³⁴, T. Brooks⁷⁶, W.K. Brooks^{31b}, G. Brown⁸², H. Brown⁷,
 P.A. Bruckman de Renstrom³⁸, D. Bruncko^{144b}, R. Bruneliere⁴⁸, S. Brunet⁶⁰, A. Bruni^{19a},
 G. Bruni^{19a}, M. Bruschi^{19a}, T. Buanes¹³, Q. Buat⁵⁵, F. Bucci⁴⁹, J. Buchanan¹¹⁸,
 P. Buchholz¹⁴¹, R.M. Buckingham¹¹⁸, A.G. Buckley⁴⁵, S.I. Buda^{25a}, I.A. Budagov⁶⁴,
 B. Budick¹⁰⁸, V. Büscher⁸¹, L. Bugge¹¹⁷, O. Bulekov⁹⁶, A.C. Bundock⁷³, M. Bune⁴²,
 T. Buran¹¹⁷, H. Burckhart²⁹, S. Burdin⁷³, T. Burgess¹³, S. Burke¹²⁹, E. Busato³³,
 P. Bussey⁵³, C.P. Buszello¹⁶⁶, B. Butler¹⁴³, J.M. Butler²¹, C.M. Buttar⁵³,
 J.M. Butterworth⁷⁷, W. Buttinger²⁷, S. Cabrera Urbán¹⁶⁷, D. Caforio^{19a,19b}, O. Cakir^{3a},
 P. Calafiura¹⁴, G. Calderini⁷⁸, P. Calfayan⁹⁸, R. Calkins¹⁰⁶, L.P. Caloba^{23a},
 R. Caloi^{132a,132b}, D. Calvet³³, S. Calvet³³, R. Camacho Toro³³, P. Camarri^{133a,133b},
 D. Cameron¹¹⁷, L.M. Caminada¹⁴, S. Campana²⁹, M. Campanelli⁷⁷, V. Canale^{102a,102b},
 F. Canelli^{30,g}, A. Canepa^{159a}, J. Cantero⁸⁰, R. Cantrill⁷⁶, L. Capasso^{102a,102b},
 M.D.M. Capeans Garrido²⁹, I. Caprini^{25a}, M. Caprini^{25a}, D. Capriotti⁹⁹, M. Capua^{36a,36b},
 R. Caputo⁸¹, R. Cardarelli^{133a}, T. Carli²⁹, G. Carlino^{102a}, L. Carminati^{89a,89b}, B. Caron⁸⁵,
 S. Caron¹⁰⁴, E. Carquin^{31b}, G.D. Carrillo Montoya¹⁷³, A.A. Carter⁷⁵, J.R. Carter²⁷,
 J. Carvalho^{124a,h}, D. Casadei¹⁰⁸, M.P. Casado¹¹, M. Cascella^{122a,122b}, C. Caso^{50a,50b,*},
 A.M. Castaneda Hernandez^{173,i}, E. Castaneda-Miranda¹⁷³, V. Castillo Gimenez¹⁶⁷,
 N.F. Castro^{124a}, G. Cataldi^{72a}, P. Catastini⁵⁷, A. Catinaccio²⁹, J.R. Catmore²⁹, A. Cattai²⁹,
 G. Cattani^{133a,133b}, S. Caughron⁸⁸, P. Cavalleri⁷⁸, D. Cavalli^{89a}, M. Cavalli-Sforza¹¹,
 V. Cavasinni^{122a,122b}, F. Ceradini^{134a,134b}, A.S. Cerqueira^{23b}, A. Cerri²⁹, L. Cerrito⁷⁵,
 F. Cerutti⁴⁷, S.A. Cetin^{18b}, A. Chafaq^{135a}, D. Chakraborty¹⁰⁶, I. Chalupkova¹²⁶, K. Chan²,

B. Chapleau⁸⁵, J.D. Chapman²⁷, J.W. Chapman⁸⁷, E. Chareyre⁷⁸, D.G. Charlton¹⁷,
 V. Chavda⁸², C.A. Chavez Barajas²⁹, S. Cheatham⁸⁵, S. Chekanov⁵, S.V. Chekulaev^{159a},
 G.A. Chelkov⁶⁴, M.A. Chelstowska¹⁰⁴, C. Chen⁶³, H. Chen²⁴, S. Chen^{32c}, X. Chen¹⁷³,
 Y. Chen³⁴, A. Cheplakov⁶⁴, R. Cherkaoui El Moursli^{135e}, V. Chernyatin²⁴, E. Cheu⁶,
 S.L. Cheung¹⁵⁸, L. Chevalier¹³⁶, G. Chiefari^{102a,102b}, L. Chikovani^{51a}, J.T. Childers²⁹,
 A. Chilingarov⁷¹, G. Chiodini^{72a}, A.S. Chisholm¹⁷, R.T. Chislett⁷⁷, A. Chitan^{25a},
 M.V. Chizhov⁶⁴, G. Choudalakis³⁰, S. Chouridou¹³⁷, I.A. Christidi⁷⁷, A. Christov⁴⁸,
 D. Chromek-Burckhart²⁹, M.L. Chu¹⁵¹, J. Chudoba¹²⁵, G. Ciapetti^{132a,132b}, A.K. Ciftci^{3a},
 R. Ciftci^{3a}, D. Cinca³³, V. Cindro⁷⁴, C. Ciocca^{19a,19b}, A. Ciocio¹⁴, M. Cirilli⁸⁷,
 P. Cirkovic^{12b}, M. Citterio^{89a}, M. Ciubancan^{25a}, A. Clark⁴⁹, P.J. Clark⁴⁵, R.N. Clarke¹⁴,
 W. Cleland¹²³, J.C. Clemens⁸³, B. Clement⁵⁵, C. Clement^{146a,146b}, Y. Coadou⁸³,
 M. Cobal^{164a,164c}, A. Coccaro¹³⁸, J. Cochran⁶³, J.G. Cogan¹⁴³, J. Coggeshall¹⁶⁵,
 E. Cogneras¹⁷⁸, J. Colas⁴, A.P. Colijn¹⁰⁵, N.J. Collins¹⁷, C. Collins-Tooth⁵³, J. Collot⁵⁵,
 T. Colombo^{119a,119b}, G. Colon⁸⁴, P. Conde Muiño^{124a}, E. Coniavitis¹¹⁸, M.C. Conidi¹¹,
 S.M. Consonni^{89a,89b}, V. Consorti⁴⁸, S. Constantinescu^{25a}, C. Conta^{119a,119b}, G. Conti⁵⁷,
 F. Conventi^{102a,j}, M. Cooke¹⁴, B.D. Cooper⁷⁷, A.M. Cooper-Sarkar¹¹⁸, K. Copic¹⁴,
 T. Cornelissen¹⁷⁵, M. Corradi^{19a}, F. Corriveau^{85,k}, A. Cortes-Gonzalez¹⁶⁵, G. Cortiana⁹⁹,
 G. Costa^{89a}, M.J. Costa¹⁶⁷, D. Costanzo¹³⁹, T. Costin³⁰, D. Côté²⁹, L. Courneyea¹⁶⁹,
 G. Cowan⁷⁶, C. Cowden²⁷, B.E. Cox⁸², K. Cranmer¹⁰⁸, F. Crescioli^{122a,122b},
 M. Cristinziani²⁰, G. Crosetti^{36a,36b}, R. Crupi^{72a,72b}, S. Crépe-Renaudin⁵⁵, C.-M. Cuciuc^{25a},
 C. Cuenca Almenar¹⁷⁶, T. Cuhadar Donszelmann¹³⁹, M. Curatolo⁴⁷, C.J. Curtis¹⁷,
 C. Cuthbert¹⁵⁰, P. Cwetanski⁶⁰, H. Czirr¹⁴¹, P. Czodrowski⁴³, Z. Czyczula¹⁷⁶, S. D'Auria⁵³,
 M. D'Onofrio⁷³, A. D'Orazio^{132a,132b}, M.J. Da Cunha Sargedas De Sousa^{124a}, C. Da Via⁸²,
 W. Dabrowski³⁷, A. Dafinca¹¹⁸, T. Dai⁸⁷, C. Dallapiccola⁸⁴, M. Dam³⁵, M. Dameri^{50a,50b},
 D.S. Damiani¹³⁷, H.O. Danielsson²⁹, V. Dao⁴⁹, G. Darbo^{50a}, G.L. Darlea^{25b}, W. Davey²⁰,
 T. Davidek¹²⁶, N. Davidson⁸⁶, R. Davidson⁷¹, E. Davies^{118,c}, M. Davies⁹³, A.R. Davison⁷⁷,
 Y. Davygora^{58a}, E. Dawe¹⁴², I. Dawson¹³⁹, R.K. Daya-Ishmukhametova²², K. De⁷,
 R. de Asmundis^{102a}, S. De Castro^{19a,19b}, S. De Cecco⁷⁸, J. de Graat⁹⁸, N. De Groot¹⁰⁴,
 P. de Jong¹⁰⁵, C. De La Taille¹¹⁵, H. De la Torre⁸⁰, F. De Lorenzi⁶³, L. de Mora⁷¹,
 L. De Nooij¹⁰⁵, D. De Pedis^{132a}, A. De Salvo^{132a}, U. De Sanctis^{164a,164c}, A. De Santo¹⁴⁹,
 J.B. De Vivie De Regie¹¹⁵, G. De Zorzi^{132a,132b}, W.J. Dearnaley⁷¹, R. Debbe²⁴,
 C. Debenedetti⁴⁵, B. Dechenaux⁵⁵, D.V. Dedovich⁶⁴, J. Degenhardt¹²⁰, C. Del Papa^{164a,164c},
 J. Del Peso⁸⁰, T. Del Prete^{122a,122b}, T. Delemontex⁵⁵, M. Deliyergiyev⁷⁴, A. Dell'Acqua²⁹,
 L. Dell'Asta²¹, M. Della Pietra^{102a,j}, D. della Volpe^{102a,102b}, M. Delmastro⁴, P.A. Delsart⁵⁵,
 C. Deluca¹⁰⁵, S. Demers¹⁷⁶, M. Demichev⁶⁴, B. Demirkoz^{11,l}, J. Deng¹⁶³, S.P. Denisov¹²⁸,
 D. Derendarz³⁸, J.E. Derkaoui^{135d}, F. Derue⁷⁸, P. Dervan⁷³, K. Desch²⁰, E. Devetak¹⁴⁸,
 P.O. Deviveiros¹⁰⁵, A. Dewhurst¹²⁹, B. DeWilde¹⁴⁸, S. Dhaliwal¹⁵⁸, R. Dhullipudi^{24,m},
 A. Di Ciaccio^{133a,133b}, L. Di Ciaccio⁴, A. Di Girolamo²⁹, B. Di Girolamo²⁹,
 S. Di Luise^{134a,134b}, A. Di Mattia¹⁷³, B. Di Micco²⁹, R. Di Nardo⁴⁷, A. Di Simone^{133a,133b},
 R. Di Sipio^{19a,19b}, M.A. Diaz^{31a}, E.B. Diehl⁸⁷, J. Dietrich⁴¹, T.A. Dietzsch^{58a}, S. Diglio⁸⁶,
 K. Dindar Yagci³⁹, J. Dingfelder²⁰, F. Dinut^{25a}, C. Dionisi^{132a,132b}, P. Dita^{25a}, S. Dita^{25a},

F. Dittus²⁹, F. Djama⁸³, T. Djobava^{51b}, M.A.B. do Vale^{23c}, A. Do Valle Wemans^{124a,n},
 T.K.O. Doan⁴, M. Dobbs⁸⁵, R. Dobinson^{29,*}, D. Dobos²⁹, E. Dobson^{29,o}, J. Dodd³⁴,
 C. Doglioni⁴⁹, T. Doherty⁵³, Y. Doi^{65,*}, J. Dolejsi¹²⁶, I. Dolenc⁷⁴, Z. Dolezal¹²⁶,
 B.A. Dolgoshein^{96,*}, T. Dohmae¹⁵⁵, M. Donadelli^{23d}, J. Donini³³, J. Dopke²⁹, A. Doria^{102a},
 A. Dos Anjos¹⁷³, A. Dotti^{122a,122b}, M.T. Dova⁷⁰, A.D. Doxiadis¹⁰⁵, A.T. Doyle⁵³, M. Dris⁹,
 J. Dubbert⁹⁹, S. Dube¹⁴, E. Duchovni¹⁷², G. Duckeck⁹⁸, A. Dudarev²⁹, F. Dudziak⁶³,
 M. Dührssen²⁹, I.P. Duerdoth⁸², L. Duflot¹¹⁵, M-A. Dufour⁸⁵, M. Dunford²⁹,
 H. Duran Yildiz^{3a}, R. Duxfield¹³⁹, M. Dwuznik³⁷, F. Dydak²⁹, M. Düren⁵², J. Ebke⁹⁸,
 S. Eckweiler⁸¹, K. Edmonds⁸¹, W. Edson¹, C.A. Edwards⁷⁶, N.C. Edwards⁵³,
 W. Ehrenfeld⁴¹, T. Eifert¹⁴³, G. Eigen¹³, K. Einsweiler¹⁴, E. Eisenhandler⁷⁵, T. Ekelof¹⁶⁶,
 M. El Kacimi^{135c}, M. Ellert¹⁶⁶, S. Elles⁴, F. Ellinghaus⁸¹, K. Ellis⁷⁵, N. Ellis²⁹,
 J. Elmsheuser⁹⁸, M. Elsing²⁹, D. Emeljanov¹²⁹, R. Engelmann¹⁴⁸, A. Engl⁹⁸, B. Epp⁶¹,
 J. Erdmann⁵⁴, A. Ereditato¹⁶, D. Eriksson^{146a}, J. Ernst¹, M. Ernst²⁴, J. Ernwein¹³⁶,
 D. Errede¹⁶⁵, S. Errede¹⁶⁵, E. Ertel⁸¹, M. Escalier¹¹⁵, H. Esch⁴², C. Escobar¹²³,
 X. Espinal Curull¹¹, B. Esposito⁴⁷, F. Etienne⁸³, A.I. Etienvre¹³⁶, E. Etzion¹⁵³,
 D. Evangelakou⁵⁴, H. Evans⁶⁰, L. Fabbri^{19a,19b}, C. Fabre²⁹, R.M. Fakhrutdinov¹²⁸,
 S. Falciano^{132a}, Y. Fang¹⁷³, M. Fanti^{89a,89b}, A. Farbin⁷, A. Farilla^{134a}, J. Farley¹⁴⁸,
 T. Farooque¹⁵⁸, S. Farrell¹⁶³, S.M. Farrington¹¹⁸, P. Farthouat²⁹, P. Fassnacht²⁹,
 D. Fassouliotis⁸, B. Fatholahzadeh¹⁵⁸, A. Favareto^{89a,89b}, L. Fayard¹¹⁵, S. Fazio^{36a,36b},
 R. Febbraro³³, P. Federic^{144a}, O.L. Fedin¹²¹, W. Fedorko⁸⁸, M. Fehling-Kaschek⁴⁸,
 L. Feligioni⁸³, D. Fellmann⁵, C. Feng^{32d}, E.J. Feng⁵, A.B. Fenyuk¹²⁸, J. Ferencei^{144b},
 W. Fernando⁵, S. Ferrag⁵³, J. Ferrando⁵³, V. Ferrara⁴¹, A. Ferrari¹⁶⁶, P. Ferrari¹⁰⁵,
 R. Ferrari^{119a}, D.E. Ferreira de Lima⁵³, A. Ferrer¹⁶⁷, D. Ferrere⁴⁹, C. Ferretti⁸⁷,
 A. Ferretto Parodi^{50a,50b}, M. Fiascaris³⁰, F. Fiedler⁸¹, A. Filipčić⁷⁴, F. Filthaut¹⁰⁴,
 M. Fincke-Keeler¹⁶⁹, M.C.N. Fiolhais^{124a,h}, L. Fiorini¹⁶⁷, A. Firan³⁹, G. Fischer⁴¹,
 M.J. Fisher¹⁰⁹, M. Flechl⁴⁸, I. Fleck¹⁴¹, J. Fleckner⁸¹, P. Fleischmann¹⁷⁴, S. Fleischmann¹⁷⁵,
 T. Flick¹⁷⁵, A. Floderus⁷⁹, L.R. Flores Castillo¹⁷³, M.J. Flowerdew⁹⁹, T. Fonseca Martin¹⁶,
 A. Formica¹³⁶, A. Forti⁸², D. Fortin^{159a}, D. Fournier¹¹⁵, H. Fox⁷¹, P. Francavilla¹¹,
 M. Franchini^{19a,19b}, S. Franchino^{119a,119b}, D. Francis²⁹, T. Frank¹⁷², S. Franz²⁹,
 M. Fraternali^{119a,119b}, S. Fratina¹²⁰, S.T. French²⁷, C. Friedrich⁴¹, F. Friedrich⁴³,
 R. Froeschl²⁹, D. Froidevaux²⁹, J.A. Frost²⁷, C. Fukunaga¹⁵⁶, E. Fullana Torregrosa²⁹,
 B.G. Fulson¹⁴³, J. Fuster¹⁶⁷, C. Gabaldon²⁹, O. Gabizon¹⁷², T. Gadfort²⁴, S. Gadomski⁴⁹,
 G. Gagliardi^{50a,50b}, P. Gagnon⁶⁰, C. Galea⁹⁸, E.J. Gallas¹¹⁸, V. Gallo¹⁶, B.J. Gallop¹²⁹,
 P. Gallus¹²⁵, K.K. Gan¹⁰⁹, Y.S. Gao^{143,e}, A. Gaponenko¹⁴, F. Garbersson¹⁷⁶,
 M. Garcia-Sciveres¹⁴, C. García¹⁶⁷, J.E. García Navarro¹⁶⁷, R.W. Gardner³⁰, N. Garelli²⁹,
 H. Garitaonandia¹⁰⁵, V. Garonne²⁹, J. Garvey¹⁷, C. Gatti⁴⁷, G. Gaudio^{119a}, B. Gaur¹⁴¹,
 L. Gauthier¹³⁶, P. Gauzzi^{132a,132b}, I.L. Gavrilenko⁹⁴, C. Gay¹⁶⁸, G. Gaycken²⁰, E.N. Gazis⁹,
 P. Ge^{32d}, Z. Gecse¹⁶⁸, C.N.P. Gee¹²⁹, D.A.A. Geerts¹⁰⁵, Ch. Geich-Gimbel²⁰,
 K. Gellerstedt^{146a,146b}, C. Gemme^{50a}, A. Gemmell⁵³, M.H. Genest⁵⁵, S. Gentile^{132a,132b},
 M. George⁵⁴, S. George⁷⁶, P. Gerlach¹⁷⁵, A. Gershon¹⁵³, C. Geweniger^{58a}, H. Ghazlane^{135b},
 N. Ghodbane³³, B. Giacobbe^{19a}, S. Giagu^{132a,132b}, V. Giakoumopoulou⁸, V. Giangiobbe¹¹,

F. Gianotti²⁹, B. Gibbard²⁴, A. Gibson¹⁵⁸, S.M. Gibson²⁹, D. Gillberg²⁸, A.R. Gillman¹²⁹,
 D.M. Gingrich^{2,d}, J. Ginzburg¹⁵³, N. Giokaris⁸, M.P. Giordani^{164c}, R. Giordano^{102a,102b},
 F.M. Giorgi¹⁵, P. Giovannini⁹⁹, P.F. Giraud¹³⁶, D. Giugni^{89a}, M. Giunta⁹³, P. Giusti^{19a},
 B.K. Gjelsten¹¹⁷, L.K. Gladilin⁹⁷, C. Glasman⁸⁰, J. Glatzer⁴⁸, A. Glazov⁴¹, K.W. Glitza¹⁷⁵,
 G.L. Glonti⁶⁴, J.R. Goddard⁷⁵, J. Godfrey¹⁴², J. Godlewski²⁹, M. Goebel⁴¹, T. Göpfert⁴³,
 C. Goeringer⁸¹, C. Gössling⁴², S. Goldfarb⁸⁷, T. Golling¹⁷⁶, A. Gomes^{124a,b},
 L.S. Gomez Fajardo⁴¹, R. Gonçalo⁷⁶, J. Goncalves Pinto Firmino Da Costa⁴¹, L. Gonella²⁰,
 S. Gonzalez¹⁷³, S. González de la Hoz¹⁶⁷, G. Gonzalez Parra¹¹, M.L. Gonzalez Silva²⁶,
 S. Gonzalez-Sevilla⁴⁹, J.J. Goodson¹⁴⁸, L. Goossens²⁹, P.A. Gorbounov⁹⁵, H.A. Gordon²⁴,
 I. Gorelov¹⁰³, G. Gorfine¹⁷⁵, B. Gorini²⁹, E. Gorini^{72a,72b}, A. Gorišek⁷⁴, E. Gornicki³⁸,
 B. Gosdzik⁴¹, A.T. Goshaw⁵, M. Gosselink¹⁰⁵, M.I. Gostkin⁶⁴, I. Gough Eschrich¹⁶³,
 M. Gouighri^{135a}, D. Goujdami^{135c}, M.P. Goulette⁴⁹, A.G. Goussiou¹³⁸, C. Goy⁴,
 S. Gozpinar²², I. Grabowska-Bold³⁷, P. Grafström^{19a,19b}, K.-J. Grahn⁴¹, F. Grancagnolo^{72a},
 S. Grancagnolo¹⁵, V. Grassi¹⁴⁸, V. Gratchev¹²¹, N. Grau³⁴, H.M. Gray²⁹, J.A. Gray¹⁴⁸,
 E. Graziani^{134a}, O.G. Grebenyuk¹²¹, T. Greenshaw⁷³, Z.D. Greenwood^{24,m}, K. Gregersen³⁵,
 I.M. Gregor⁴¹, P. Grenier¹⁴³, J. Griffiths¹³⁸, N. Grigalashvili⁶⁴, A.A. Grillo¹³⁷,
 S. Grinstein¹¹, Y.V. Grishkevich⁹⁷, J.-F. Grivaz¹¹⁵, E. Gross¹⁷², J. Grosse-Knetter⁵⁴,
 J. Groth-Jensen¹⁷², K. Grybel¹⁴¹, D. Guest¹⁷⁶, C. Guicheney³³, A. Guida^{72a,72b},
 S. Guindon⁵⁴, U. Gul⁵³, H. Guler^{85,p}, J. Gunther¹²⁵, B. Guo¹⁵⁸, J. Guo³⁴, P. Gutierrez¹¹¹,
 N. Guttman¹⁵³, O. Gutzwiller¹⁷³, C. Guyot¹³⁶, C. Gwenlan¹¹⁸, C.B. Gwilliam⁷³, A. Haas¹⁴³,
 S. Haas²⁹, C. Haber¹⁴, H.K. Hadavand³⁹, D.R. Hadley¹⁷, P. Haefner²⁰, F. Hahn²⁹,
 S. Haider²⁹, Z. Hajduk³⁸, H. Hakobyan¹⁷⁷, D. Hall¹¹⁸, J. Haller⁵⁴, K. Hamacher¹⁷⁵,
 P. Hamal¹¹³, M. Hamer⁵⁴, A. Hamilton^{145b,q}, S. Hamilton¹⁶¹, L. Han^{32b}, K. Hanagaki¹¹⁶,
 K. Hanawa¹⁶⁰, M. Hance¹⁴, C. Handel⁸¹, P. Hanke^{58a}, J.R. Hansen³⁵, J.B. Hansen³⁵,
 J.D. Hansen³⁵, P.H. Hansen³⁵, P. Hansson¹⁴³, K. Hara¹⁶⁰, G.A. Hare¹³⁷, T. Harenberg¹⁷⁵,
 S. Harkusha⁹⁰, D. Harper⁸⁷, R.D. Harrington⁴⁵, O.M. Harris¹³⁸, J. Hartert⁴⁸, F. Hartjes¹⁰⁵,
 T. Haruyama⁶⁵, A. Harvey⁵⁶, S. Hasegawa¹⁰¹, Y. Hasegawa¹⁴⁰, S. Hassani¹³⁶, S. Haug¹⁶,
 M. Hauschild²⁹, R. Hauser⁸⁸, M. Havranek²⁰, C.M. Hawkes¹⁷, R.J. Hawkings²⁹,
 A.D. Hawkins⁷⁹, D. Hawkins¹⁶³, T. Hayakawa⁶⁶, T. Hayashi¹⁶⁰, D. Hayden⁷⁶, C.P. Hays¹¹⁸,
 H.S. Hayward⁷³, S.J. Haywood¹²⁹, M. He^{32d}, S.J. Head¹⁷, V. Hedberg⁷⁹, L. Heelan⁷,
 S. Heim⁸⁸, B. Heinemann¹⁴, S. Heisterkamp³⁵, L. Helary²¹, C. Heller⁹⁸, M. Heller²⁹,
 S. Hellman^{146a,146b}, D. Hellmich²⁰, C. Hensens¹¹, R.C.W. Henderson⁷¹, M. Henke^{58a},
 A. Henrichs⁵⁴, A.M. Henriques Correia²⁹, S. Henrot-Versille¹¹⁵, C. Hensel⁵⁴, T. Henß¹⁷⁵,
 C.M. Hernandez⁷, Y. Hernández Jiménez¹⁶⁷, R. Herrberg¹⁵, G. Herten⁴⁸, R. Hertenberger⁹⁸,
 L. Hervas²⁹, G.G. Hesketh⁷⁷, N.P. Hessey¹⁰⁵, E. Higón-Rodríguez¹⁶⁷, J.C. Hill²⁷,
 K.H. Hiller⁴¹, S. Hillert²⁰, S.J. Hillier¹⁷, I. Hinchliffe¹⁴, E. Hines¹²⁰, M. Hirose¹¹⁶,
 F. Hirsch⁴², D. Hirschbuehl¹⁷⁵, J. Hobbs¹⁴⁸, N. Hod¹⁵³, M.C. Hodgkinson¹³⁹, P. Hodgson¹³⁹,
 A. Hoecker²⁹, M.R. Hoferkamp¹⁰³, J. Hoffman³⁹, D. Hoffmann⁸³, M. Hohlfeld⁸¹,
 M. Holder¹⁴¹, S.O. Holmgren^{146a}, T. Holy¹²⁷, J.L. Holzbauer⁸⁸, T.M. Hong¹²⁰,
 L. Hooft van Huysduynen¹⁰⁸, C. Horn¹⁴³, S. Horner⁴⁸, J.-Y. Hostachy⁵⁵, S. Hou¹⁵¹,
 A. Hoummada^{135a}, J. Howard¹¹⁸, J. Howarth⁸², I. Hristova¹⁵, J. Hrivnac¹¹⁵, T. Hryn'ova⁴,

P.J. Hsu⁸¹, S.-C. Hsu¹⁴, Z. Hubacek¹²⁷, F. Hubaut⁸³, F. Huegging²⁰, A. Huettmann⁴¹,
 T.B. Huffman¹¹⁸, E.W. Hughes³⁴, G. Hughes⁷¹, M. Huhtinen²⁹, M. Hurwitz¹⁴,
 U. Husemann⁴¹, N. Huseynov^{64,r}, J. Huston⁸⁸, J. Huth⁵⁷, G. Iacobucci⁴⁹, G. Iakovidis⁹,
 M. Ibbotson⁸², I. Ibragimov¹⁴¹, L. Iconomidou-Fayard¹¹⁵, J. Idarraga¹¹⁵, P. Iengo^{102a},
 O. Igonkina¹⁰⁵, Y. Ikegami⁶⁵, M. Ikeno⁶⁵, D. Iliadis¹⁵⁴, N. Ilic¹⁵⁸, T. Ince²⁰,
 J. Inigo-Golfin²⁹, P. Ioannou⁸, M. Iodice^{134a}, K. Iordanidou⁸, V. Ippolito^{132a,132b},
 A. Irles Quiles¹⁶⁷, C. Isaksson¹⁶⁶, M. Ishino⁶⁷, M. Ishitsuka¹⁵⁷, R. Ishmukhametov³⁹,
 C. Issever¹¹⁸, S. Istin^{18a}, A.V. Ivashin¹²⁸, W. Iwanski³⁸, H. Iwasaki⁶⁵, J.M. Izen⁴⁰,
 V. Izzo^{102a}, B. Jackson¹²⁰, J.N. Jackson⁷³, P. Jackson¹⁴³, M.R. Jaekel²⁹, V. Jain⁶⁰,
 K. Jakobs⁴⁸, S. Jakobsen³⁵, T. Jakoubek¹²⁵, J. Jakubek¹²⁷, D.K. Jana¹¹¹, E. Jansen⁷⁷,
 H. Jansen²⁹, A. Jantsch⁹⁹, M. Janus⁴⁸, G. Jarlskog⁷⁹, L. Jeanty⁵⁷, I. Jen-La Plante³⁰,
 P. Jenni²⁹, A. Jeremie⁴, P. Jez³⁵, S. Jézéquel⁴, M.K. Jha^{19a}, H. Ji¹⁷³, W. Ji⁸¹, J. Jia¹⁴⁸,
 Y. Jiang^{32b}, M. Jimenez Belenguer⁴¹, S. Jin^{32a}, O. Jinnouchi¹⁵⁷, M.D. Joergensen³⁵,
 D. Joffe³⁹, M. Johansen^{146a,146b}, K.E. Johansson^{146a}, P. Johansson¹³⁹, S. Johnert⁴¹,
 K.A. Johns⁶, K. Jon-And^{146a,146b}, G. Jones¹⁷⁰, R.W.L. Jones⁷¹, T.J. Jones⁷³, C. Joram²⁹,
 P.M. Jorge^{124a}, K.D. Joshi⁸², J. Jovicevic¹⁴⁷, T. Jovin^{12b}, X. Ju¹⁷³, C.A. Jung⁴²,
 R.M. Jungst²⁹, V. Juranek¹²⁵, P. Jussel⁶¹, A. Juste Rozas¹¹, S. Kabana¹⁶, M. Kaci¹⁶⁷,
 A. Kaczmarska³⁸, P. Kadlecik³⁵, M. Kado¹¹⁵, H. Kagan¹⁰⁹, M. Kagan⁵⁷, E. Kajomovitz¹⁵²,
 S. Kalinin¹⁷⁵, L.V. Kalinovskaya⁶⁴, S. Kama³⁹, N. Kanaya¹⁵⁵, M. Kaneda²⁹, S. Kaneti²⁷,
 T. Kanno¹⁵⁷, V.A. Kantserov⁹⁶, J. Kanzaki⁶⁵, B. Kaplan¹⁷⁶, A. Kapliy³⁰, J. Kaplon²⁹,
 D. Kar⁵³, M. Karagounis²⁰, K. Karakostas⁹, M. Karnevskiy⁴¹, V. Kartvelishvili⁷¹,
 A.N. Karyukhin¹²⁸, L. Kashif¹⁷³, G. Kasieczka^{58b}, R.D. Kass¹⁰⁹, A. Kastanas¹³,
 M. Kataoka⁴, Y. Kataoka¹⁵⁵, E. Katsoufis⁹, J. Katzy⁴¹, V. Kaushik⁶, K. Kawagoe⁶⁹,
 T. Kawamoto¹⁵⁵, G. Kawamura⁸¹, M.S. Kayl¹⁰⁵, V.A. Kazanin¹⁰⁷, M.Y. Kazarinov⁶⁴,
 R. Keeler¹⁶⁹, R. Kehoe³⁹, M. Keil⁵⁴, G.D. Kekelidze⁶⁴, J.S. Keller¹³⁸, M. Kenyon⁵³,
 O. Kepka¹²⁵, N. Kerschen²⁹, B.P. Kerševan⁷⁴, S. Kersten¹⁷⁵, K. Kessoku¹⁵⁵, J. Keung¹⁵⁸,
 F. Khalil-zada¹⁰, H. Khandanyan¹⁶⁵, A. Khanov¹¹², D. Kharchenko⁶⁴, A. Khodinov⁹⁶,
 A. Khomich^{58a}, T.J. Khoo²⁷, G. Khoriauli²⁰, A. Khoroshilov¹⁷⁵, V. Khovanskiy⁹⁵,
 E. Khramov⁶⁴, J. Khubua^{51b}, H. Kim^{146a,146b}, S.H. Kim¹⁶⁰, N. Kimura¹⁷¹, O. Kind¹⁵,
 B.T. King⁷³, M. King⁶⁶, R.S.B. King¹¹⁸, J. Kirk¹²⁹, A.E. Kiryunin⁹⁹, T. Kishimoto⁶⁶,
 D. Kisielewska³⁷, T. Kittelmann¹²³, E. Kladiva^{144b}, M. Klein⁷³, U. Klein⁷³,
 K. Kleinknecht⁸¹, M. Klemetti⁸⁵, A. Klier¹⁷², P. Klimek^{146a,146b}, A. Klimentov²⁴,
 R. Klingenberg⁴², J.A. Klinger⁸², E.B. Klinkby³⁵, T. Klioutchnikova²⁹, P.F. Klok¹⁰⁴,
 S. Klous¹⁰⁵, E.-E. Kluge^{58a}, T. Kluge⁷³, P. Kluit¹⁰⁵, S. Kluth⁹⁹, N.S. Knecht¹⁵⁸,
 E. Kneringer⁶¹, E.B.F.G. Knoops⁸³, A. Knue⁵⁴, B.R. Ko⁴⁴, T. Kobayashi¹⁵⁵, M. Kobel⁴³,
 M. Kocian¹⁴³, P. Kodys¹²⁶, K. Köneke²⁹, A.C. König¹⁰⁴, S. Koenig⁸¹, L. Köpke⁸¹,
 F. Koetsveld¹⁰⁴, P. Koevesarki²⁰, T. Koffas²⁸, E. Koffeman¹⁰⁵, L.A. Kogan¹¹⁸,
 S. Kohlmann¹⁷⁵, F. Kohn⁵⁴, Z. Kohout¹²⁷, T. Kohriki⁶⁵, T. Koi¹⁴³, G.M. Kolachev¹⁰⁷,
 H. Kolanoski¹⁵, V. Kolesnikov⁶⁴, I. Koletsou^{89a}, J. Koll⁸⁸, M. Kollefrath⁴⁸, A.A. Komar⁹⁴,
 Y. Komori¹⁵⁵, T. Kondo⁶⁵, T. Kono^{41,s}, A.I. Kononov⁴⁸, R. Konoplich^{108,t},
 N. Konstantinidis⁷⁷, S. Koperny³⁷, K. Korcyl³⁸, K. Kordas¹⁵⁴, A. Korn¹¹⁸, A. Korol¹⁰⁷,

I. Korolkov¹¹, E.V. Korolkova¹³⁹, V.A. Korotkov¹²⁸, O. Kortner⁹⁹, S. Kortner⁹⁹,
 V.V. Kostyukhin²⁰, S. Kotov⁹⁹, V.M. Kotov⁶⁴, A. Kotwal⁴⁴, C. Kourkoumelis⁸,
 V. Kouskoura¹⁵⁴, A. Koutsman^{159a}, R. Kowalewski¹⁶⁹, T.Z. Kowalski³⁷, W. Kozanecki¹³⁶,
 A.S. Kozhin¹²⁸, V. Kral¹²⁷, V.A. Kramarenko⁹⁷, G. Kramberger⁷⁴, M.W. Krasny⁷⁸,
 A. Krasznahorkay¹⁰⁸, J. Kraus⁸⁸, J.K. Kraus²⁰, S. Kreiss¹⁰⁸, F. Krejci¹²⁷, J. Kretzschmar⁷³,
 N. Krieger⁵⁴, P. Krieger¹⁵⁸, K. Kroeninger⁵⁴, H. Kroha⁹⁹, J. Kroll¹²⁰, J. Kroseberg²⁰,
 J. Krstic^{12a}, U. Kruchonak⁶⁴, H. Krüger²⁰, T. Kruker¹⁶, N. Krumnack⁶³,
 Z.V. Krumshateyn⁶⁴, A. Kruth²⁰, T. Kubota⁸⁶, S. Kuday^{3a}, S. Kuehn⁴⁸, A. Kugel^{58c},
 T. Kuhl⁴¹, D. Kuhn⁶¹, V. Kukhtin⁶⁴, Y. Kulchitsky⁹⁰, S. Kuleshov^{31b}, C. Kummer⁹⁸,
 M. Kuna⁷⁸, J. Kunkle¹²⁰, A. Kupco¹²⁵, H. Kurashige⁶⁶, M. Kurata¹⁶⁰, Y.A. Kurochkin⁹⁰,
 V. Kus¹²⁵, E.S. Kuwertz¹⁴⁷, M. Kuze¹⁵⁷, J. Kvita¹⁴², R. Kwee¹⁵, A. La Rosa⁴⁹,
 L. La Rotonda^{36a,36b}, L. Labarga⁸⁰, J. Labbe⁴, S. Lablak^{135a}, C. Lacasta¹⁶⁷,
 F. Lacava^{132a,132b}, H. Lacker¹⁵, D. Lacour⁷⁸, V.R. Lacuesta¹⁶⁷, E. Ladygin⁶⁴, R. Lafaye⁴,
 B. Laforge⁷⁸, T. Lagouri⁸⁰, S. Lai⁴⁸, E. Laisne⁵⁵, M. Lamanna²⁹, L. Lambourne⁷⁷,
 C.L. Lampen⁶, W. Lampl⁶, E. Lancon¹³⁶, U. Landgraf⁴⁸, M.P.J. Landon⁷⁵, J.L. Lane⁸²,
 V.S. Lang^{58a}, C. Lange⁴¹, A.J. Lankford¹⁶³, F. Lanni²⁴, K. Lantzsch¹⁷⁵, S. Laplace⁷⁸,
 C. Lapoire²⁰, J.F. Laporte¹³⁶, T. Lari^{89a}, A. Larner¹¹⁸, M. Lassnig²⁹, P. Laurelli⁴⁷,
 V. Lavorini^{36a,36b}, W. Lavrijsen¹⁴, P. Laycock⁷³, O. Le Dortz⁷⁸, E. Le Guirriec⁸³,
 C. Le Maner¹⁵⁸, E. Le Menedeu¹¹, T. LeCompte⁵, F. Ledroit-Guillon⁵⁵, H. Lee¹⁰⁵,
 J.S.H. Lee¹¹⁶, S.C. Lee¹⁵¹, L. Lee¹⁷⁶, M. Lefebvre¹⁶⁹, M. Legendre¹³⁶, F. Legger⁹⁸,
 C. Leggett¹⁴, M. Lehmacher²⁰, G. Lehmann Miotto²⁹, X. Lei⁶, M.A.L. Leite^{23d},
 R. Leitner¹²⁶, D. Lellouch¹⁷², B. Lemmer⁵⁴, V. Lendermann^{58a}, K.J.C. Leney^{145b},
 T. Lenz¹⁰⁵, G. Lenzen¹⁷⁵, B. Lenzi²⁹, K. Leonhardt⁴³, S. Leontsinis⁹, F. Lepold^{58a},
 C. Leroy⁹³, J-R. Lessard¹⁶⁹, C.G. Lester²⁷, C.M. Lester¹²⁰, J. Levêque⁴, D. Levin⁸⁷,
 L.J. Levinson¹⁷², A. Lewis¹¹⁸, G.H. Lewis¹⁰⁸, A.M. Leyko²⁰, M. Leyton¹⁵, B. Li⁸³, H. Li^{173,u},
 S. Li^{32b,v}, X. Li⁸⁷, Z. Liang^{118,w}, H. Liao³³, B. Liberti^{133a}, P. Lichard²⁹, M. Lichtnecker⁹⁸,
 K. Lie¹⁶⁵, W. Liebig¹³, C. Limbach²⁰, A. Limosani⁸⁶, M. Limper⁶², S.C. Lin^{151,x},
 F. Linde¹⁰⁵, J.T. Linnemann⁸⁸, E. Lipeles¹²⁰, A. Lipniacka¹³, T.M. Liss¹⁶⁵, D. Lissauer²⁴,
 A. Lister⁴⁹, A.M. Litke¹³⁷, C. Liu²⁸, D. Liu¹⁵¹, H. Liu⁸⁷, J.B. Liu⁸⁷, L. Liu⁸⁷, M. Liu^{32b},
 Y. Liu^{32b}, M. Livan^{119a,119b}, S.S.A. Livermore¹¹⁸, A. Lleres⁵⁵, J. Llorente Merino⁸⁰,
 S.L. Lloyd⁷⁵, E. Lobodzinska⁴¹, P. Loch⁶, W.S. Lockman¹³⁷, T. Loddenkoetter²⁰,
 F.K. Loebinger⁸², A. Loginov¹⁷⁶, C.W. Loh¹⁶⁸, T. Lohse¹⁵, K. Lohwasser⁴⁸, M. Lokajicek¹²⁵,
 V.P. Lombardo⁴, R.E. Long⁷¹, L. Lopes^{124a}, D. Lopez Mateos⁵⁷, J. Lorenz⁹⁸,
 N. Lorenzo Martinez¹¹⁵, M. Losada¹⁶², P. Loscutoff¹⁴, F. Lo Sterzo^{132a,132b}, M.J. Losty^{159a},
 X. Lou⁴⁰, A. Lounis¹¹⁵, K.F. Loureiro¹⁶², J. Love²¹, P.A. Love⁷¹, A.J. Lowe^{143,e}, F. Lu^{32a},
 H.J. Lubatti¹³⁸, C. Luci^{132a,132b}, A. Lucotte⁵⁵, A. Ludwig⁴³, D. Ludwig⁴¹, I. Ludwig⁴⁸,
 J. Ludwig⁴⁸, F. Luehring⁶⁰, G. Luijckx¹⁰⁵, W. Lukas⁶¹, D. Lumb⁴⁸, L. Luminari^{132a},
 E. Lund¹¹⁷, B. Lund-Jensen¹⁴⁷, B. Lundberg⁷⁹, J. Lundberg^{146a,146b}, O. Lundberg^{146a,146b},
 J. Lundquist³⁵, M. Lungwitz⁸¹, D. Lynn²⁴, E. Lytken⁷⁹, H. Ma²⁴, L.L. Ma¹⁷³,
 G. Maccarrone⁴⁷, A. Macchiolo⁹⁹, B. Maček⁷⁴, J. Machado Miguens^{124a}, R. Mackeprang³⁵,
 R.J. Madaras¹⁴, W.F. Mader⁴³, R. Maenner^{58c}, T. Maeno²⁴, P. Mättig¹⁷⁵, S. Mättig⁴¹,

L. Magnoni²⁹, E. Magradze⁵⁴, K. Mahboubi⁴⁸, S. Mahmoud⁷³, G. Mahout¹⁷, C. Maiani¹³⁶,
 C. Maidantchik^{23a}, A. Maio^{124a,b}, S. Majewski²⁴, Y. Makida⁶⁵, N. Makovec¹¹⁵, P. Mal¹³⁶,
 B. Malaescu²⁹, Pa. Malecki³⁸, P. Malecki³⁸, V.P. Maleev¹²¹, F. Malek⁵⁵, U. Mallik⁶²,
 D. Malon⁵, C. Malone¹⁴³, S. Maltezos⁹, V. Malyshev¹⁰⁷, S. Malyukov²⁹, R. Mameghani⁹⁸,
 J. Mamuzic^{12b}, A. Manabe⁶⁵, L. Mandelli^{89a}, I. Mandić⁷⁴, R. Mandrysch¹⁵, J. Maneira^{124a},
 P.S. Mangeard⁸⁸, L. Manhaes de Andrade Filho^{23a}, A. Mann⁵⁴, P.M. Manning¹³⁷,
 A. Manousakis-Katsikakis⁸, B. Mansoulie¹³⁶, A. Mapelli²⁹, L. Mapelli²⁹, L. March⁸⁰,
 J.F. Marchand²⁸, F. Marchese^{133a,133b}, G. Marchiori⁷⁸, M. Marcisovsky¹²⁵, C.P. Marino¹⁶⁹,
 F. Marroquin^{23a}, Z. Marshall²⁹, F.K. Martens¹⁵⁸, L.F. Marti¹⁶, S. Marti-Garcia¹⁶⁷,
 B. Martin²⁹, B. Martin⁸⁸, J.P. Martin⁹³, T.A. Martin¹⁷, V.J. Martin⁴⁵,
 B. Martin dit Latour⁴⁹, S. Martin-Haugh¹⁴⁹, M. Martinez¹¹, V. Martinez Outschoorn⁵⁷,
 A.C. Martyniuk¹⁶⁹, M. Marx⁸², F. Marzano^{132a}, A. Marzin¹¹¹, L. Masetti⁸¹, T. Mashimo¹⁵⁵,
 R. Mashinistov⁹⁴, J. Masik⁸², A.L. Maslennikov¹⁰⁷, I. Massa^{19a,19b}, G. Massaro¹⁰⁵,
 N. Massol⁴, A. Mastroberardino^{36a,36b}, T. Masubuchi¹⁵⁵, P. Matricon¹¹⁵, H. Matsunaga¹⁵⁵,
 T. Matsushita⁶⁶, C. Mattravers^{118,c}, J. Maurer⁸³, S.J. Maxfield⁷³, A. Mayne¹³⁹,
 R. Mazini¹⁵¹, M. Mazur²⁰, L. Mazzaferro^{133a,133b}, M. Mazzanti^{89a}, S.P. Mc Kee⁸⁷,
 A. McCarn¹⁶⁵, R.L. McCarthy¹⁴⁸, T.G. McCarthy²⁸, N.A. McCubbin¹²⁹, K.W. McFarlane⁵⁶,
 J.A. MCFayden¹³⁹, H. McGlone⁵³, G. Mchedlidze^{51b}, T. McLaughlan¹⁷, S.J. McMahan¹²⁹,
 R.A. McPherson^{169,k}, A. Meade⁸⁴, J. Mechnich¹⁰⁵, M. Mechtel¹⁷⁵, M. Medinnis⁴¹,
 R. Meera-Lebbai¹¹¹, T. Meguro¹¹⁶, R. Mehdiyev⁹³, S. Mehlhase³⁵, A. Mehta⁷³, K. Meier^{58a},
 B. Meirose⁷⁹, C. Melachrinou³⁰, B.R. Mellado Garcia¹⁷³, F. Meloni^{89a,89b},
 L. Mendoza Navas¹⁶², Z. Meng^{151,u}, A. Mengarelli^{19a,19b}, S. Menke⁹⁹, E. Meoni¹⁶¹,
 K.M. Mercurio⁵⁷, P. Mermod⁴⁹, L. Merola^{102a,102b}, C. Meroni^{89a}, F.S. Merritt³⁰,
 H. Merritt¹⁰⁹, A. Messina^{29,y}, J. Metcalfe¹⁰³, A.S. Mete¹⁶³, C. Meyer⁸¹, C. Meyer³⁰,
 J-P. Meyer¹³⁶, J. Meyer¹⁷⁴, J. Meyer⁵⁴, T.C. Meyer²⁹, W.T. Meyer⁶³, J. Miao^{32d},
 S. Michal²⁹, L. Micu^{25a}, R.P. Middleton¹²⁹, S. Migas⁷³, L. Mijović¹³⁶, G. Mikenberg¹⁷²,
 M. Mikestikova¹²⁵, M. Mikuž⁷⁴, D.W. Miller³⁰, R.J. Miller⁸⁸, W.J. Mills¹⁶⁸, C. Mills⁵⁷,
 A. Milov¹⁷², D.A. Milstead^{146a,146b}, D. Milstein¹⁷², A.A. Minaenko¹²⁸, M. Miñano Moya¹⁶⁷,
 I.A. Minashvili⁶⁴, A.I. Mincer¹⁰⁸, B. Mindur³⁷, M. Mineev⁶⁴, Y. Ming¹⁷³, L.M. Mir¹¹,
 G. Mirabelli^{132a}, J. Mitrevski¹³⁷, V.A. Mitsou¹⁶⁷, S. Mitsui⁶⁵, P.S. Miyagawa¹³⁹,
 J.U. Mjörnmark⁷⁹, T. Moa^{146a,146b}, V. Moeller²⁷, K. Mönig⁴¹, N. Möser²⁰, S. Mohapatra¹⁴⁸,
 W. Mohr⁴⁸, R. Moles-Valls¹⁶⁷, J. Monk⁷⁷, E. Monnier⁸³, J. Montejo Berlingen¹¹,
 S. Montesano^{89a,89b}, F. Monticelli⁷⁰, S. Monzani^{19a,19b}, R.W. Moore², G.F. Moorhead⁸⁶,
 C. Mora Herrera⁴⁹, A. Moraes⁵³, N. Morange¹³⁶, J. Morel⁵⁴, G. Morello^{36a,36b}, D. Moreno⁸¹,
 M. Moreno Llácer¹⁶⁷, P. Morettini^{50a}, M. Morgenstern⁴³, M. Morii⁵⁷, A.K. Morley²⁹,
 G. Mornacchi²⁹, J.D. Morris⁷⁵, L. Morvaj¹⁰¹, H.G. Moser⁹⁹, M. Mosidze^{51b}, J. Moss¹⁰⁹,
 R. Mount¹⁴³, E. Mountricha^{9,z}, S.V. Mouraviev⁹⁴, E.J.W. Moyse⁸⁴, F. Mueller^{58a},
 J. Mueller¹²³, K. Mueller²⁰, T.A. Müller⁹⁸, T. Mueller⁸¹, D. Muenstermann²⁹,
 Y. Munwes¹⁵³, W.J. Murray¹²⁹, I. Mussche¹⁰⁵, E. Musto^{102a,102b}, A.G. Myagkov¹²⁸,
 M. Myska¹²⁵, J. Nadal¹¹, K. Nagai¹⁶⁰, K. Nagano⁶⁵, A. Nagarkar¹⁰⁹, Y. Nagasaka⁵⁹,
 M. Nagel⁹⁹, A.M. Nairz²⁹, Y. Nakahama²⁹, K. Nakamura¹⁵⁵, T. Nakamura¹⁵⁵, I. Nakano¹¹⁰,

G. Nanava²⁰, A. Napier¹⁶¹, R. Narayan^{58b}, M. Nash^{77,c}, T. Nattermann²⁰, T. Naumann⁴¹,
 G. Navarro¹⁶², H.A. Neal⁸⁷, P.Yu. Nechaeva⁹⁴, T.J. Neep⁸², A. Negri^{119a,119b}, G. Negri²⁹,
 S. Nektarijevic⁴⁹, A. Nelson¹⁶³, T.K. Nelson¹⁴³, S. Nemecek¹²⁵, P. Nemethy¹⁰⁸,
 A.A. Nepomuceno^{23a}, M. Nessi^{29,aa}, M.S. Neubauer¹⁶⁵, A. Neusiedl⁸¹, R.M. Neves¹⁰⁸,
 P. Nevski²⁴, P.R. Newman¹⁷, V. Nguyen Thi Hong¹³⁶, R.B. Nickerson¹¹⁸, R. Nicolaidou¹³⁶,
 B. Nicquevert²⁹, F. Niedercorn¹¹⁵, J. Nielsen¹³⁷, N. Nikiforou³⁴, A. Nikiforov¹⁵,
 V. Nikolaenko¹²⁸, I. Nikolic-Audit⁷⁸, K. Nikolics⁴⁹, K. Nikolopoulos²⁴, H. Nilsen⁴⁸,
 P. Nilsson⁷, Y. Ninomiya¹⁵⁵, A. Nisati^{132a}, R. Nisius⁹⁹, T. Nobe¹⁵⁷, L. Nodulman⁵,
 M. Nomachi¹¹⁶, I. Nomidis¹⁵⁴, M. Nordberg²⁹, P.R. Norton¹²⁹, J. Novakova¹²⁶, M. Nozaki⁶⁵,
 L. Nozka¹¹³, I.M. Nugent^{159a}, A.-E. Nuncio-Quiroz²⁰, G. Nunes Hanninger⁸⁶,
 T. Nunnemann⁹⁸, E. Nurse⁷⁷, B.J. O'Brien⁴⁵, S.W. O'Neale^{17,*}, D.C. O'Neil¹⁴²,
 V. O'Shea⁵³, L.B. Oakes⁹⁸, F.G. Oakham^{28,d}, H. Oberlack⁹⁹, J. Ocariz⁷⁸, A. Ochi⁶⁶,
 S. Oda⁶⁹, S. Odaka⁶⁵, J. Odier⁸³, H. Ogren⁶⁰, A. Oh⁸², S.H. Oh⁴⁴, C.C. Ohm^{146a,146b},
 T. Ohshima¹⁰¹, H. Okawa¹⁶³, Y. Okumura³⁰, T. Okuyama¹⁵⁵, A. Olariu^{25a},
 A.G. Olchevski⁶⁴, S.A. Olivares Pino^{31a}, M. Oliveira^{124a,h}, D. Oliveira Damazio²⁴,
 E. Oliver Garcia¹⁶⁷, D. Olivito¹²⁰, A. Olszewski³⁸, J. Olszowska³⁸, A. Onofre^{124a,ab},
 P.U.E. Onyisi³⁰, C.J. Oram^{159a}, M.J. Oreglia³⁰, Y. Oren¹⁵³, D. Orestano^{134a,134b},
 N. Orlando^{72a,72b}, I. Orlov¹⁰⁷, C. Oropeza Barrera⁵³, R.S. Orr¹⁵⁸, B. Osculati^{50a,50b},
 R. Ospanov¹²⁰, C. Osuna¹¹, G. Otero y Garzon²⁶, J.P. Ottersbach¹⁰⁵, M. Ouchrif^{135d},
 E.A. Ouellette¹⁶⁹, F. Ould-Saada¹¹⁷, A. Ouraou¹³⁶, Q. Ouyang^{32a}, A. Ovcharova¹⁴,
 M. Owen⁸², S. Owen¹³⁹, V.E. Ozcan^{18a}, N. Ozturk⁷, A. Pacheco Pages¹¹,
 C. Padilla Aranda¹¹, S. Pagan Griso¹⁴, E. Paganis¹³⁹, F. Paige²⁴, P. Pais⁸⁴, K. Pajchel¹¹⁷,
 G. Palacino^{159b}, C.P. Paleari⁶, S. Palestini²⁹, D. Pallin³³, A. Palma^{124a}, J.D. Palmer¹⁷,
 Y.B. Pan¹⁷³, E. Panagiotopoulou⁹, P. Pani¹⁰⁵, N. Panikashvili⁸⁷, S. Panitkin²⁴,
 D. Pantea^{25a}, A. Papadelis^{146a}, Th.D. Papadopoulou⁹, A. Paramonov⁵,
 D. Paredes Hernandez³³, W. Park^{24,ac}, M.A. Parker²⁷, F. Parodi^{50a,50b}, J.A. Parsons³⁴,
 U. Parzefall⁴⁸, S. Pashapour⁵⁴, E. Pasqualucci^{132a}, S. Passaggio^{50a}, A. Passeri^{134a},
 F. Pastore^{134a,134b}, Fr. Pastore⁷⁶, G. Pásztor^{49,ad}, S. Pataria¹⁷⁵, N. Patel¹⁵⁰, J.R. Pater⁸²,
 S. Patricelli^{102a,102b}, T. Pauly²⁹, M. Pecsny^{144a}, M.I. Pedraza Morales¹⁷³,
 S.V. Peleganchuk¹⁰⁷, D. Pelikan¹⁶⁶, H. Peng^{32b}, B. Penning³⁰, A. Penson³⁴, J. Penwell⁶⁰,
 M. Perantoni^{23a}, K. Perez^{34,ae}, T. Perez Cavalcanti⁴¹, E. Perez Codina^{159a}, M.T. Pérez
 García-Estanz¹⁶⁷, V. Perez Reale³⁴, L. Perini^{89a,89b}, H. Pernegger²⁹, R. Perrino^{72a},
 P. Perrodo⁴, V.D. Peshekhonov⁶⁴, K. Peters²⁹, B.A. Petersen²⁹, J. Petersen²⁹,
 T.C. Petersen³⁵, E. Petit⁴, A. Petridis¹⁵⁴, C. Petridou¹⁵⁴, E. Petrolo^{132a},
 F. Petrucci^{134a,134b}, D. Petschull⁴¹, M. Petteni¹⁴², R. Pezoa^{31b}, A. Phan⁸⁶, P.W. Phillips¹²⁹,
 G. Piacquadio²⁹, A. Picazio⁴⁹, E. Piccaro⁷⁵, M. Piccinini^{19a,19b}, S.M. Piec⁴¹, R. Piegai²⁶,
 D.T. Pignotti¹⁰⁹, J.E. Pilcher³⁰, A.D. Pilkington⁸², J. Pina^{124a,b}, M. Pinamonti^{164a,164c},
 A. Pinder¹¹⁸, J.L. Pinfold², B. Pinto^{124a}, C. Pizio^{89a,89b}, M. Plamondon¹⁶⁹, M.-A. Pleier²⁴,
 E. Plotnikova⁶⁴, A. Poblaguev²⁴, S. Poddar^{58a}, F. Podlyski³³, L. Poggioli¹¹⁵,
 T. Poghosyan²⁰, M. Pohl⁴⁹, G. Polesello^{119a}, A. Policicchio^{36a,36b}, A. Polini^{19a}, J. Poll⁷⁵,
 V. Polychronakos²⁴, D. Pomeroy²², K. Pommès²⁹, L. Pontecorvo^{132a}, B.G. Pope⁸⁸,

G.A. Popeneciu^{25a}, D.S. Popovic^{12a}, A. Poppleton²⁹, X. Portell Bueso²⁹, G.E. Pospelov⁹⁹, S. Pospisil¹²⁷, I.N. Potrap⁹⁹, C.J. Potter¹⁴⁹, C.T. Potter¹¹⁴, G. Poulard²⁹, J. Poveda⁶⁰, V. Pozdnyakov⁶⁴, R. Prabhu⁷⁷, P. Pralavorio⁸³, A. Pranko¹⁴, S. Prasad²⁹, R. Pravahan²⁴, S. Prell⁶³, K. Pretzl¹⁶, D. Price⁶⁰, J. Price⁷³, L.E. Price⁵, D. Prieur¹²³, M. Primavera^{72a}, K. Prokofiev¹⁰⁸, F. Prokoshin^{31b}, S. Protopopescu²⁴, J. Proudfoot⁵, X. Prudent⁴³, M. Przybycien³⁷, H. Przysieszniak⁴, S. Psoroulas²⁰, E. Ptacek¹¹⁴, E. Pueschel⁸⁴, J. Purdham⁸⁷, M. Purohit^{24,ac}, P. Puzo¹¹⁵, Y. Pylypchenko⁶², J. Qian⁸⁷, A. Quadt⁵⁴, D.R. Quarrie¹⁴, W.B. Quayle¹⁷³, F. Quinonez^{31a}, M. Raas¹⁰⁴, V. Radescu⁴¹, P. Radloff¹¹⁴, T. Rador^{18a}, F. Ragusa^{89a,89b}, G. Rahal¹⁷⁸, A.M. Rahimi¹⁰⁹, D. Rahm²⁴, S. Rajagopalan²⁴, M. Rammensee⁴⁸, M. Rammes¹⁴¹, A.S. Randle-Conde³⁹, K. Randrianarivony²⁸, F. Rauscher⁹⁸, T.C. Rave⁴⁸, M. Raymond²⁹, A.L. Read¹¹⁷, D.M. Rebutti^{119a,119b}, A. Redelbach¹⁷⁴, G. Redlinger²⁴, R. Reece¹²⁰, K. Reeves⁴⁰, E. Reinherz-Aronis¹⁵³, A. Reinsch¹¹⁴, I. Reisinger⁴², C. Rembser²⁹, Z.L. Ren¹⁵¹, A. Renaud¹¹⁵, M. Rescigno^{132a}, S. Resconi^{89a}, B. Resende¹³⁶, P. Reznicek⁹⁸, R. Rezvani¹⁵⁸, R. Richter⁹⁹, E. Richter-Was^{4,af}, M. Ridel⁷⁸, M. Rijpstra¹⁰⁵, M. Rijssenbeek¹⁴⁸, A. Rimoldi^{119a,119b}, L. Rinaldi^{19a}, R.R. Rios³⁹, I. Riu¹¹, G. Rivoltella^{89a,89b}, F. Rizatdinova¹¹², E. Rizvi⁷⁵, S.H. Robertson^{85,k}, A. Robichaud-Veronneau¹¹⁸, D. Robinson²⁷, J.E.M. Robinson⁷⁷, A. Robson⁵³, J.G. Rocha de Lima¹⁰⁶, C. Roda^{122a,122b}, D. Roda Dos Santos²⁹, A. Roe⁵⁴, S. Roe²⁹, O. Røhne¹¹⁷, S. Rolli¹⁶¹, A. Romaniouk⁹⁶, M. Romano^{19a,19b}, G. Romeo²⁶, E. Romero Adam¹⁶⁷, L. Roos⁷⁸, E. Ros¹⁶⁷, S. Rosati^{132a}, K. Rosbach⁴⁹, A. Rose¹⁴⁹, M. Rose⁷⁶, G.A. Rosenbaum¹⁵⁸, E.I. Rosenberg⁶³, P.L. Rosendahl¹³, O. Rosenthal¹⁴¹, L. Rosselet⁴⁹, V. Rossetti¹¹, E. Rossi^{132a,132b}, L.P. Rossi^{50a}, M. Rotaru^{25a}, I. Roth¹⁷², J. Rothberg¹³⁸, D. Rousseau¹¹⁵, C.R. Royon¹³⁶, A. Rozanov⁸³, Y. Rozen¹⁵², X. Ruan^{32a,ag}, F. Rubbo¹¹, I. Rubinskiy⁴¹, B. Ruckert⁹⁸, N. Ruckstuhl¹⁰⁵, V.I. Rud⁹⁷, C. Rudolph⁴³, G. Rudolph⁶¹, F. Rühr⁶, A. Ruiz-Martinez⁶³, L. Romyantsev⁶⁴, Z. Rurikova⁴⁸, N.A. Rusakovich⁶⁴, J.P. Rutherford⁶, C. Ruwiedel¹⁴, P. Ruzicka¹²⁵, Y.F. Ryabov¹²¹, P. Ryan⁸⁸, M. Rybar¹²⁶, G. Rybkin¹¹⁵, N.C. Ryder¹¹⁸, A.F. Saavedra¹⁵⁰, I. Sadeh¹⁵³, H.F-W. Sadrozinski¹³⁷, R. Sadykov⁶⁴, F. Safai Tehrani^{132a}, H. Sakamoto¹⁵⁵, G. Salamanna⁷⁵, A. Salamon^{133a}, M. Saleem¹¹¹, D. Salek²⁹, D. Salihagic⁹⁹, A. Salnikov¹⁴³, J. Salt¹⁶⁷, B.M. Salvachua Ferrando⁵, D. Salvatore^{36a,36b}, F. Salvatore¹⁴⁹, A. Salvucci¹⁰⁴, A. Salzburger²⁹, D. Sampsonidis¹⁵⁴, B.H. Samset¹¹⁷, A. Sanchez^{102a,102b}, V. Sanchez Martinez¹⁶⁷, H. Sandaker¹³, H.G. Sander⁸¹, M.P. Sanders⁹⁸, M. Sandhoff¹⁷⁵, T. Sandoval²⁷, C. Sandoval¹⁶², R. Sandstroem⁹⁹, D.P.C. Sankey¹²⁹, A. Sansoni⁴⁷, C. Santamarina Rios⁸⁵, C. Santoni³³, R. Santonico^{133a,133b}, H. Santos^{124a}, J.G. Saraiva^{124a}, T. Sarangi¹⁷³, E. Sarkisyan-Grinbaum⁷, F. Sarri^{122a,122b}, G. Sartiso¹⁷⁵, O. Sasaki⁶⁵, N. Sasao⁶⁷, I. Satsounkevitch⁹⁰, G. Sauvage⁴, E. Sauvan⁴, J.B. Sauvan¹¹⁵, P. Savard^{158,d}, V. Savinov¹²³, D.O. Savu²⁹, L. Sawyer^{24,m}, D.H. Saxon⁵³, J. Saxon¹²⁰, C. Sbarra^{19a}, A. Sbrizzi^{19a,19b}, O. Scallion⁹³, D.A. Scannicchio¹⁶³, M. Scarcella¹⁵⁰, J. Schaarschmidt¹¹⁵, P. Schacht⁹⁹, D. Schaefer¹²⁰, U. Schäfer⁸¹, S. Schaepe²⁰, S. Schaetzel^{58b}, A.C. Schaffer¹¹⁵, D. Schaile⁹⁸, R.D. Schamberger¹⁴⁸, A.G. Schamov¹⁰⁷, V. Scharf^{58a}, V.A. Schegelsky¹²¹, D. Scheirich⁸⁷, M. Schernau¹⁶³, M.I. Scherzer³⁴, C. Schiavi^{50a,50b}, J. Schieck⁹⁸,

M. Schioppa^{36a,36b}, S. Schlenker²⁹, E. Schmidt⁴⁸, K. Schmieden²⁰, C. Schmitt⁸¹,
S. Schmitt^{58b}, M. Schmitz²⁰, B. Schneider¹⁶, U. Schnoor⁴³, A. Schoening^{58b},
A.L.S. Schorlemmer⁵⁴, M. Schott²⁹, D. Schouten^{159a}, J. Schovancova¹²⁵, M. Schram⁸⁵,
C. Schroeder⁸¹, N. Schroer^{58c}, M.J. Schultens²⁰, J. Schultes¹⁷⁵, H.-C. Schultz-Coulon^{58a},
H. Schulz¹⁵, M. Schumacher⁴⁸, B.A. Schumm¹³⁷, Ph. Schune¹³⁶, C. Schwanenberger⁸²,
A. Schwartzman¹⁴³, Ph. Schwemling⁷⁸, R. Schwienhorst⁸⁸, R. Schwierz⁴³, J. Schwindling¹³⁶,
T. Schwindt²⁰, M. Schwoerer⁴, G. Sciolla²², W.G. Scott¹²⁹, J. Searcy¹¹⁴, G. Sedov⁴¹,
E. Sedykh¹²¹, S.C. Seidel¹⁰³, A. Seiden¹³⁷, F. Seifert⁴³, J.M. Seixas^{23a}, G. Sekhniaidze^{102a},
S.J. Sekula³⁹, K.E. Selbach⁴⁵, D.M. Seliverstov¹²¹, B. Sellden^{146a}, G. Sellers⁷³,
M. Seman^{144b}, N. Semprini-Cesari^{19a,19b}, C. Serfon⁹⁸, L. Serin¹¹⁵, L. Serkin⁵⁴, R. Seuster⁹⁹,
H. Severini¹¹¹, A. Sfyrila²⁹, E. Shabalina⁵⁴, M. Shamim¹¹⁴, L.Y. Shan^{32a}, J.T. Shank²¹,
Q.T. Shao⁸⁶, M. Shapiro¹⁴, P.B. Shatalov⁹⁵, K. Shaw^{164a,164c}, D. Sherman¹⁷⁶,
P. Sherwood⁷⁷, A. Shibata¹⁰⁸, S. Shimizu²⁹, M. Shimojima¹⁰⁰, T. Shin⁵⁶, M. Shiyakova⁶⁴,
A. Shmeleva⁹⁴, M.J. Shochet³⁰, D. Short¹¹⁸, S. Shrestha⁶³, E. Shulga⁹⁶, M.A. Shupe⁶,
P. Sicho¹²⁵, A. Sidoti^{132a}, F. Siegert⁴⁸, Dj. Sijacki^{12a}, O. Silbert¹⁷², J. Silva^{124a}, Y. Silver¹⁵³,
D. Silverstein¹⁴³, S.B. Silverstein^{146a}, V. Simak¹²⁷, O. Simard¹³⁶, Lj. Simic^{12a}, S. Simion¹¹⁵,
E. Simioni⁸¹, B. Simmons⁷⁷, R. Simoniello^{89a,89b}, M. Simonyan³⁵, P. Sinervo¹⁵⁸,
N.B. Sinev¹¹⁴, V. Sipica¹⁴¹, G. Siragusa¹⁷⁴, A. Sircar²⁴, A.N. Sisakyan⁶⁴,
S.Yu. Sivoklokov⁹⁷, J. Sjölin^{146a,146b}, T.B. Sjursen¹³, L.A. Skinnari¹⁴, H.P. Skottowe⁵⁷,
K. Skovpen¹⁰⁷, P. Skubic¹¹¹, M. Slater¹⁷, T. Slavicek¹²⁷, K. Sliwa¹⁶¹, V. Smakhtin¹⁷²,
B.H. Smart⁴⁵, S.Yu. Smirnov⁹⁶, Y. Smirnov⁹⁶, L.N. Smirnova⁹⁷, O. Smirnova⁷⁹,
B.C. Smith⁵⁷, D. Smith¹⁴³, K.M. Smith⁵³, M. Smizanska⁷¹, K. Smolek¹²⁷, A.A. Snesarev⁹⁴,
S.W. Snow⁸², J. Snow¹¹¹, S. Snyder²⁴, R. Sobie^{169,k}, J. Sodomka¹²⁷, A. Soffer¹⁵³,
C.A. Solans¹⁶⁷, M. Solar¹²⁷, J. Solc¹²⁷, E.Yu. Soldatov⁹⁶, U. Soldevila¹⁶⁷,
E. Solfaroli Camillocci^{132a,132b}, A.A. Solodkov¹²⁸, O.V. Solovyanov¹²⁸, N. Soni⁸⁶,
V. Sopko¹²⁷, B. Sopko¹²⁷, M. Sosebee⁷, R. Soualah^{164a,164c}, A. Soukharev¹⁰⁷,
S. Spagnolo^{72a,72b}, F. Spanò⁷⁶, R. Spighi^{19a}, G. Spigo²⁹, F. Spila^{132a,132b}, R. Spiwoks²⁹,
M. Spousta¹²⁶, T. Spreitzer¹⁵⁸, B. Spurlock⁷, R.D. St. Denis⁵³, J. Stahlman¹²⁰,
R. Stamen^{58a}, E. Stanecka³⁸, R.W. Stanek⁵, C. Stanescu^{134a}, M. Stanescu-Bellu⁴¹,
S. Stapnes¹¹⁷, E.A. Starchenko¹²⁸, J. Stark⁵⁵, P. Staroba¹²⁵, P. Starovoitov⁴¹,
R. Staszewski³⁸, A. Staude⁹⁸, P. Stavina^{144a}, G. Steele⁵³, P. Steinbach⁴³, P. Steinberg²⁴,
I. Stekl¹²⁷, B. Stelzer¹⁴², H.J. Stelzer⁸⁸, O. Stelzer-Chilton^{159a}, H. Stenzel⁵², S. Stern⁹⁹,
G.A. Stewart²⁹, J.A. Stillings²⁰, M.C. Stockton⁸⁵, K. Stoerig⁴⁸, G. Stoicea^{25a}, S. Stonjek⁹⁹,
P. Strachota¹²⁶, A.R. Stradling⁷, A. Straessner⁴³, J. Strandberg¹⁴⁷, S. Strandberg^{146a,146b},
A. Strandlie¹¹⁷, M. Strang¹⁰⁹, E. Strauss¹⁴³, M. Strauss¹¹¹, P. Strizenec^{144b}, R. Ströhmer¹⁷⁴,
D.M. Strom¹¹⁴, J.A. Strong^{76,*}, R. Stroynowski³⁹, J. Strube¹²⁹, B. Stugu¹³, I. Stumer^{24,*},
J. Stupak¹⁴⁸, P. Sturm¹⁷⁵, N.A. Styles⁴¹, D.A. Soh^{151,w}, D. Su¹⁴³, HS. Subramania²,
A. Succurro¹¹, Y. Sugaya¹¹⁶, C. Suhr¹⁰⁶, M. Suk¹²⁶, V.V. Sulin⁹⁴, S. Sultansoy^{3d},
T. Sumida⁶⁷, X. Sun⁵⁵, J.E. Sundermann⁴⁸, K. Suruliz¹³⁹, G. Susinno^{36a,36b},
M.R. Sutton¹⁴⁹, Y. Suzuki⁶⁵, Y. Suzuki⁶⁶, M. Svatos¹²⁵, S. Swedish¹⁶⁸, I. Sykora^{144a},
T. Sykora¹²⁶, J. Sánchez¹⁶⁷, D. Ta¹⁰⁵, K. Tackmann⁴¹, A. Taffard¹⁶³, R. Tafirout^{159a},

N. Taiblum¹⁵³, Y. Takahashi¹⁰¹, H. Takai²⁴, R. Takashima⁶⁸, H. Takeda⁶⁶, T. Takeshita¹⁴⁰,
 Y. Takubo⁶⁵, M. Talby⁸³, A. Talyshev^{107,f}, M.C. Tamsett²⁴, J. Tanaka¹⁵⁵, R. Tanaka¹¹⁵,
 S. Tanaka¹³¹, S. Tanaka⁶⁵, A.J. Tanasijczuk¹⁴², K. Tani⁶⁶, N. Tannoury⁸³, S. Tapprogge⁸¹,
 D. Tardif¹⁵⁸, S. Tarem¹⁵², F. Tarrade²⁸, G.F. Tartarelli^{89a}, P. Tas¹²⁶, M. Tasevsky¹²⁵,
 E. Tassi^{36a,36b}, M. Tatarkhanov¹⁴, Y. Tayalati^{135d}, C. Taylor⁷⁷, F.E. Taylor⁹²,
 G.N. Taylor⁸⁶, W. Taylor^{159b}, M. Teinturier¹¹⁵, M. Teixeira Dias Castanheira⁷⁵,
 P. Teixeira-Dias⁷⁶, K.K. Temming⁴⁸, H. Ten Kate²⁹, P.K. Teng¹⁵¹, S. Terada⁶⁵,
 K. Terashi¹⁵⁵, J. Terron⁸⁰, M. Testa⁴⁷, R.J. Teuscher^{158,k}, J. Therhaag²⁰,
 T. Theveneaux-Pelzer⁷⁸, S. Thoma⁴⁸, J.P. Thomas¹⁷, E.N. Thompson³⁴, P.D. Thompson¹⁷,
 P.D. Thompson¹⁵⁸, A.S. Thompson⁵³, L.A. Thomsen³⁵, E. Thomson¹²⁰, M. Thomson²⁷,
 R.P. Thun⁸⁷, F. Tian³⁴, M.J. Tibbetts¹⁴, T. Tic¹²⁵, V.O. Tikhomirov⁹⁴, Y.A. Tikhonov^{107,f},
 S. Timoshenko⁹⁶, P. Tipton¹⁷⁶, F.J. Tique Aires Viegas²⁹, S. Tisserant⁸³, T. Todorov⁴,
 S. Todorova-Nova¹⁶¹, B. Toggerson¹⁶³, J. Tojo⁶⁹, S. Tokár^{144a}, K. Tokushuku⁶⁵,
 K. Tollefson⁸⁸, M. Tomoto¹⁰¹, L. Tompkins³⁰, K. Toms¹⁰³, A. Tonoyan¹³, C. Topfel¹⁶,
 N.D. Topilin⁶⁴, I. Torchiani²⁹, E. Torrence¹¹⁴, H. Torres⁷⁸, E. Torró Pastor¹⁶⁷, J. Toth^{83,ad},
 F. Touchard⁸³, D.R. Tovey¹³⁹, T. Trefzger¹⁷⁴, L. Tremblet²⁹, A. Tricoli²⁹, I.M. Trigger^{159a},
 S. Trincaz-Duvoid⁷⁸, M.F. Tripiana⁷⁰, W. Trischuk¹⁵⁸, B. Trocmé⁵⁵, C. Troncon^{89a},
 M. Trotter-McDonald¹⁴², M. Trzebinski³⁸, A. Trzupek³⁸, C. Tsarouchas²⁹, J.C-L. Tseng¹¹⁸,
 M. Tsiakiris¹⁰⁵, P.V. Tsiarehka⁹⁰, D. Tsionou^{4,ah}, G. Tsipolitis⁹, S. Tsiskaridze¹¹,
 V. Tsiskaridze⁴⁸, E.G. Tskhadadze^{51a}, I.I. Tsukerman⁹⁵, V. Tsulaia¹⁴, J.-W. Tsung²⁰,
 S. Tsuno⁶⁵, D. Tsybychev¹⁴⁸, A. Tua¹³⁹, A. Tudorache^{25a}, V. Tudorache^{25a}, J.M. Tuggle³⁰,
 M. Turala³⁸, D. Turecek¹²⁷, I. Turk Cakir^{3e}, E. Turlay¹⁰⁵, R. Turra^{89a,89b}, P.M. Tuts³⁴,
 A. Tykhonov⁷⁴, M. Tylmad^{146a,146b}, M. Tyndel¹²⁹, G. Tzanakos⁸, K. Uchida²⁰, I. Ueda¹⁵⁵,
 R. Ueno²⁸, M. Uglan¹³, M. Uhlenbrock²⁰, M. Uhrmacher⁵⁴, F. Ukegawa¹⁶⁰, G. Unal²⁹,
 A. Undrus²⁴, G. Unel¹⁶³, Y. Unno⁶⁵, D. Urbaniec³⁴, G. Usai⁷, M. Uslenghi^{119a,119b},
 L. Vacavant⁸³, V. Vacek¹²⁷, B. Vachon⁸⁵, S. Vahsen¹⁴, J. Valenta¹²⁵, P. Valente^{132a},
 S. Valentinetti^{19a,19b}, A. Valero¹⁶⁷, S. Valkar¹²⁶, E. Valladolid Gallego¹⁶⁷, S. Vallecorsa¹⁵²,
 J.A. Valls Ferrer¹⁶⁷, H. van der Graaf¹⁰⁵, E. van der Kraaij¹⁰⁵, R. Van Der Leeuw¹⁰⁵,
 E. van der Poel¹⁰⁵, D. van der Ster²⁹, N. van Eldik²⁹, P. van Gemmeren⁵, I. van Vulpen¹⁰⁵,
 M. Vanadia⁹⁹, W. Vandelli²⁹, A. Vaniachine⁵, P. Vankov⁴¹, F. Vannucci⁷⁸, R. Vari^{132a},
 T. Varol⁸⁴, D. Varouchas¹⁴, A. Vartapetian⁷, K.E. Varvell¹⁵⁰, V.I. Vassilakopoulos⁵⁶,
 F. Vazeille³³, T. Vazquez Schroeder⁵⁴, G. Vegni^{89a,89b}, J.J. Veillet¹¹⁵, F. Veloso^{124a},
 R. Veness²⁹, S. Veneziano^{132a}, A. Ventura^{72a,72b}, D. Ventura⁸⁴, M. Venturi⁴⁸, N. Venturi¹⁵⁸,
 V. Vercesi^{119a}, M. Verducci¹³⁸, W. Verkerke¹⁰⁵, J.C. Vermeulen¹⁰⁵, A. Vest⁴³,
 M.C. Vetterli^{142,d}, I. Vichou¹⁶⁵, T. Vickey^{145b,ai}, O.E. Vickey Boeriu^{145b},
 G.H.A. Viehhauser¹¹⁸, S. Viel¹⁶⁸, M. Villa^{19a,19b}, M. Villaplana Perez¹⁶⁷, E. Vilucchi⁴⁷,
 M.G. Vincker²⁸, E. Vinek²⁹, V.B. Vinogradov⁶⁴, M. Virchaux^{136,*}, J. Virzi¹⁴, O. Vitells¹⁷²,
 M. Viti⁴¹, I. Vivarelli⁴⁸, F. Vives Vaque², S. Vlachos⁹, D. Vladoiu⁹⁸, M. Vlasak¹²⁷,
 A. Vogel²⁰, P. Vokac¹²⁷, G. Volpi⁴⁷, M. Volpi⁸⁶, G. Volpini^{89a}, H. von der Schmitt⁹⁹,
 J. von Loeben⁹⁹, H. von Radziewski⁴⁸, E. von Toerne²⁰, V. Vorobel¹²⁶, V. Vorwerk¹¹,
 M. Vos¹⁶⁷, R. Voss²⁹, T.T. Voss¹⁷⁵, J.H. Vossebeld⁷³, N. Vranjes¹³⁶,

M. Vranjes Milosavljevic¹⁰⁵, V. Vrba¹²⁵, M. Vreeswijk¹⁰⁵, T. Vu Anh⁴⁸, R. Vuillermet²⁹,
I. Vukotic¹¹⁵, W. Wagner¹⁷⁵, P. Wagner¹²⁰, H. Wahlen¹⁷⁵, S. Wahrmund⁴³,
J. Wakabayashi¹⁰¹, S. Walch⁸⁷, J. Walder⁷¹, R. Walker⁹⁸, W. Walkowiak¹⁴¹, R. Wall¹⁷⁶,
P. Waller⁷³, C. Wang⁴⁴, H. Wang¹⁷³, H. Wang^{32b,aj}, J. Wang¹⁵¹, J. Wang⁵⁵, R. Wang¹⁰³,
S.M. Wang¹⁵¹, T. Wang²⁰, A. Warburton⁸⁵, C.P. Ward²⁷, M. Warsinsky⁴⁸, A. Washbrook⁴⁵,
C. Wasicki⁴¹, P.M. Watkins¹⁷, A.T. Watson¹⁷, I.J. Watson¹⁵⁰, M.F. Watson¹⁷, G. Watts¹³⁸,
S. Watts⁸², A.T. Waugh¹⁵⁰, B.M. Waugh⁷⁷, M. Weber¹²⁹, M.S. Weber¹⁶, P. Weber⁵⁴,
A.R. Weidberg¹¹⁸, P. Weigell⁹⁹, J. Weingarten⁵⁴, C. Weiser⁴⁸, H. Wellenstein²²,
P.S. Wells²⁹, T. Wenaus²⁴, D. Wendland¹⁵, Z. Weng^{151,w}, T. Wengler²⁹, S. Wenig²⁹,
N. Wermes²⁰, M. Werner⁴⁸, P. Werner²⁹, M. Werth¹⁶³, M. Wessels^{58a}, J. Wetter¹⁶¹,
C. Weydert⁵⁵, K. Whalen²⁸, S.J. Wheeler-Ellis¹⁶³, A. White⁷, M.J. White⁸⁶,
S. White^{122a,122b}, S.R. Whitehead¹¹⁸, D. Whiteson¹⁶³, D. Whittington⁶⁰, F. Wicke¹¹⁵,
D. Wicke¹⁷⁵, F.J. Wickens¹²⁹, W. Wiedenmann¹⁷³, M. Wielers¹²⁹, P. Wienemann²⁰,
C. Wiglesworth⁷⁵, L.A.M. Wiik-Fuchs⁴⁸, P.A. Wijeratne⁷⁷, A. Wildauer¹⁶⁷, M.A. Wildt^{41,s},
I. Wilhelm¹²⁶, H.G. Wilkens²⁹, J.Z. Will⁹⁸, E. Williams³⁴, H.H. Williams¹²⁰, W. Willis³⁴,
S. Willocq⁸⁴, J.A. Wilson¹⁷, M.G. Wilson¹⁴³, A. Wilson⁸⁷, I. Wingerter-Seez⁴,
S. Winkelmann⁴⁸, F. Winklmeier²⁹, M. Wittgen¹⁴³, S.J. Wollstadt⁸¹, M.W. Wolter³⁸,
H. Wolters^{124a,h}, W.C. Wong⁴⁰, G. Wooden⁸⁷, B.K. Wosiek³⁸, J. Wotschack²⁹,
M.J. Woudstra⁸², K.W. Wozniak³⁸, K. Wraight⁵³, C. Wright⁵³, M. Wright⁵³, B. Wrona⁷³,
S.L. Wu¹⁷³, X. Wu⁴⁹, Y. Wu^{32b,ak}, E. Wulf³⁴, B.M. Wynne⁴⁵, S. Xella³⁵, M. Xiao¹³⁶,
S. Xie⁴⁸, C. Xu^{32b,z}, D. Xu¹³⁹, B. Yabsley¹⁵⁰, S. Yacoob^{145b}, M. Yamada⁶⁵,
H. Yamaguchi¹⁵⁵, A. Yamamoto⁶⁵, K. Yamamoto⁶³, S. Yamamoto¹⁵⁵, T. Yamamura¹⁵⁵,
T. Yamanaka¹⁵⁵, J. Yamaoka⁴⁴, T. Yamazaki¹⁵⁵, Y. Yamazaki⁶⁶, Z. Yan²¹, H. Yang⁸⁷,
U.K. Yang⁸², Y. Yang⁶⁰, Z. Yang^{146a,146b}, S. Yanush⁹¹, L. Yao^{32a}, Y. Yao¹⁴, Y. Yasu⁶⁵,
G.V. Ybeles Smit¹³⁰, J. Ye³⁹, S. Ye²⁴, M. Yilmaz^{3c}, R. Yoosoofmiya¹²³, K. Yorita¹⁷¹,
R. Yoshida⁵, C. Young¹⁴³, C.J. Young¹¹⁸, S. Youssef²¹, D. Yu²⁴, J. Yu⁷, J. Yu¹¹², L. Yuan⁶⁶,
A. Yurkewicz¹⁰⁶, B. Zabinski³⁸, R. Zaidan⁶², A.M. Zaitsev¹²⁸, Z. Zajacova²⁹,
L. Zanello^{132a,132b}, D. Zanzi⁹⁹, A. Zaytsev¹⁰⁷, C. Zeitnitz¹⁷⁵, M. Zeman¹²⁵, A. Zemla³⁸,
C. Zender²⁰, O. Zenin¹²⁸, T. Ženiš^{144a}, Z. Zinonos^{122a,122b}, S. Zenz¹⁴, D. Zerwas¹¹⁵,
G. Zevi della Porta⁵⁷, Z. Zhan^{32d}, D. Zhang^{32b,aj}, H. Zhang⁸⁸, J. Zhang⁵, X. Zhang^{32d},
Z. Zhang¹¹⁵, L. Zhao¹⁰⁸, T. Zhao¹³⁸, Z. Zhao^{32b}, A. Zhemchugov⁶⁴, J. Zhong¹¹⁸, B. Zhou⁸⁷,
N. Zhou¹⁶³, Y. Zhou¹⁵¹, C.G. Zhu^{32d}, H. Zhu⁴¹, J. Zhu⁸⁷, Y. Zhu^{32b}, X. Zhuang⁹⁸,
V. Zhuravlov⁹⁹, D. Zieminska⁶⁰, N.I. Zimin⁶⁴, R. Zimmermann²⁰, S. Zimmermann²⁰,
S. Zimmermann⁴⁸, M. Ziolkowski¹⁴¹, R. Zitoun⁴, L. Živković³⁴, V.V. Zmouchko^{128,*},
G. Zobernig¹⁷³, A. Zoccoli^{19a,19b}, M. zur Nedden¹⁵, V. Zutshi¹⁰⁶, L. Zwalinski²⁹.

¹ University at Albany, Albany NY, United States of America

² Department of Physics, University of Alberta, Edmonton AB, Canada

³ ^(a)Department of Physics, Ankara University, Ankara; ^(b)Department of Physics,

Dumlupinar University, Kutahya; ^(c)Department of Physics, Gazi University, Ankara;

^(d)Division of Physics, TOBB University of Economics and Technology, Ankara; ^(e)Turkish

Atomic Energy Authority, Ankara, Turkey

⁴ LAPP, CNRS/IN2P3 and Université de Savoie, Annecy-le-Vieux, France

⁵ High Energy Physics Division, Argonne National Laboratory, Argonne IL, United States of America

⁶ Department of Physics, University of Arizona, Tucson AZ, United States of America

⁷ Department of Physics, The University of Texas at Arlington, Arlington TX, United States of America

⁸ Physics Department, University of Athens, Athens, Greece

⁹ Physics Department, National Technical University of Athens, Zografou, Greece

¹⁰ Institute of Physics, Azerbaijan Academy of Sciences, Baku, Azerbaijan

¹¹ Institut de Física d'Altes Energies and Departament de Física de la Universitat Autònoma de Barcelona and ICREA, Barcelona, Spain

¹² ^(a)Institute of Physics, University of Belgrade, Belgrade; ^(b)Vinca Institute of Nuclear Sciences, University of Belgrade, Belgrade, Serbia

¹³ Department for Physics and Technology, University of Bergen, Bergen, Norway

¹⁴ Physics Division, Lawrence Berkeley National Laboratory and University of California, Berkeley CA, United States of America

¹⁵ Department of Physics, Humboldt University, Berlin, Germany

¹⁶ Albert Einstein Center for Fundamental Physics and Laboratory for High Energy Physics, University of Bern, Bern, Switzerland

¹⁷ School of Physics and Astronomy, University of Birmingham, Birmingham, United Kingdom

¹⁸ ^(a)Department of Physics, Bogazici University, Istanbul; ^(b)Division of Physics, Dogus University, Istanbul; ^(c)Department of Physics Engineering, Gaziantep University, Gaziantep; ^(d)Department of Physics, Istanbul Technical University, Istanbul, Turkey

¹⁹ ^(a)INFN Sezione di Bologna; ^(b)Dipartimento di Fisica, Università di Bologna, Bologna, Italy

²⁰ Physikalisches Institut, University of Bonn, Bonn, Germany

²¹ Department of Physics, Boston University, Boston MA, United States of America

²² Department of Physics, Brandeis University, Waltham MA, United States of America

²³ ^(a)Universidade Federal do Rio De Janeiro COPPE/EE/IF, Rio de Janeiro; ^(b)Federal University of Juiz de Fora (UFJF), Juiz de Fora; ^(c)Federal University of Sao Joao del Rei (UFSJ), Sao Joao del Rei; ^(d)Instituto de Fisica, Universidade de Sao Paulo, Sao Paulo, Brazil

²⁴ Physics Department, Brookhaven National Laboratory, Upton NY, United States of America

²⁵ ^(a)National Institute of Physics and Nuclear Engineering, Bucharest; ^(b)University Politehnica Bucharest, Bucharest; ^(c)West University in Timisoara, Timisoara, Romania

²⁶ Departamento de Física, Universidad de Buenos Aires, Buenos Aires, Argentina

²⁷ Cavendish Laboratory, University of Cambridge, Cambridge, United Kingdom

²⁸ Department of Physics, Carleton University, Ottawa ON, Canada

- ²⁹ CERN, Geneva, Switzerland
- ³⁰ Enrico Fermi Institute, University of Chicago, Chicago IL, United States of America
- ³¹ ^(a)Departamento de Física, Pontificia Universidad Católica de Chile, Santiago;
- ^(b)Departamento de Física, Universidad Técnica Federico Santa María, Valparaíso, Chile
- ³² ^(a)Institute of High Energy Physics, Chinese Academy of Sciences, Beijing; ^(b)Department of Modern Physics, University of Science and Technology of China, Anhui; ^(c)Department of Physics, Nanjing University, Jiangsu; ^(d)School of Physics, Shandong University, Shandong, China
- ³³ Laboratoire de Physique Corpusculaire, Clermont Université and Université Blaise Pascal and CNRS/IN2P3, Aubiere Cedex, France
- ³⁴ Nevis Laboratory, Columbia University, Irvington NY, United States of America
- ³⁵ Niels Bohr Institute, University of Copenhagen, Kobenhavn, Denmark
- ³⁶ ^(a)INFN Gruppo Collegato di Cosenza; ^(b)Dipartimento di Fisica, Università della Calabria, Arcavata di Rende, Italy
- ³⁷ AGH University of Science and Technology, Faculty of Physics and Applied Computer Science, Krakow, Poland
- ³⁸ The Henryk Niewodniczanski Institute of Nuclear Physics, Polish Academy of Sciences, Krakow, Poland
- ³⁹ Physics Department, Southern Methodist University, Dallas TX, United States of America
- ⁴⁰ Physics Department, University of Texas at Dallas, Richardson TX, United States of America
- ⁴¹ DESY, Hamburg and Zeuthen, Germany
- ⁴² Institut für Experimentelle Physik IV, Technische Universität Dortmund, Dortmund, Germany
- ⁴³ Institut für Kern- und Teilchenphysik, Technical University Dresden, Dresden, Germany
- ⁴⁴ Department of Physics, Duke University, Durham NC, United States of America
- ⁴⁵ SUPA - School of Physics and Astronomy, University of Edinburgh, Edinburgh, United Kingdom
- ⁴⁶ Fachhochschule Wiener Neustadt, Johannes Gutenbergstrasse 32700 Wiener Neustadt, Austria
- ⁴⁷ INFN Laboratori Nazionali di Frascati, Frascati, Italy
- ⁴⁸ Fakultät für Mathematik und Physik, Albert-Ludwigs-Universität, Freiburg i.Br., Germany
- ⁴⁹ Section de Physique, Université de Genève, Geneva, Switzerland
- ⁵⁰ ^(a)INFN Sezione di Genova; ^(b)Dipartimento di Fisica, Università di Genova, Genova, Italy
- ⁵¹ ^(a)E.Andronikashvili Institute of Physics, Tbilisi State University, Tbilisi; ^(b)High Energy Physics Institute, Tbilisi State University, Tbilisi, Georgia
- ⁵² II Physikalisches Institut, Justus-Liebig-Universität Giessen, Giessen, Germany
- ⁵³ SUPA - School of Physics and Astronomy, University of Glasgow, Glasgow, United

Kingdom

⁵⁴ II Physikalisches Institut, Georg-August-Universität, Göttingen, Germany

⁵⁵ Laboratoire de Physique Subatomique et de Cosmologie, Université Joseph Fourier and CNRS/IN2P3 and Institut National Polytechnique de Grenoble, Grenoble, France

⁵⁶ Department of Physics, Hampton University, Hampton VA, United States of America

⁵⁷ Laboratory for Particle Physics and Cosmology, Harvard University, Cambridge MA, United States of America

⁵⁸ ^(a)Kirchhoff-Institut für Physik, Ruprecht-Karls-Universität Heidelberg, Heidelberg;

^(b)Physikalisches Institut, Ruprecht-Karls-Universität Heidelberg, Heidelberg; ^(c)ZITI Institut für technische Informatik, Ruprecht-Karls-Universität Heidelberg, Mannheim, Germany

⁵⁹ Faculty of Applied Information Science, Hiroshima Institute of Technology, Hiroshima, Japan

⁶⁰ Department of Physics, Indiana University, Bloomington IN, United States of America

⁶¹ Institut für Astro- und Teilchenphysik, Leopold-Franzens-Universität, Innsbruck, Austria

⁶² University of Iowa, Iowa City IA, United States of America

⁶³ Department of Physics and Astronomy, Iowa State University, Ames IA, United States of America

⁶⁴ Joint Institute for Nuclear Research, JINR Dubna, Dubna, Russia

⁶⁵ KEK, High Energy Accelerator Research Organization, Tsukuba, Japan

⁶⁶ Graduate School of Science, Kobe University, Kobe, Japan

⁶⁷ Faculty of Science, Kyoto University, Kyoto, Japan

⁶⁸ Kyoto University of Education, Kyoto, Japan

⁶⁹ Department of Physics, Kyushu University, Fukuoka, Japan

⁷⁰ Instituto de Física La Plata, Universidad Nacional de La Plata and CONICET, La Plata, Argentina

⁷¹ Physics Department, Lancaster University, Lancaster, United Kingdom

⁷² ^(a)INFN Sezione di Lecce; ^(b)Dipartimento di Matematica e Fisica, Università del Salento, Lecce, Italy

⁷³ Oliver Lodge Laboratory, University of Liverpool, Liverpool, United Kingdom

⁷⁴ Department of Physics, Jožef Stefan Institute and University of Ljubljana, Ljubljana, Slovenia

⁷⁵ School of Physics and Astronomy, Queen Mary University of London, London, United Kingdom

⁷⁶ Department of Physics, Royal Holloway University of London, Surrey, United Kingdom

⁷⁷ Department of Physics and Astronomy, University College London, London, United Kingdom

⁷⁸ Laboratoire de Physique Nucléaire et de Hautes Energies, UPMC and Université Paris-Diderot and CNRS/IN2P3, Paris, France

⁷⁹ Fysiska institutionen, Lunds universitet, Lund, Sweden

⁸⁰ Departamento de Física Teórica C-15, Universidad Autónoma de Madrid, Madrid, Spain

- ⁸¹ Institut für Physik, Universität Mainz, Mainz, Germany
- ⁸² School of Physics and Astronomy, University of Manchester, Manchester, United Kingdom
- ⁸³ CPPM, Aix-Marseille Université and CNRS/IN2P3, Marseille, France
- ⁸⁴ Department of Physics, University of Massachusetts, Amherst MA, United States of America
- ⁸⁵ Department of Physics, McGill University, Montreal QC, Canada
- ⁸⁶ School of Physics, University of Melbourne, Victoria, Australia
- ⁸⁷ Department of Physics, The University of Michigan, Ann Arbor MI, United States of America
- ⁸⁸ Department of Physics and Astronomy, Michigan State University, East Lansing MI, United States of America
- ⁸⁹ ^(a)INFN Sezione di Milano; ^(b)Dipartimento di Fisica, Università di Milano, Milano, Italy
- ⁹⁰ B.I. Stepanov Institute of Physics, National Academy of Sciences of Belarus, Minsk, Republic of Belarus
- ⁹¹ National Scientific and Educational Centre for Particle and High Energy Physics, Minsk, Republic of Belarus
- ⁹² Department of Physics, Massachusetts Institute of Technology, Cambridge MA, United States of America
- ⁹³ Group of Particle Physics, University of Montreal, Montreal QC, Canada
- ⁹⁴ P.N. Lebedev Institute of Physics, Academy of Sciences, Moscow, Russia
- ⁹⁵ Institute for Theoretical and Experimental Physics (ITEP), Moscow, Russia
- ⁹⁶ Moscow Engineering and Physics Institute (MEPhI), Moscow, Russia
- ⁹⁷ Skobeltsyn Institute of Nuclear Physics, Lomonosov Moscow State University, Moscow, Russia
- ⁹⁸ Fakultät für Physik, Ludwig-Maximilians-Universität München, München, Germany
- ⁹⁹ Max-Planck-Institut für Physik (Werner-Heisenberg-Institut), München, Germany
- ¹⁰⁰ Nagasaki Institute of Applied Science, Nagasaki, Japan
- ¹⁰¹ Graduate School of Science and Kobayashi-Maskawa Institute, Nagoya University, Nagoya, Japan
- ¹⁰² ^(a)INFN Sezione di Napoli; ^(b)Dipartimento di Scienze Fisiche, Università di Napoli, Napoli, Italy
- ¹⁰³ Department of Physics and Astronomy, University of New Mexico, Albuquerque NM, United States of America
- ¹⁰⁴ Institute for Mathematics, Astrophysics and Particle Physics, Radboud University Nijmegen/Nikhef, Nijmegen, Netherlands
- ¹⁰⁵ Nikhef National Institute for Subatomic Physics and University of Amsterdam, Amsterdam, Netherlands
- ¹⁰⁶ Department of Physics, Northern Illinois University, DeKalb IL, United States of America
- ¹⁰⁷ Budker Institute of Nuclear Physics, SB RAS, Novosibirsk, Russia

- ¹⁰⁸ Department of Physics, New York University, New York NY, United States of America
- ¹⁰⁹ Ohio State University, Columbus OH, United States of America
- ¹¹⁰ Faculty of Science, Okayama University, Okayama, Japan
- ¹¹¹ Homer L. Dodge Department of Physics and Astronomy, University of Oklahoma, Norman OK, United States of America
- ¹¹² Department of Physics, Oklahoma State University, Stillwater OK, United States of America
- ¹¹³ Palacký University, RCPTM, Olomouc, Czech Republic
- ¹¹⁴ Center for High Energy Physics, University of Oregon, Eugene OR, United States of America
- ¹¹⁵ LAL, Université Paris-Sud and CNRS/IN2P3, Orsay, France
- ¹¹⁶ Graduate School of Science, Osaka University, Osaka, Japan
- ¹¹⁷ Department of Physics, University of Oslo, Oslo, Norway
- ¹¹⁸ Department of Physics, Oxford University, Oxford, United Kingdom
- ¹¹⁹ ^(a)INFN Sezione di Pavia; ^(b)Dipartimento di Fisica, Università di Pavia, Pavia, Italy
- ¹²⁰ Department of Physics, University of Pennsylvania, Philadelphia PA, United States of America
- ¹²¹ Petersburg Nuclear Physics Institute, Gatchina, Russia
- ¹²² ^(a)INFN Sezione di Pisa; ^(b)Dipartimento di Fisica E. Fermi, Università di Pisa, Pisa, Italy
- ¹²³ Department of Physics and Astronomy, University of Pittsburgh, Pittsburgh PA, United States of America
- ¹²⁴ ^(a)Laboratorio de Instrumentacao e Fisica Experimental de Particulas - LIP, Lisboa, Portugal; ^(b)Departamento de Fisica Teorica y del Cosmos and CAFPE, Universidad de Granada, Granada, Spain
- ¹²⁵ Institute of Physics, Academy of Sciences of the Czech Republic, Praha, Czech Republic
- ¹²⁶ Faculty of Mathematics and Physics, Charles University in Prague, Praha, Czech Republic
- ¹²⁷ Czech Technical University in Prague, Praha, Czech Republic
- ¹²⁸ State Research Center Institute for High Energy Physics, Protvino, Russia
- ¹²⁹ Particle Physics Department, Rutherford Appleton Laboratory, Didcot, United Kingdom
- ¹³⁰ Physics Department, University of Regina, Regina SK, Canada
- ¹³¹ Ritsumeikan University, Kusatsu, Shiga, Japan
- ¹³² ^(a)INFN Sezione di Roma I; ^(b)Dipartimento di Fisica, Università La Sapienza, Roma, Italy
- ¹³³ ^(a)INFN Sezione di Roma Tor Vergata; ^(b)Dipartimento di Fisica, Università di Roma Tor Vergata, Roma, Italy
- ¹³⁴ ^(a)INFN Sezione di Roma Tre; ^(b)Dipartimento di Fisica, Università Roma Tre, Roma, Italy
- ¹³⁵ ^(a)Faculté des Sciences Ain Chock, Réseau Universitaire de Physique des Hautes Energies - Université Hassan II, Casablanca; ^(b)Centre National de l'Energie des Sciences

Techniques Nucleaires, Rabat; ^(c)Faculté des Sciences Semlalia, Université Cadi Ayyad, LPHEA-Marrakech; ^(d)Faculté des Sciences, Université Mohamed Premier and LPTPM, Oujda; ^(e)Faculté des sciences, Université Mohammed V-Agdal, Rabat, Morocco

¹³⁶ DSM/IRFU (Institut de Recherches sur les Lois Fondamentales de l'Univers), CEA Saclay (Commissariat à l'Energie Atomique), Gif-sur-Yvette, France

¹³⁷ Santa Cruz Institute for Particle Physics, University of California Santa Cruz, Santa Cruz CA, United States of America

¹³⁸ Department of Physics, University of Washington, Seattle WA, United States of America

¹³⁹ Department of Physics and Astronomy, University of Sheffield, Sheffield, United Kingdom

¹⁴⁰ Department of Physics, Shinshu University, Nagano, Japan

¹⁴¹ Fachbereich Physik, Universität Siegen, Siegen, Germany

¹⁴² Department of Physics, Simon Fraser University, Burnaby BC, Canada

¹⁴³ SLAC National Accelerator Laboratory, Stanford CA, United States of America

¹⁴⁴ ^(a)Faculty of Mathematics, Physics & Informatics, Comenius University, Bratislava; ^(b)Department of Subnuclear Physics, Institute of Experimental Physics of the Slovak Academy of Sciences, Kosice, Slovak Republic

¹⁴⁵ ^(a)Department of Physics, University of Johannesburg, Johannesburg; ^(b)School of Physics, University of the Witwatersrand, Johannesburg, South Africa

¹⁴⁶ ^(a)Department of Physics, Stockholm University; ^(b)The Oskar Klein Centre, Stockholm, Sweden

¹⁴⁷ Physics Department, Royal Institute of Technology, Stockholm, Sweden

¹⁴⁸ Departments of Physics & Astronomy and Chemistry, Stony Brook University, Stony Brook NY, United States of America

¹⁴⁹ Department of Physics and Astronomy, University of Sussex, Brighton, United Kingdom

¹⁵⁰ School of Physics, University of Sydney, Sydney, Australia

¹⁵¹ Institute of Physics, Academia Sinica, Taipei, Taiwan

¹⁵² Department of Physics, Technion: Israel Institute of Technology, Haifa, Israel

¹⁵³ Raymond and Beverly Sackler School of Physics and Astronomy, Tel Aviv University, Tel Aviv, Israel

¹⁵⁴ Department of Physics, Aristotle University of Thessaloniki, Thessaloniki, Greece

¹⁵⁵ International Center for Elementary Particle Physics and Department of Physics, The University of Tokyo, Tokyo, Japan

¹⁵⁶ Graduate School of Science and Technology, Tokyo Metropolitan University, Tokyo, Japan

¹⁵⁷ Department of Physics, Tokyo Institute of Technology, Tokyo, Japan

¹⁵⁸ Department of Physics, University of Toronto, Toronto ON, Canada

¹⁵⁹ ^(a)TRIUMF, Vancouver BC; ^(b)Department of Physics and Astronomy, York University, Toronto ON, Canada

¹⁶⁰ Institute of Pure and Applied Sciences, University of Tsukuba, 1-1-1 Tennodai, Tsukuba, Ibaraki 305-8571, Japan

¹⁶¹ Science and Technology Center, Tufts University, Medford MA, United States of America

¹⁶² Centro de Investigaciones, Universidad Antonio Narino, Bogota, Colombia

¹⁶³ Department of Physics and Astronomy, University of California Irvine, Irvine CA, United States of America

¹⁶⁴ ^(a)INFN Gruppo Collegato di Udine; ^(b)ICTP, Trieste; ^(c)Dipartimento di Chimica, Fisica e Ambiente, Università di Udine, Udine, Italy

¹⁶⁵ Department of Physics, University of Illinois, Urbana IL, United States of America

¹⁶⁶ Department of Physics and Astronomy, University of Uppsala, Uppsala, Sweden

¹⁶⁷ Instituto de Física Corpuscular (IFIC) and Departamento de Física Atómica, Molecular y Nuclear and Departamento de Ingeniería Electrónica and Instituto de Microelectrónica de Barcelona (IMB-CNM), University of Valencia and CSIC, Valencia, Spain

¹⁶⁸ Department of Physics, University of British Columbia, Vancouver BC, Canada

¹⁶⁹ Department of Physics and Astronomy, University of Victoria, Victoria BC, Canada

¹⁷⁰ Department of Physics, University of Warwick, Coventry, United Kingdom

¹⁷¹ Waseda University, Tokyo, Japan

¹⁷² Department of Particle Physics, The Weizmann Institute of Science, Rehovot, Israel

¹⁷³ Department of Physics, University of Wisconsin, Madison WI, United States of America

¹⁷⁴ Fakultät für Physik und Astronomie, Julius-Maximilians-Universität, Würzburg, Germany

¹⁷⁵ Fachbereich C Physik, Bergische Universität Wuppertal, Wuppertal, Germany

¹⁷⁶ Department of Physics, Yale University, New Haven CT, United States of America

¹⁷⁷ Yerevan Physics Institute, Yerevan, Armenia

¹⁷⁸ Domaine scientifique de la Doua, Centre de Calcul CNRS/IN2P3, Villeurbanne Cedex, France

^a Also at Laboratório de Instrumentação e Física Experimental de Partículas - LIP, Lisboa, Portugal

^b Also at Faculdade de Ciências and CFNUL, Universidade de Lisboa, Lisboa, Portugal

^c Also at Particle Physics Department, Rutherford Appleton Laboratory, Didcot, United Kingdom

^d Also at TRIUMF, Vancouver BC, Canada

^e Also at Department of Physics, California State University, Fresno CA, United States of America

^f Also at Novosibirsk State University, Novosibirsk, Russia

^g Also at Fermilab, Batavia IL, United States of America

^h Also at Department of Physics, University of Coimbra, Coimbra, Portugal

ⁱ Also at Department of Physics, UASLP, San Luis Potosi, Mexico

^j Also at Università di Napoli Parthenope, Napoli, Italy

^k Also at Institute of Particle Physics (IPP), Canada

^l Also at Department of Physics, Middle East Technical University, Ankara, Turkey

^m Also at Louisiana Tech University, Ruston LA, United States of America

ⁿ Also at Dep Física and CEFITEC of Faculdade de Ciências e Tecnologia, Universidade

Nova de Lisboa, Caparica, Portugal

^o Also at Department of Physics and Astronomy, University College London, London, United Kingdom

^p Also at Group of Particle Physics, University of Montreal, Montreal QC, Canada

^q Also at Department of Physics, University of Cape Town, Cape Town, South Africa

^r Also at Institute of Physics, Azerbaijan Academy of Sciences, Baku, Azerbaijan

^s Also at Institut für Experimentalphysik, Universität Hamburg, Hamburg, Germany

^t Also at Manhattan College, New York NY, United States of America

^u Also at School of Physics, Shandong University, Shandong, China

^v Also at CPPM, Aix-Marseille Université and CNRS/IN2P3, Marseille, France

^w Also at School of Physics and Engineering, Sun Yat-sen University, Guanzhou, China

^x Also at Academia Sinica Grid Computing, Institute of Physics, Academia Sinica, Taipei, Taiwan

^y Also at Dipartimento di Fisica, Università La Sapienza, Roma, Italy

^z Also at DSM/IRFU (Institut de Recherches sur les Lois Fondamentales de l'Univers), CEA Saclay (Commissariat à l'Energie Atomique), Gif-sur-Yvette, France

^{aa} Also at Section de Physique, Université de Genève, Geneva, Switzerland

^{ab} Also at Departamento de Fisica, Universidade de Minho, Braga, Portugal

^{ac} Also at Department of Physics and Astronomy, University of South Carolina, Columbia SC, United States of America

^{ad} Also at Institute for Particle and Nuclear Physics, Wigner Research Centre for Physics, Budapest, Hungary

^{ae} Also at California Institute of Technology, Pasadena CA, United States of America

^{af} Also at Institute of Physics, Jagiellonian University, Krakow, Poland

^{ag} Also at LAL, Université Paris-Sud and CNRS/IN2P3, Orsay, France

^{ah} Also at Department of Physics and Astronomy, University of Sheffield, Sheffield, United Kingdom

^{ai} Also at Department of Physics, Oxford University, Oxford, United Kingdom

^{aj} Also at Institute of Physics, Academia Sinica, Taipei, Taiwan

^{ak} Also at Department of Physics, The University of Michigan, Ann Arbor MI, United States of America

* Deceased